Acta Universitatis Agriculturae Sueciae

Doctoral Thesis No. 2026:34
Faculty of Natural Resources and Agricultural Sciences

Untargeted analysis of per- and polyfluoroalkyl substances

An analysis of contaminated waters and advanced treatment processes

Svante Bertil Rehnstam

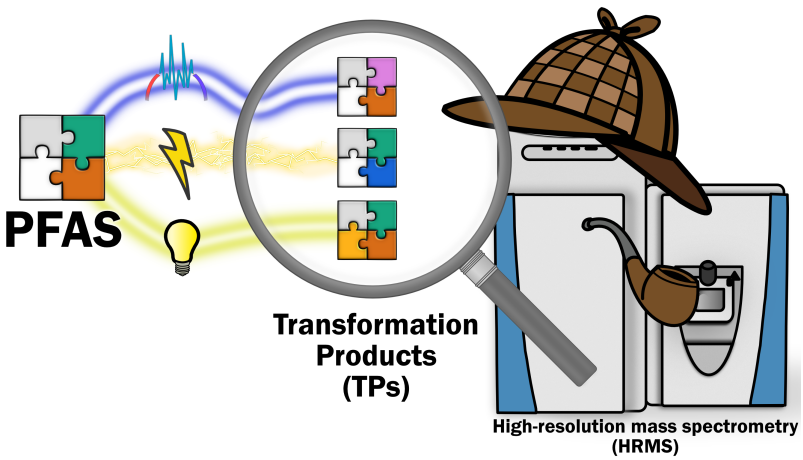

Untargeted analysis of per- and polyfluoroalkyl substances

An analysis of contaminated waters and advanced treatment processes

Svante Bertil Rehnstam
Faculty of Natural Resources and Agricultural Sciences
Department of Aquatic Sciences and Assessment
Uppsala

SLU
SWEDISH UNIVERSITY OF AGRICULTURAL SCIENCES

DOCTORAL THESIS
Uppsala 2026

Acta Universitatis Agriculturae Sueciae
2026:34

Cover: Screening for transformation product suspects using high-resolution mass spectrometry. Techniques include electrochemical oxidation, ultraviolet degradation, and plasma degradation. (Original work of Svante Rehnstam. Made using Affinity Designer®)

ISSN 1652-6880
ISBN (print version) 978-91-8124-251-5
ISBN (electronic version) 978-91-8124-281-2
https://doi.org/10.54612/a.5d1sn7i5s9

Swedish University of Agricultural Sciences, Department of Aquatic Sciences and Assessment , Uppsala, Sweden

Print: SLU Grafisk service, Uppsala 2026

Untargeted analysis of per- and polyfluoroalkyl substances

Abstract

Per- and polyfluoroalkyl substances (PFAS) are persistent and widespread environmental contaminants. As a result, destructive treatment techniques have been developed to degrade these pollutants. However, such processes may generate transformation products (TPs), whose identities and potential risks remain unknown. This thesis investigates the formation of TPs using high-resolution mass spectrometry (HRMS). The processes investigated include electrochemical oxidation, ultraviolet (UV) degradation, and plasma degradation. An untargeted HRMS workflow was developed and validated against an in-house targeted PFAS method.

The findings elucidated the formation of TPs resulting from the electrochemical oxidation treatment in groundwater and landfill leachate. During treatment, ammonia present in the sample was oxidised to reactive nitro-substances that subsequently reacted with the PFAS present in the matrix leading to the formation of TPs such as perfluoroalkane sulfonhyponitrites (FASHN). The plasma degradation study further highlighted the influence of sample matrices on TP formation. A new class of PFAS, not previously reported, was detected, termed two-to-one fluorotelomer ethers (2:1-FtE), likely originating from larger precursor compounds. This class of PFAS had a consistent backbone but featured diverse functional groups.

The UV degradation study was performed in ultrapure water spiked with PFAS and induced the formation of hydrogen-substituted and unsaturated PFAS species. The treatment also revealed extensive isomerisation and the previously unreported di-hydrogen-substituted unsaturated PFOS (H_2-UPFOS).

Toxicity evaluation using *in silico* predictions showed that some PFAS TPs were predicted to be more toxic than their precursors. Notably, H_2-UPFOS and the novel 2:1-FtE exhibited the highest predicted toxicity. This thesis demonstrates that untargeted HRMS can identify novel and potentially toxic PFAS TPs, improving the evaluation of PFAS remediation technologies.

Keywords: organic micropollutants; suspect screening; non-target sceening; destructive treatment processes; transformation products; water analysis

Förutsättningslös analys av per- och polyfluorerade alkylsubstanser

Abstrakt

Per- och polyfluorerade alkylsubstanser (PFAS) är organiska miljöföroreningar som är persistenta och globalt spridda. På grund av detta så utvecklas nya metoder för att bryta ner dem. När PFAS bryts ner i behandlingsprocesser kan de bilda stabila transformationsprodukter (TP) vars identiteter och potentiella hälsorisker är okända. Denna avhandling undersöker bildningen av TP med hjälp av högupplöst masspektrometri (HRMS). Processerna som undersöktes var elektrokemisk oxidering (EO), ultraviolett strålning (UV) och plasmadegradering. För att kunna studera bildning av TP utvecklades en förutsättningslös HRMS-metod som validerades mot en intern riktad analysmetod.

Ett av fynden var att TP bildades i grundvatten och lakvatten som behandlats med EO. Oxideringen av ammoniak som fanns i proverna hade skapat reaktiva nitrogrupper som reagerade med PFAS som också fanns i proverna. Detta ledde till bildningen av en ny TP som identifierades som perfluoralkan sulfonhyponitriter (FASHN). Studien med plasmabehandling påvisade återigen det inflytande som provmatrisen kan ha vid bildning av TP. En ny PFAS-klass som inte rapporterats tidigare detekterades, 2:1 fluorotelomer eter (2:1-FtE). Ämnet hade troligen bildats från en prekursor i matrisen. Denna hypotes stöds av att 2:1-FtE tycks ha behållit en PFAS ryggrad, men hade många olika funktionsgrupper utöver det. Behandlingen med UV-strålning gjordes i ultrarent vatten spikat med PFAS och inducerade bildning av vätesubstituerade och omättade PFAS. Processen skapade också många olika isomerer. Det är första gången som divätesubstituerad och omättad PFOS (H_2-UPFOS) identifierades som en TP av UV-strålning. En utvärdering av toxiciteten för TP-fynden gjordes med *in silico*-verktyg. Det visade sig att många TP var mer giftiga än ursprungsmolekylerna. Bland annat så rankades H_2-UPFOS och 2:1-FtE högst bland alla detekterade ämnen.

Denna avhandling demonstrerar att förutsättningslös HRMS-analys kan identifiera tidigare okända TP från PFAS. Kunskap om oönskade TP kan användas för att förbättra utvärderingar av reningstekniker för nedbrytning av PFAS.

Nyckelord: högupplöst masspektrometri, suspect screening, förutsättningslös analys, nedbrytningstekniker, transformationsprodukter, vattenanalys, organiska miljöföroreningar

Contents

List of publications

This thesis is based on the work contained in the following papers, referred to by Roman numerals in the text:

I. Rehnstam, S., Czeschka, M.-B. & Ahrens, L. (2023). Suspect screening and total oxidizable precursor (TOP) assay as tools for characterization of per- and polyfluoroalkyl substance (PFAS)-contaminated groundwater and treated landfill leachate. Chemosphere, 334, 138925. https://doi.org/10.1016/j.chemosphere.2023.138925.

II. Rehnstam, S., Smith, S.J. & Ahrens, L. (2024). Suspect and non-target screening of per- and polyfluoroalkyl substances (PFAS) and other halogenated substances in electrochemically oxidized landfill leachate and groundwater. Journal of Hazardous Materials, 480 (May), 136316. https://doi.org/10.1016/j.jhazmat.2024.136316.

III. Rehnstam, S., Luo, S., Löffler, P., Lai, F.Y., Wei, Z., Ahrens, L. UV degradation of per- and polyfluoroalkyl substances – suspect screening of transformation products and toxicity predictions (manuscript).

IV. Rehnstam, S., Thagard, S.M., Ahrens, L. Plasma treatment of industrial wastewater – untargeted analysis of PFAS (manuscript).

The contribution of Svante Bertil Rehnstam to the papers included in this thesis was as follows:

I. Contributed to the planning of the study design, conducted the instrumental analysis for high-resolution mass spectrometry data, data analysis, writing of the original draft, visualisation of figures, and editing and revising drafts.

II. Conducted the instrumental analysis for high-resolution mass spectrometry data, data analysis, writing of the original draft, visualisation of figures, and editing and revising drafts.

III. Conducted the instrumental analysis for high-resolution mass spectrometry data, data analysis, writing of the original draft, visualisation of figures, and editing and revising drafts

IV. Conducted the instrumental analysis for high-resolution mass spectrometry data, data analysis, toxicity predictions, writing of the original draft, visualisation of figures, and editing and revising drafts,

Additional publications

The author has contributed to the following papers which are not included in the thesis:

I. Löffler, P., Rehnstam, S., Ahrens, L., Lai, F.Y. & Celma, A. (2025). Long-Term System Suitability Evaluation for Mass Accuracy in the Analysis of Small Molecules by High-Resolution Mass Spectrometry. Journal of the American Society for Mass Spectrometry, 36 (9), 2005–2012. https://doi.org/10.1021/jasms.5c00128

II. Kong, Z.H., Stangl, M., Oester, R., Rehnstam, S., Futter, M., Siddique, A.B., Bundschuh, M. & Mckie, B.G. (2026). Medical facemask waste alters detritus decomposition and fungal communities in a freshwater pond. Scientific Reports, 16 (1), 10597. https://doi.org/10.1038/s41598-026-45795-5

List of tables

List of figures

Abbreviations

2:1-FtE	Two-to-one fluorotelomer ether
a.u.	Arbitrary unit
AFFF	Aqueous film-forming foams
AGC	Automatic gain control
C	Carbon
CD	Compound Discoverer
DDA	Data-dependent acquisition
DUPFOS	Diunsaturated perfluorooctanesulfonic acid
EOF	Extractable organic fluorine
ESI-	Electrospray negative ion mode
FASA	Perfluoroalkyl sulfonamide
FASASA	Perfluoroalkyl sulfonamide sulfonic acid
FASHN	Perfluoroalkane sulfonhyponitrite
GAC	Granular activated carbon
H_2-UPFOS	di-hydrogen-substituted unsaturated perfluorooctanesulfonic acid
H-PFCA	Hydrogen-substituted perfluoroalkyl carboxylic acid
HRAM	High-resolution accurate masses
HRMS	High-resolution mass spectrometry
H-UPFOS	Hydrogen substituted perfluorooctanesulfonic acid
IX	Anion exchange
KMD	Kendrick Mass Defect
LC-MS/MS	Liquid chromatography tandem mass spectrometry
LOD	Limit of detection

LOQ	Limit of quantification
m	Mass
MD	Mass Defect
Me-FASASi	N-methyl perfluoroalkane sulfonamide sulfinic acid
MeOH-FASA	N-methanol perfluoroalkyl sulfonamide
MS	Mass spectrometry
N-EtFASAA	N-ethyl perfluoroalkyl sulfonamidoacetic acid
N-EtFOSAA	N-ethyl perfluorooctanesulfonamidoacetic acid
N-MeFASAA	N-methyl perfluoroalkyl sulfonamidoacetic acid
N-MeFOSAA	N-methyl perfluorooctanesulfonamidoacetic acid
N-SPAmP-FHxSA	N-sulfopropyldimethylammonio propyl perfluorohexanesulfonamide
N-SPAmP-FHxSAA	N-sulfopropyldimethylammoniopropyl-perfluorohexanesulfonamido acetic acid
N-SPAmP-FHxSAPS	N-sulfopropyldimethylammoniopropyl perfluorohexane sulfonamidopropylsulfonate
OECD	Organisation for Economic Co-operation and Development
PFAS	Per- and polyfluoroalkyl substances
PFBS	Perfluorobutanesulfonic acid
PFC	Perfluorinated compounds
PFCA	Perfluoroalkyl carboxylic acid
PFdiCA	Perfluoroalkanedicarboxylic acid
PFECHS	Perfluoroethylcyclohexansulfonic acid
PFESA	Perfluoroethersulfonic acid
PFHxDiA	Perfluorohexanedicarboxylic acid
PFHxS	Perfluorohexanesulfonic acid
PFOCHS	Polyfluorooxacyclohexane propane sulfonic acid

PFOS	Perfluorooctanesulfonic acid
PFPeDiA	Perfluoropentanedicarboxylic acid
PFSA	Perfluoroalkanesulfonic acid
ppm	Parts-per-million
SLE	Suspect list exchange
SST	System suitability test
SusDat	NORMAN Substance database
TOPA	Total oxidizable precursor assay
TP	Transformation product
UV	Ultraviolet
UVCB	Substances of unknown or variable composition, complex reaction products, or biological materials

AI declaration

This thesis reflects my own scholarly work, and I am responsible for its contents and accuracy throughout. When writing the thesis, the generative AI tool Gemini was utilised for two main reasons. First was for assistance when writing code in R, however, only strictly for the generation of figures. The second was to improve phrasing and general language.

Content from the generative AI was carefully reviewed for errors in language and intent. All data, interpretations of data, and conclusions are my own.

1. Background

1.1 What are PFAS?

Per- and polyfluoroalkyl substances are a class of anthropogenic chemicals abbreviated as PFAS. They have previously been referred to as perfluorinated compounds (PFC), and going even further back in time, simply as fluorinated surfactants (Kissa 2001; Corsini et al. 2014). Although there has been previous work aimed at harmonising the definition of PFAS, the most widely used definition is currently provided by the Organisation for Economic Co-operation and Development (OECD), which defines PFAS as substances containing at minimum one "fully fluorinated methyl or methylene carbon atom" (OECD 2021). This means that at least one $-CF_3$ or $-CF_2-$ moiety must be present for a compound to be classified as a PFAS. This class comprises a large and structurally diverse group of chemicals. PFAS are broadly categorised into two groups based on their chemical structure. Perfluoroalkyl substances contain an alkyl chain where all available carbon bonds are saturated with fluorine. Polyfluoroalkyl substances, however, are only partially fluorinated, meaning their carbon chains contain hydrogen or other atoms alongside fluorine. Furthermore, there are both long-chain and short-chain PFAS. This categorisation is based on the length of the per or polyfluorinated carbon chain. Long chain PFAS are defined as having a carbon chain length of eight or more in perfluoroalkyl carboxylic acids (PFCA) and six or more in non-carboxylic acids such as perfluoroalkanesulfonic acids (PFSA) (OECD 2022). In Figure 1 a PFSA with a perfluorinated carbon chain of eight, perfluorooctanesulfonic acid (PFOS) is displayed.

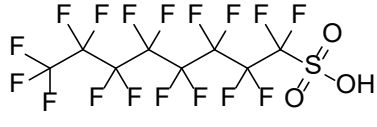

Figure 1. A skeleton structure of perfluorooctanesulfonic acid (PFOS).

Based on the OECD definition and data from online databases, there are currently over 7 million unique PFAS with almost 250,000 compounds containing more than one single CF_2 or CF_3 moiety. (Schymanski et al. 2023; PubChem n.d.). In the 20th century, PFAS was mainly produced by

companies such as DuPont and 3M, where they were synthesised both as niche industrial chemicals and as components of widely recognised commercial products such as Teflon® and Scotchgard® (Kissa 2001; Gaber et al. 2023). Since then, they have found widespread global use, being utilised in applications ranging from heavy industry to common household items. Some notable uses include aqueous film-forming foams (AFFF), water and dirt repellents, and food packaging (Glüge et al. 2020). Several chemical and physical properties have driven their extensive use, primarily their amphiphilic properties as well as their exceptional thermal and chemical stability which arises from the strength of the carbon-fluorine bond (Moody & Field 2000). Unfortunately, the same properties that make PFAS highly stable and useful have also rightfully earned them the infamous designation of "forever chemicals".

1.2 Why are PFAS a concern?

The designation "forever chemical" refers to the fact that PFAS persist in water, soil, the atmosphere, wildlife, and in human tissues for extremely long periods. Their widespread use has caused an ubiquitous contamination of our environment, and their fate and transport have been extensively documented in studies across the world (Giesy & Kannan 2001; Lau et al. 2007; Ahrens et al. 2010). The combination of continuous environmental exposure and negligible natural degradation results in the accumulation of PFAS in organisms across different trophic levels, including humans (Haukås et al. 2007; Graber et al. 2019). Although PFAS are not known for their acute toxicity, the constant exposure and accumulation is a threat to the environment (Zhang et al. 2026). These concerns have prompted regulatory efforts to restrict or ban PFAS, such as the inclusion of PFOS under the Stockholm Convention on Persistent Organic Pollutants (UNEP 2009). However, the ban on individual PFAS have proven ineffective as for every banned chemical, industry often introduces structurally similar substitutes and analogues that are different enough to pass legal scrutiny (Lu et al. 2019; Hamid et al. 2024). This challenge is analogous to the Hydra of Lerna in Greek mythology, where removing one head resulted in the growth of two more (Euripides & Halleran 1988). Similar difficulties are faced when trying to remediate PFAS, as traditional treatment techniques are largely ineffective at degrading PFAS, as is described below. (Lenka et al. 2021).

1.3 Current remediation methods and their limitations

1.3.1 Advanced treatment techniques

To protect our environmental and human health, significant research has focused on advancing remediation strategies. Due to the inherent difficulty of degrading PFAS, new and more effective techniques must be developed. Current techniques used for remediation are primarily removal rather than destruction, which means that PFAS are displaced from the water to another phase rather than degraded *in situ*. These techniques include sorbent-based removal methods such as sorption onto granular activated carbon (GAC) and anion exchange (IX) processes (Cantoni et al. 2021; Cheng et al. 2025). Both sorbent-based approaches will eventually become saturated by the matrix present in the water, including both PFAS and other chemicals, meaning that there is a need for the regeneration or replacement of the sorbents. In the case of GAC, the sorbent is typically transported to a separate facility and regenerated thermally (Vakili et al. 2024). Similarly, IX resins require regeneration using large volumes of chemical solutions, often involving organic solvents (Ellis et al. 2025). Besides GAC and IX, a wide range of alternative sorbent materials is currently being developed for the removal of PFAS (Li et al. 2023a).

Other non-destructive techniques aim to concentrate and reduce the volume of contaminated water instead of transferring PFAS onto a solid media. Examples include reverse osmosis, nanofiltration, and foam fractionation. Reverse osmosis and nanofiltration use membranes to separate water and solute from each other, resulting in a small volume of highly concentrated reject water. They are very effective techniques with high removal efficiencies, although they are also costly, partly due to membranes fouling over time and maintenance requirements (Appleman et al. 2014; Franke et al. 2021). Foam fractionation operates via a different mechanism, exploiting the surfactant properties of PFAS. Air is introduced into contaminated water, causing PFAS to adsorb at air-water interfaces and accumulate in rising bubbles. The resulting PFAS-rich foam can be collected and then collapsed, yielding a low-volume, high-concentration waste stream (McCleaf et al. 2021; Smith et al. 2022). Despite their effectiveness, these removal techniques share one major drawback: they generate secondary waste streams that require further treatment or disposal. This challenge highlights

the need for the development of advanced destructive treatment technologies capable of fully mineralising PFAS.

1.3.2 Advanced destructive treatment techniques and the analytical knowledge gap

To truly remediate PFAS they must be destroyed and ultimately mineralised to inorganic fluorine. This is exceptionally difficult, as the carbon-fluorine bond is one of the strongest bonds in organic chemistry (Moody & Field 2000). Consequently, new techniques are currently in development to degrade PFAS, and three specific techniques will be discussed briefly herein, as they are the primary techniques explored in this thesis (Table 1).

Table 1. List of three selected advanced destructive treatment techniques that are under development, including their primary mechanism and related key drivers.

Technique	Primary mechanisms	Key reactive drivers
Electrochemical oxidation	Oxidation (and reduction) at electrode surface	Hydroxyl radicals; direct electron transfer
Photochemical degradation	Photolysis; redox reactions	Hydrated electrons; reactive oxygen species
Plasma treatment	Thermal and non-thermal decomposition	High-energy electrons; radicals

The first technique is electrochemical oxidation, which uses electricity to drive oxidation reactions at electrode surfaces. Although the exact mechanism for the degradation of PFAS is still not fully agreed upon, it is commonly proposed that the process is driven mainly by direct electron transfer at the anode surface (Veciana et al. 2022). This creates a radical on the headgroup of the PFAS which initiates the defluorination reaction. Once the PFAS has become a radical, it becomes vulnerable to other reactive species present in the matrix. This whole process is then repeated as a stepwise defluorination reaction. One of the reactive species that are created by electrochemical oxidation is the hydroxyl radical. This radical is also generated at the anode surface and may then facilitate the defluorination (Veciana et al. 2022). Other hypotheses describing electrochemical oxidation pathways suggest other reactive species may facilitate the defluorination, including $O_2^{\bullet-}$ and $SO_4^{\bullet-}$ radicals (Veciana et al. 2022; Mirabediny et al. 2023). It is also possible to use this technique under reductive conditions. When performing electrochemical reduction, direct electron transfer is still

considered the main pathway (Yin et al. 2025). A PFAS may initially lose a fluorine atom at the cathode and form a radical, which then will gain another electron to form an anion, and then once back in aqueous phase, abstract a hydrogen from a H_2O molecule to create a hydrogen-substituted PFAS. This substitution may, in turn, facilitate further defluorination.

The second technique is photochemical degradation. This process mainly utilises ultraviolet (UV) radiation to generate hydrated electrons from H_2O molecules. These hydrated electrons can then attack the PFAS and exchange fluorine for hydrogen atoms, which then makes the PFAS susceptible to further reactions such as chain-shortening and additional hydrogen-fluorine substitutions. However, there are discussions on whether the hydrogen-fluorine substitution may strengthen adjacent carbon-fluorine bonds (Liu et al. 2021). The hydrated electron can reductively degrade PFAS due to its very strong reduction potential (E^o = -2.9 V, vs. standard hydrogen electrode) (Park et al. 2009). It is also a relatively long-lived species that has a half-life of $\sim 10^2$ µs. This can be compared to hydroxyl radicals and sulfate radicals that have half-lives of $\sim 10^{-3}$ and $\sim 10^1$ µs, respectively (Mukherjee et al. 2023). For a carbon-fluoride bond to break through reduction, a reduction potential more negative than -2.7 V needs to be achieved. The hydrated electron has a reduction potential more negative than -2.7 V and has a relatively long half-life, making it ideal for reducing PFAS. To increase the production of hydrated electrons, reducing agents may be used. A common reducing agent is sulfite, which can generate hydrated electrons when exposed to UV radiation (Mukherjee et al. 2023). Although this is a promising method, the efficiency of UV degradation is affected by the headgroup of the PFAS, with the carboxylic acid headgroup generally being more favourable for UV degradation than the sulfonic acid headgroup. Furthermore, the chain-length of the PFAS may also affect the defluorination (Bentel et al. 2019).

The third technique, plasma degradation, does not rely solely on one degradation pathway, i.e. oxidation or reduction, instead it uses both. It generates oxidative species such as hydroxyl radicals and reductive species such as hydrated electrons (Singh et al. 2021). The plasma itself is generated by an electrical discharge between two electrodes applied to a foam formed from argon gas. Samples are placed in a container where argon gas is

dispersed. The argon bubbles transport the contaminants to the surface and into the foam. An electric discharge can then ionise the gas-phase argon, generating plasma, which in turn interacts with the foam layer. It is in the foam layer that the reactive species are generated and can react with the PFAS (Stratton et al. 2017; Li et al. 2023b). Due to the many different reactive species, it is difficult to pinpoint exactly which process primarily drives PFAS degradation in this treatment technique. However, the bubble-foam interface is particularly advantageous for PFAS treatment. This mechanism is similar to that of foam fractionation, a technique which also disperses gas in contaminated samples to generate a highly concentrated PFAS foam (Smith et al. 2022).

To summarise, all three methods can degrade PFAS. Electrochemical oxidation uses primarily oxidation through direct electron transfer, UV primarily relies on hydrated electrons, and plasma uses various reactive species and mechanisms. The efficiency of these methods, as measured by targeted analysis, usually depends on the chain-length of PFAS as well as their headgroup. Sometimes treatment trains are implemented to reduce the overall volume that is treated. Pre-concentration steps such as foam fractionation or membrane techniques may give a concentrated waste stream with lower volumes to treat (Lu et al. 2020). These techniques are not yet standardised or implemented at full-scale. Further considerations regarding energy consumption, scope of the treatment, degradation efficiency, and transformation products (TP) formation must be considered before scaling up from a laboratory scale (Junker et al. 2025).

Commonly, the success of a treatment technique is evaluated using targeted analytical methods. Such methods rely on the use of analytical standards. Combining advanced sample preparation with analytical methods such as liquid chromatography coupled to tandem mass spectrometry (LC-MS/MS) can provide sensitive, precise, and accurate quantification (Taylor & Sapozhnikova 2022). However, the main limitation of these methods is that only pre-defined target compounds can be detected and quantified. If TPs are formed during treatment and corresponding analytical standards are unavailable, these compounds will remain undetected.

One approach to overcome this limitation is to measure the total PFAS using total oxidisable precursor assay (TOPA) (Houtz & Sedlak 2012). Using the TOPA it is possible to convert precursors into their terminal forms, i.e., legacy PFSA and PFCA. However, this method does not cover all PFAS and does not identify exact precursor structures. Another method is to analyse extractable organic fluorine (EOF) using combustion ion chromatography (Kaiser et al. 2021). However, such approaches provide only total fluorine measurements, indicating the fraction of fluorine not accounted for by targeted LC-MS/MS analysis.

While informative, these bulk measurements do not provide structural or mechanistic insight into the identity of unknown compounds, thereby limiting our ability to fully understand PFAS degradation pathways (Smith et al. 2024). This analytical gap highlights the need for complementary approaches capable of identifying unknown TPs and elucidating degradation mechanisms.

1.4 The shift to untargeted analysis

Environmental analytical chemistry increasingly requires approaches beyond the use of authentic analytical standards, as environmental matrices are highly complex and the number of potential analytes are too many to be comprehensively covered by targeted methods. The degradation of PFAS needs to be investigated in detail, and identifying TPs is essential for both optimising degradation processes and understanding the underlying reaction mechanisms. However, this is inherently not possible with traditional targeted analysis, hence there is a need for the development of new analytical strategies. This limitation can be overcome through the use of high-resolution mass spectrometry (HRMS). This state-of-the-art mass spectrometric instrumentation presents the opportunity to explore a chemical space that was previously unknown. By acquiring high-resolution accurate mass (HRAM) data, it becomes possible to derive molecular formulas and generate structural information (Kind & Fiehn 2007). The data obtained from HRMS is extremely complex, and one set of samples may result in thousands of features per sample. Combining HRMS with advanced data-processing workflows facilitates the prioritisation and identification of relevant compounds, effectively enabling the detection of the proverbial “needle in

the haystack". This approach allows for the detection of compounds for which no authentic standards exist, including previously unreported compounds. New methods for PFAS analysis using software are quickly developing and what used to be a novel method just a few years ago is standard practice today (Gago-Ferrero et al. 2015; Koelmel et al. 2020; Getzinger et al. 2021; Bugsel et al. 2023). Without untargeted analysis, uncharacterised chemical releases can expose ecosystems and human populations to entirely undetected threats. Untargeted approaches, including suspect and non-target screening have become more popular in recent years, but these methods are rarely combined with the development of treatment techniques and evaluation of PFAS treatment technologies remains limited.

2. Aims and objectives

This PhD thesis aims to advance the field of environmental remediation by integrating HRMS analysis with advanced destructive treatment techniques. By developing analytical techniques using state-of-the-art instrumentation and software, this thesis aims at detecting and identifying TPs to aid in future endeavours to optimise and improve treatment technologies. Ultimately this work aims to reduce PFAS contamination and mitigate the associated environmental and health risks. A summary of the findings and can be seen in Figure 2.
The papers presented in this thesis, in the form of published articles or manuscripts, had the following goals and sub-goals:

I. Develop an in-house methodology for the screening and identification of PFAS using untargeted analysis techniques (**Papers I & II**)

    i. Create a suspect and non-target screening workflow applicable to a wide range of environmental matrices
    ii. Identify points of improvement to enable continuous methodological refinement

II. Identify TPs across different advanced destructive treatment processes (**Papers II, III & IV**)

    i. Detect and identify TPs associated with specific treatment processes and degradation pathways
    ii. Propose structurally plausible candidates for newly identified compounds

III. Evaluate the toxicity and environmental hazard of identified TPs (**Papers II, III, & IV**)

    i. Assess whether overall toxicity changes before and after treatment
    ii. Evaluate the relative toxicity of individual TPs and their potential environmental impact

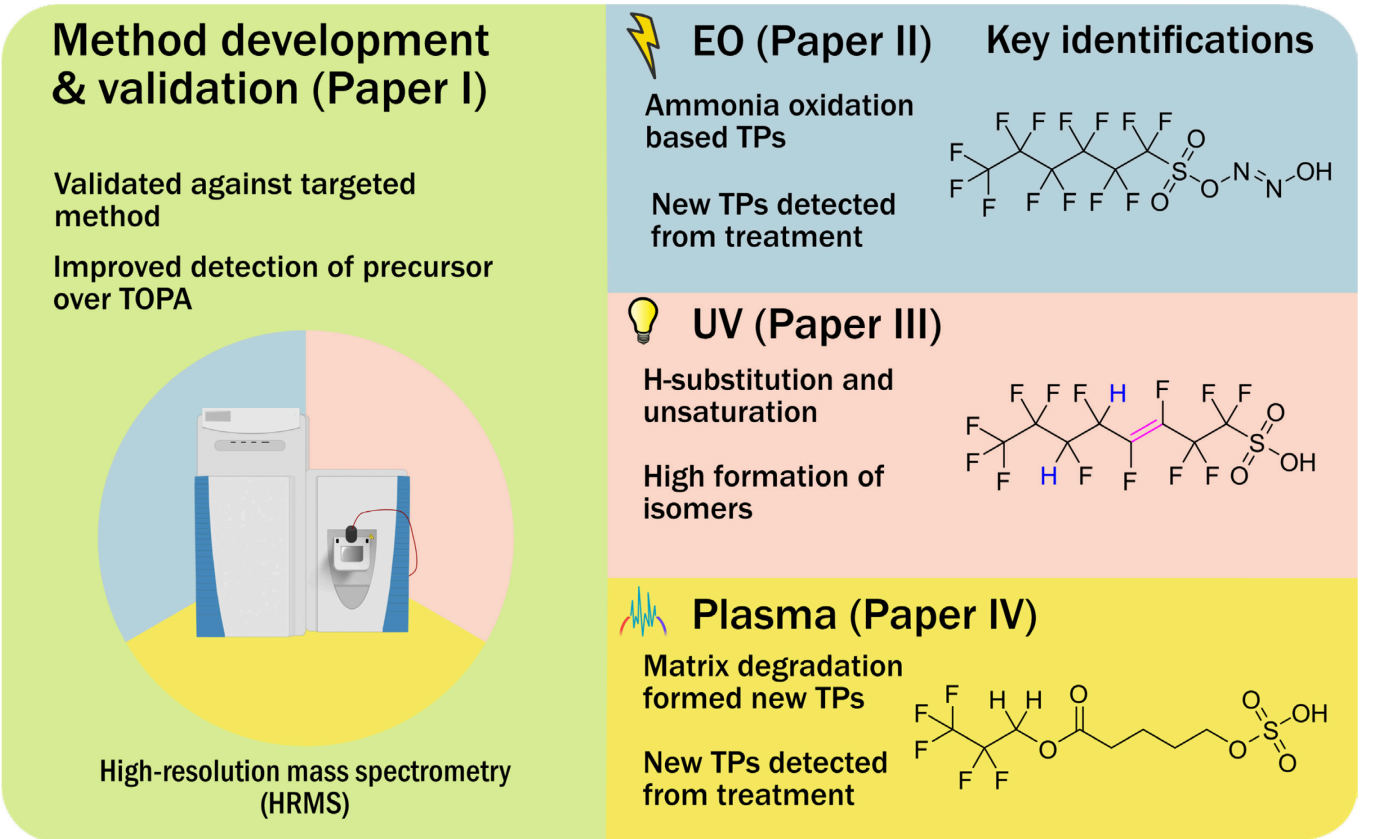

Figure 2. Summary of key findings from each paper and aims in the thesis as well as key identified PFAS

3. Materials & Methods

3.1 Tested treatment technologies

Three different treatment techniques were investigated in this thesis: electrochemical oxidation (**Paper II**), photochemical degradation (**Paper III**), and plasma degradation (**Paper IV**). All three techniques were monitored using time series to assess the evolution of TPs over time. All treatment technique experiments were performed by collaborating researchers (**Paper II**) and external research groups (**Papers III and IV**). Treatment techniques were performed on real in-field samples (**Papers II and IV**) and samples produced in the laboratory by spiking water with PFAS standards (**Paper III**).

3.2 Sample preparation

Solid-phase extraction was used for samples with low concentrations of PFAS and was performed using weak-anion exchange cartridges (**Papers I and II**) according to validated extraction protocols (Gobelius et al. 2018). Samples produced from UV degradation were directly injected on the instrument with no prior sample preparation (**Paper III**). Plasma-treated samples were diluted tenfold before injection into the instrument because of predicted high levels of PFAS (**Paper IV**).

3.3 Instrument analysis

3.3.1 Targeted analysis

The targeted analysis was performed using an AB SCIEX ExionLC TripleQuad 3500 system which is a LC-MS/MS system (**Papers I and II**). The method was developed and validated by another researcher in the group and is described in detail in their published article (Smith et al. 2022). Instrument parameters for each compound analysed was optimised by adjusting the declustering potential, collision energies, and collision cell exit potentials. The calibration curve was an external calibration curve with 10 points including stable isotope labelled internal standards.

3.3.2 Untargeted analysis

The analyses (**Papers I, II, III, and IV**) were performed on a Vanquish Horizon liquid chromatography system coupled to a QExactive Focus Orbitrap mass spectrometer (Thermo Fisher Scientific, Bremen, Germany). The samples (10 µL) were injected in triplicate on the system with a LC TriPlus RSH autosampler (CTC Analytics, Zwingen, Switzerland). Chromatographic separation of the samples was performed on a Waters ACQUITY UPLC BEH C18 (1.7 µm, 2.1 x 50 mm) analytical column, equipped with a Waters ACQUITY UPLC BEH C18 VanGuard pre-column. The column temperature was held at a constant 40 ºC. The mobile phases used consisted of ultrapure water generated with a purification cartridge (Milli-Q, and Milli-Q LC-Pak) with 5 mM ammonium acetate as solvent A and LC-MS grade methanol (LiChrosolv, Merck) with 5 mM ammonium acetate as solvent B with a flow of 0.3 mL/min and the gradient program is provided in Table 2. The samples were ionised in negative ion mode (ESI-) on an Ion Max heated electrospray ion source (HESI-II, Thermo Fisher Scientific). The ion source settings are detailed in Table 3.

Table 2. Mobile phase gradient program used for the untargeted analysis using LC-HRMS

Time (min)	% Solvent A	% Solvent B
0.00	90	10
1.00	90	10
13.00	5	95
15.00	5	95
15.10	90	10
17.00	90	10

Table 3. Ion source settings (ESI-) used in all experiments

Parameter	Value
Sheath gas flow rate (a.u.)	45
Auxiliary gas flow rate (a.u.)	10
Sweep gas flow rate (a.u.)	0
Spray voltage (kV)	-2.7
Capillary temperature (ºC)	300
S-lens RF level (a.u.)	50
Auxiliary gas heater temperature (ºC)	400

The mass spectrometer was set to acquire MS^1 data in a range from 100 to 1000 *m*/*z*. Acquisition was performed with a resolving power of 70 000 at 200 *m*/*z* with an automatic gain control (AGC) target set to 1 x 10^6 a.u. Maximum ion trapping time was set to automatic, and data were acquired using a single microscan. The spectrum data type was set to profile mode.

For MS^2 data acquisition, the instrument was set to obtain data using the data-dependent acquisition (DDA) mode (Discovery mode). The resolving power was set to 35 000 at 200 *m*/*z*. Stepped collision energies of 10 and 30 eV were applied. For consistent acquisition of mass spectra, the ion trapping time was set to a maximum of 100 ms. To maximise the amount of MS^2 data acquired per analysis, the loop count was set to the maximum value of 3. The intensity threshold was set to 2.0 x 10^4 and the dynamic exclusion was set to 3 s.

The isolation window and isolation offset were optimised for obtaining as pure MS^2 spectra as possible for PFAS with few impurities. This was done by setting the isolation window to 0.5 *m*/*z* and the isolation offset to -0.2 *m*/*z*. This is further discussed and explained in Section 3.5.3 (MS^1 based non-target strategies).

The instrument was always calibrated before use, and for ensuring that the acquisition of HRAM was of high quality an internal system suitability test (SST) was developed and is described in detail elsewhere (Löffler et al. 2025). After calibrating the instrument, the SST solution was injected to ensure that the calibration was performed successfully. The acquired HRAM

were compared to the monoisotopic masses of the chemicals present in the SST solution and mass accuracy was recorded in mass deviation expressed as a difference of parts-per-million (ppm) *m*/*z*. If the mass accuracy was within the set ±3 ppm threshold, the SST was considered passed; if above these thresholds the system was recalibrated. The SST solution was also injected post-analysis to ensure that a mass accuracy drift had not occurred during the time of analysis.

Blanks included field blanks, laboratory blanks, solid-phase extraction blanks, and instrument blanks.

3.4 Software

3.4.1 Compound Discoverer

Compound Discoverer (CD) (Thermo Fisher Scientific, California) was the main software used for the small molecule feature detection and identification in this thesis. The software performs peak picking, feature grouping, blank subtraction, peak rating, and contains many automated compound identification tools that can be customised according to the research objectives. Throughout the PhD project the software has been updated regularly, and with each update new tools and functions became available. The different versions used in the PhD thesis were CD 3.3 (**Paper I**), CD 3.4 (**Papers II and, III**) and CD 3.5 (**Paper IV**).

3.4.2 FluoroMatch

FluoroMatch is a software developed by the Innovate Omics Group and was first published in 2020 (Koelmel et al. 2020). It is freely available and open source. When it was released, no comparable software existed that was free, open-source, and designed for the untargeted analysis of PFAS. A notable feature that was unique to FluoroMatch at the time of release was the PFAS fragment library, which includes annotated *m*/*z* obtained from fragmenting PFAS. This library is a very powerful tool for prioritising features when performing untargeted PFAS analysis. The fragment library was later adapted and incorporated into the Compound Discoverer workflow in the CD 3.3 SP2 update (Tautenhahn 2023).

3.4.3 Toxicity prediction software

In **Papers III and IV**, *in silico* software for toxicity predictions were used to evaluate the relative environmental toxicity of identified PFAS and PFAS TPs. The two software used were VEGA (**Paper III)** and TRIDENT (**Papers III and IV**) (Danieli et al. 2023; Gustavsson et al. 2026).

3.4.4 R and R-studio

In **Papers I, II, III, and IV**, R and R-studio were used to wrangle data, make the in-house code for identifying homologous series, and for making figures (R Core Team 2025). In addition to base R and R-studio, the tidyverse package was used in all codes written (Wickham et al. 2019).

3.5 Untargeted strategies

3.5.1 Communicating confidence

Untargeted analysis does not rely on the use of analytical standards but can incorporate them to improve confidence in an identification of a compound. However, due to the nature of the wide scope of suspect and non-target screening approaches, analytical standards are often unavailable for many detected features. To be transparent in compound identification, confidence levels are assigned to each feature. In 2014, a level system for communicating the confidence of an identification was proposed (Schymanski et al. 2014). This system was further developed and specialised for communicating confidence when identifying PFAS (Charbonnet et al. 2022). An adapted and simplified overview of these confidence levels is presented in Table 4. All confidence levels presented in this thesis and **Papers I, II, III, and IV** follow this way of communicating the confidence of identifications.

Table 4. Adapted simplified table of the different confidence levels for identifying PFAS (Charbonnet et al. 2022)

Level	Identification Confidence
1a	Confirmed by reference standard
1b	Indistinguishable from reference standard
2a	Probable by library spectral match
2b	Probable by diagnostic fragmentation evidence
2c	Probable by diagnostic homologue evidence
3a	Positional isomer candidates
3b	Fragmentation-based candidate
3c	Circumstantial candidate with fragmentation evidence
3d	Circumstantial candidate with homologue evidence
4	Unequivocal molecular formula
5a	PFAS suspect screening exact mass match
5b	Nontarget PFAS exact mass of interest

3.5.2 Suspect screening

Suspect screening is the most effective method to screen environmental samples for large numbers of known or expected chemicals using HRMS. The HRAM acquired are compared to a list of recorded monoisotopic masses calculated from molecular formulas of known compounds (Krauss et al. 2010). This is the first step beyond targeted analysis, as it eliminates the need for analytical standards and instead relies on curated suspect lists containing molecular formula information. There are many efforts to provide up-to-date and high-quality suspect lists for the scientific community. One such effort is the NORMAN Suspect List Exchange (SLE) which is an online and publicly available database of suspect lists (Mohammed Taha et al. 2022). The NORMAN Substance Database (SusDat) is a database that has gathered the information about each compound that can be found in all the featured suspect lists. It enables users to customise a suspect list by selecting one or several classes of compounds and/or suspect lists and then downloading all that information for local use. This database is continuously updated as new suspect lists and compounds are added to the SLE.

In this PhD thesis, two types of suspect screening approaches were utilised: offline and online suspect screening. Offline suspect screening refers to the

use of pre-defined locally stored suspect lists curated by the researcher, containing compounds relevant to the study. In contrast, online suspect screening utilises real-time matching of HRAM data against external databases via internet access, rather than relying solely on local files. An example of such a database is the EPA DSSTox database, a curated resource of environmentally relevant and potentially toxic compounds (CCTE 2025).

In **Paper I** the following databases were used for matching compounds: EPA DSSTox, EPA Toxcast, FDA, MassBank, MolBank, PubMed, Royal Society of Chemistry, and Sigma-Aldrich. For **Papers II, III, and IV** only EPA DSSTox was used as an online database.

For suspect screening it is also possible to take advantage of online databases for fragmentation evidence. In this thesis, three such databases were used: mzCloud (Thermo Fisher Scientific, California, USA) (**Papers I, II, III, and IV**), an online database containing recorded MS^2 spectra for thousands of compounds; MassBank (EU) (**Papers II, III, and IV**) and MassBank of North America (**Papers II, III, and IV**), both of which are community-driven repositories for mass spectrometric data.

The offline suspect lists used in this thesis can be divided into two categories:
1. List of known compounds verified by one or more sources.
2. List of compounds generated using *in silico* tools.

The suspect lists in the first category were obtained from the NORMAN SusDat system (**Papers I and II**), the NIST PFAS suspect list (**Papers II, III, and IV**), the CompTox EPA PFAS list (**Papers II, III, and IV**), and a suspect list made by Thermo Fisher adapted from previous untargeted PFAS literature (**Papers II, III, and IV**) (Barzen-Hanson et al. 2017).

The second category consisted of an *in silico*-generated suspect list derived from the literature (Getzinger et al. 2021). This suspect list was produced to widen the scope of suspect screening by generating predicted TPs that could then be included in suspect screening studies. Since this thesis focuses on TPs it was included as a suspect list in **Papers II, III, and IV**.

3.5.3 MS^1 based non-target strategies

While suspect screening uses HRMS to identify previously known or expected compounds, non-target screening aims to detect true unknown compounds present in a sample. As no prior information is available of these compounds, additional prioritisation strategies beyond exact mass matching are required. A summary of the strategies is displayed in Figure 3.

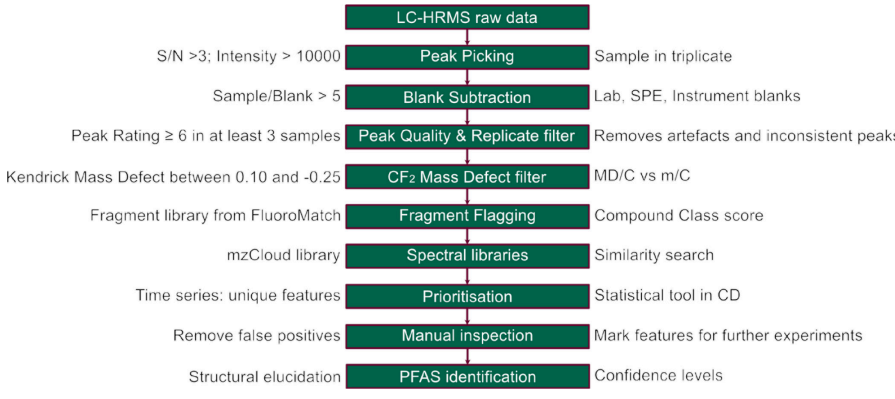

Figure 3. Summary of the workflow for analysis of PFAS using non-target screening

In this thesis, a couple of strategies were used to take advantage of the unique chemical properties of PFAS to improve the non-target screening. These approaches mainly taking advantage of the unique mass defect of fluorine. Fluorine has a monoisotopic mass of 18.998403 Da, which results in PFAS often having monoisotopic masses where the first decimal is a nine, meaning the nearest nominal mass would necessitate rounding up. Comparatively, a hydrocarbon's nearest nominal mass would necessitate rounding down. For example, the two molecules CF_4 (87.99361 Da) and CH_4 (16.03130 Da) illustrate this difference. This property can be exploited during feature prioritisation which is called Kendrick Mass Defect (KMD) approach, where most organic compounds have positive KMD values and PFAS have a close-to-zero to negative KMD values (Kendrick 1963; Barzen-Hanson et al. 2017).

One application of KMD is the calculation of CF_2-adjusted KMD values for all detected features during processing of the raw data, allowing for the removal of features that do not fall within the typical PFAS thresholds. This

reduces the total number of features considerably during the suspect and non-target screening process.

A second application of KMD is the identification of homologous series. Once the data has been processed and a feature list has been created it can be analysed using an in-house written R script (Rehnstam 2023). An example of homologous series plotted from the results obtained in **Paper I** can be seen in Figure 4 (Rehnstam et al. 2023).The script identifies compounds that differ by a CF_2 or C_2F_4 moiety and have a CF_2-adjusted KMD difference of 0.001 or less and then groups them together. It also included two constraints including increasing retention time with increasing *m/z* and a requirement that the deviation between the theoretical and observed addition/loss of CF_2 or C_2F_4 did not exceed 0.001 *m/z*.

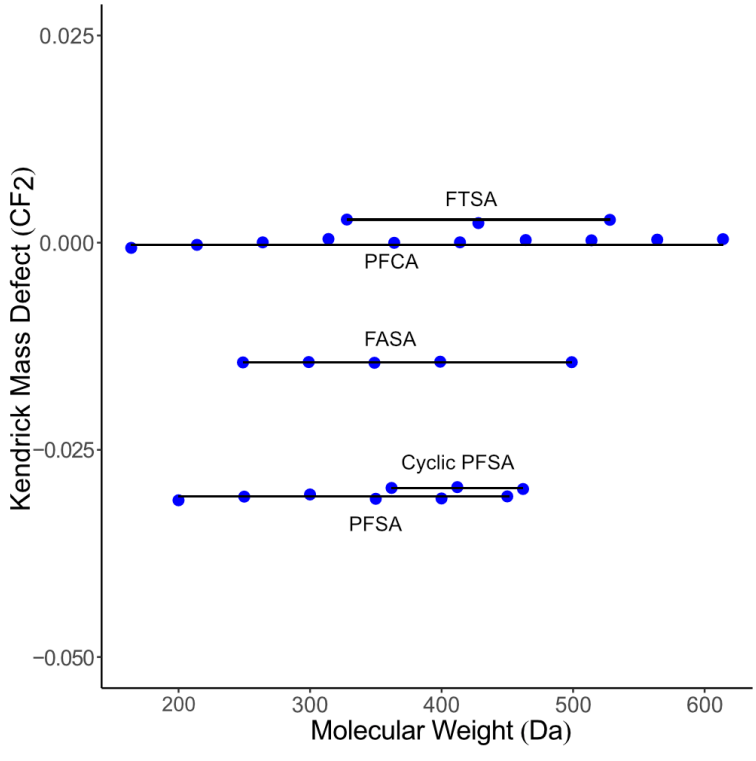

Figure 4. A KMD plot with the results from **Paper I** (Rehnstam et al. 2023) with permission from Elsevier. The plot displays five different classes of PFAS and their different homologues detected.

A third approach, also based on KMD, which was originally developed for simplifying complex food matrices using suspect and non-target screening (Kaufmann et al. 2022). This method calculates two parameters: mass defect per carbon atom (MD/C) and mass-to-carbon ratio (m/C). These two values are plotted against each other, with MD/C on the y-axis and m/C on the x-axis, for all detected features. The number of carbons in each feature is calculated based on the relative abundance of the first two isotopic peaks. Within this plot, a region defined by -0.05 to 0.025 on the y-axis (MD/C) and 10 to 100 on the x-axis (m/C) has been shown to be characteristic for PFAS (Zweigle et al. 2023).

This approach is not only used for data processing and prioritisation of features but can also be exploited when acquiring MS^2 data for PFAS. Since most PFAS will have a negative KMD, setting the offset to -0.2 *m*/*z* and the isolation window to 0.5 *m*/*z* results in preferential selection, where the mass spectrometer captures ions 0.05 *m*/*z* above the precursor ion and 0.45 *m*/*z* below the precursor ion (Figure 5). This strategy is expected to reduce the number of impurities present in a MS^2 acquisition, as most natural organic compounds have a positive KMD (Qi et al. 2022).

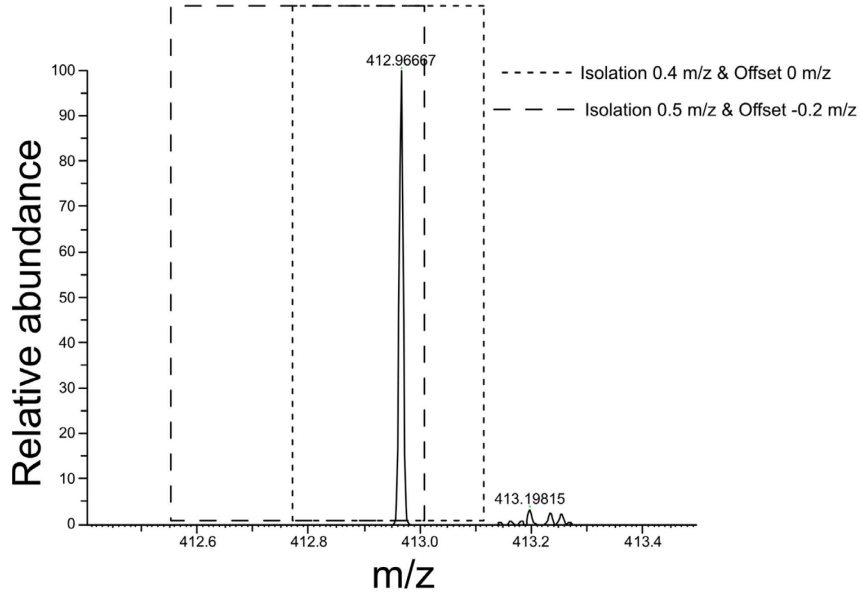

Figure 5. Settings for MS^2 acquisition, illustrating difference in offset and isolation window parameters.

3.5.4 MS^2 based non-target strategies

Maximising MS^2 coverage in suspect and non-target screening provides more comprehensive structural information and reduces the need for additional MS^2 experiments. To improve initial MS^2 data coverage before data processing, the IE Omics R script from Innovate Omics was used (Koelmel et al. 2017). This R script generates exclusion lists to trigger DDA events for lower-intensity signals, generating more MS^2 data with minimal additional effort.

When using Compound Discoverer, in addition to performing an "identity search" it is also possible to perform a "similarity search". Since there is no monoisotopic mass match performed in a similarity search, this makes it only match individual fragments from the acquired data with fragments from mzCloud's entire library. This feature may assist connecting fragments with specific structures or functional groups.

Fragment flagging was utilised to prioritise features that could potentially be PFAS when performing the suspect and non-target screening. The fragments that were obtained from the FluoroMatch suite had been adapted to work in the CD workflow following the CD 3.3 SP2 update (Koelmel et al. 2020; Tautenhahn 2023). This approach provided a fast and reliable way to prioritise PFAS-related features. Since PFAS are compounds with high degrees of fluorination, PFAS generate characteristic fragments that are distinctly unique to the substance class. However, some fragments present in the list were not exclusively unique to PFAS but also may be present in other substances classes. One such example was the SO_3^- fragment that can be observed in multiple substance classes. In the CD workflow this functionality is called the Compound Class scoring system, where each feature with MS^2 data is assigned a score. A score greater than 0 indicates that at least one diagnostic fragment could be matched to the MS^2 spectrum.

Neutral losses can also be used to prioritise PFAS features using the MS^2 data. Due to the inherent fluorinated backbone of many PFAS, several characteristic neutral losses can be observed. For example, the loss of CF_2 is commonly occurring, similarly to the identification of homologous series. Furthermore, there are fragments to identify perfluoroethers, such as CF_2O moieties which frequently occur for that class. Another example of a

common fragment is the loss of HF which is characteristic for fluorotelomers. The update to CD 3.5 introduced the ability to determine neutral losses between fragment ions, whereas previously this was only possible between the precursor and its fragments. This improvement enhances the interpretation of fragmentation pathways and structural elucidation.

4. Results & Discussion

4.1 Method development of untargeted analysis

For reference, all PFAS classes mentioned in the thesis have an example structure that may be used for reference in Table 5 listed in Section 4.4 "Example structures of PFAS classes discussed in the thesis". For exact structures, see corresponding papers and supporting information where relevant.

4.1.1 Validation of the untargeted workflow against an in-house targeted PFAS method (Paper I)

The method developed and presented in **Paper I** successfully detected nearly all compounds that were also detected in the targeted analysis. The PFAS detected included five PFCAs (C_4–C_8), five PFSAs (C_4–C_8), perfluorethylcyclohexanesulfonic acid (PFECHS), and N-ethyl perfluorooctanesulfonamidoacetic acid (N-EtFOSAA). N-methyl perfluorooctanesulfonamidoacetic acid (N-MeFOSAA) was the only compound not detected as it was present at concentrations close to the limit of quantification (LOQ) of the targeted method and as such was below the limit of detection (LOD) of the HRMS method. This demonstrates that the HRMS method is a robust and reliable approach capable of achieving performance comparable to targeted methods even when applied to complex matrices such as landfill leachate and groundwater (Bugsel et al. 2023).

Additionally, the suspect and non-target screening workflow identified six more PFAS with a confidence level of 3a or higher that were not included in the targeted analysis in landfill leachate and groundwater samples. These compounds were identified by investigating homologous series, as all were homologues of compounds already detected by the targeted method. This showcased that the instrumental method and the software workflow was able to perform suspect and non-target screening of PFAS, while also extending detection beyond the limitations of targeted analysis.

Suspect screening and TOPA were both performed on the same samples in this study to evaluate whether TOPA can be used as sample prioritisation tool. Although there were changes in concentrations observed by using

TOPA, these changes were either negligible or showed decreases after TOPA. If precursors are present, concentrations of legacy PFAS are expected to increase rather than decrease (Houtz et al. 2013). However, it is important to note that TOPA does not transform all precursor compounds, and some PFAS remain unaffected by the assay (Ateia et al. 2023). This is also supported by the results in **Paper I**, where six PFAS standards were subjected to TOPA; PFECHS, perfluoroundecanoic acid, and perfluorotridecanoic acid did not undergo oxidation or transformation. Nevertheless, if a large number of samples are subjected to TOPA and subsequently analysed using targeted methods, the results may help prioritise which samples should undergo non-target analysis.

4.1.2 Detection of PFAS classes before application of destructive techniques

The developed method was applied in **Papers II, III and IV** for suspect and non-target screening of PFAS. In this section, the focus is on the detection of PFAS classes before application of destructive techniques and did not transform as a result of the treatment processes. These compounds are important to consider, as they are often overlooked in targeted analysis and yet contribute to the total PFAS burden in the environment (Smith et al. 2024). In addition to the PFAS discussed in this section, there were also PFAS detected that are normally present in targeted analyses, including PFCAs (C_4–C_{10}) and PFSAs (C_3–C_8). Each following PFAS class is discussed individually to contextualise them in their matrix and the broader environmental perspective.

Perfluoroethylcyclohexanesulfonic acid (PFECHS) was detected in both **Papers I and II**. The two additional homologues (cyclic-PFSA) identified were structurally related compounds with shorter perfluorinated side chains, including a perfluoromethyl analogue and a structure lacking the side chain entirely, and only maintaining its perfluorinated cyclohexanesulfonic acid structure. Despite PFECHS being an eight-carbon PFAS, it is not related to PFOS (De Silva et al. 2011). Notably, whenever this class was detected (**Papers I and II**), the two shorter-chain homologues were also detected, suggesting that they may originate as impurities or degradation by-products from PFECHS. Previous studies have also reported the detection of methylated analogues in the environment when detecting PFECHS (Wang et

al. 2016). In this thesis, both times this class was detected in landfill leachate, indicating a potential link to waste-related sources (**Papers I and II**).

Perfluoroalkyl sulfonamides (FASA) are known intermediates in the degradation of precursors to legacy PFSA and are therefore commonly detected in environmental samples (Zhao et al. 2018; Chen et al. 2022). In **Papers I and II**, several homologues (C_3–C_6, and C_8) not included in the targeted analysis were identified. Since they are precursors and may transform to terminal PFSA or PFCA over time (Rhoads et al. 2008), monitoring their presence is important for understanding PFAS transformation pathways and environmental impact.

Similarly, n-methyl and n-ethyl perfluoroalkyl sulfonamidoacetic acids (N-MeFASAA and N-EtFASAA) are precursors that are prone to degrading into PFSA (Rhoads et al. 2008). The C_8 homologue of N-EtFASAA was detected in **Paper I**, while multiple homologues were identified in **Paper II**. For N-MeFASAA C_3 – C_6 and C_8 homologues were detected and for N-EtFASAA C_4 – C_6 and C_8 homologues were detected. The only homologue included in the targeted method were C_8 compounds (EtFOSAA and MeFOSAA). As with FASA, these compounds should be monitored due to their role as precursors and indicators of upstream contamination sources. This class has also previously been found in surface waters in Europe in other non-target screening studies (Hensema et al. 2021).

The compound that was referred to as PFOCHS (polyfluorooxacyclohexane propane sulfonic acid) in **Paper II** has been reported previously, although with a different proposed structure (Hensema et al. 2021). Previously a fluorotelomer structure was proposed, whereas in this work, a cyclic ether structure with a perfluorinated propylalkane tail has been proposed. In **Paper II**, it was detected in groundwater and landfill leachate, whereas in a previous study it has only been detected in surface water (Hensema et al. 2021), suggesting multiple modes of environmental entry pathways.

Keto-perfluoroalkylsulfonic acids (Keto-PFSA) were detected in **Paper II**. Previous studies have also identified this compound class in environments impacted by AFFF (Baduel et al. 2017; McDonough et al. 2021). It has also

been reported as a TP that may be created during electrochemical oxidation (Schaefer et al. 2018).

More compounds that were connected to AFFF formulations were N-sulfopropyldimethylammonio propyl perfluorohexanesulfonamide, N-sulfopropyldimethylammoniopropyl-perfluorohexanesulfonamido acetic acid, and N-sulfopropyldimethylammoniopropyl perfluorohexane sulfonamidopropylsulfonate. These compounds are abbreviated as N-SPAmP-FHxSA, N-SPAmP-FHxSAA, and N-SPAmP-FHxSAPS respectively (**Paper II**). These compounds were originally identified in suspect screenings performed on AFFF formulations or AFFF impacted waters (Barzen-Hanson et al. 2017). These complex PFAS precursors are known to degrade in the environment to the terminal legacy PFAS such as PFSA and PFCA (Butt et al. 2013).

Bistriflimide was detected in **Paper II**. It is a small molecule used as a reagent and catalyst in organic chemistry synthesis (Zhao & Sun 2018). Its environmental fate is relatively unknown, and further research is needed to assess its persistence and potential environmental impact.

Di-unsaturated PFOS (DUPFOS) was detected in **Paper II**. The mass spectrum did not yield diagnostic ions to determine the position of the double bonds. It has been detected in previous studies analysing AFFF formulations (Luo et al. 2020).

Perfluoroalkyl sulfonamide sulfonic acids (FASASA) were found in **Paper II** and this class has only been detected in one previous study (Ghorbani Gorji et al. 2024), in which the C_6 homologue was detected in AFFF-impacted groundwater. In this thesis, both C_6 and C_8 homologues were identified, showing that several homologues of this class could be present in other AFFF impacted sites.

Another new class of PFAS that was detected in this thesis (**Paper II**) was N-methyl perfluoroalkane sulfonamide sulfinic acid (Me-FASASi). This class has also previously been described in literature, and the findings in this thesis expand on earlier work by identifying homologues that had not been detected before. While previous studies reported only C_6 and C_8 homologues

(Dewapriya et al. 2023), this study identified C_4, C_5, and C_6 homologues. Furthermore, the findings in literature were based on blood samples from cattle, whereas in this thesis the compounds were detected in groundwater and landfill leachate, suggesting environmental persistence in nature or multiple transformation pathways.

These findings indicate a need for better methods for wide-scope screening. As many of these compounds were either detected through suspect screening or non-target screening, this underscores the current lack of understanding of the total PFAS burden in environmental waters (Jeong et al. 2022). Comparatively, conventional targeted methods appear insufficient for comprehensive PFAS assessment. However, untargeted analysis is still less developed than targeted analyses. There are efforts at harmonising and standardising reporting and methods in suspect and non-target screening studies to reach comparable reliability and acceptance as targeted studies (Hollender et al. 2023). Improved harmonisation will also facilitate more effective communication with legislators and other stakeholders (Dulio et al. 2024).

4.2 Detection of transformation products (TPs)

4.2.1 Electrochemical oxidation (**Paper II**)

The electrochemical oxidation of groundwater and landfill leachate led to the discovery of previously unreported TPs and revealed unexpected degradation pathways. Following detection and elucidation of the structure of selected TPs, it became evident that the matrix plays a large role in determining which TPs may form (Horst et al. 2020).

This was particularly highlighted by the discovery of the new class of compounds that was named perfluoroalkane sulfonhyponitrite (FASHN). This class of compound was initially discovered through fragment flagging, where the base peak of the MS^2 spectrum corresponded to the *m*/*z* of perfluorohexanesulfonic acid (PFHxS). This initially suggested the formation of an adduct during ionisation, followed by dissociation under higher-energy collision-induced dissociation. However, comparisons of retention time revealed no overlap, indicating that the signal originated from

a distinct compound rather than a mass spectrometer artefact. Further inspection of the mass spectrum revealed a neutral loss corresponding to N_2O. Discovering this neutral loss and its progressive formation over the course of electrochemical oxidation confirmed its identity as a TP. The head group was subsequently investigated through literature, where a structurally related moiety was identified in an early study published in 1935 describing intermediates in the oxidation of ammonia to nitrous acid (Corbet 1934).
Paper II builds upon a previous study that performed a comprehensive chemical analysis of the treated samples, including measurements of ammonia before and after treatment. The presence of ammonia and the identification of a hyponitrous acid functional group led to the hypothesis that incomplete oxidation of ammonia produced reactive intermediates that subsequently reacted with PFAS to form FASHN. This may have occurred following the direct electron transfer to PFAS at the cathode. At this stage, the PFAS molecules become highly susceptible to attacks by reactive species, which in this case may have been the hyponitrous acid. In addition to PFAS analysis, brominated and chlorinated compounds were identified using suspect screening. Among these, two of the chlorinated and one of the brominated TP compounds contained nitro and dinitro functional groups. This further supported the hypothesis that oxidised nitrogen species derived from ammonia participated in reactions with organic chemicals in the matrix.

Another class that was identified and that may be an intermediate was N-methanol perfluoroalkyl sulfonamide (MeOH-FASA). In contrast to FASHN, the formation of this TP can be explained more straightforwardly. The longer alkylated functional groups of AFFF-derived PFAS are more prone to degradation, on the basis that they are not perfluorinated, and therefore require less energy to undergo transformation. This class was first detected at the initial stage of treatment, and subsequently decreased in intensity over time, supporting its role as an intermediate product. Nonetheless, this finding is important, as it highlights that for any degradation technique, incomplete degradation processes can lead to the formation of short-lived TPs.

The detection of hydrogen-substituted PFSA (H-PFSA) was an unexpected finding. Electrochemical oxidation mainly relies on oxidative mechanisms, whereas hydrogen substitution is typically associated with reductive

degradation pathways (Sun et al. 2018). Although oxidation occurs at the anode via direct electron transfer, simultaneous reduction may still occur at the cathode potentially explaining this observation (Yin et al. 2025).

Finally, perfluoroethersulfonic acids (PFESA) were also detected as TPs. However, depending on the sample type, these compounds were sometimes already present prior to treatment, complicating their interpretation as solely transformation-derived products. PFESA have been previously detected in freshwater downstream of wastewater treatment plants (Strynar et al. 2015).

To the best of our knowledge, the work performed in **Paper II** represents a unique showcase of electrochemical oxidation applied to real samples and then subjected to comprehensive untargeted analysis, with only one comparable study reported in the literature (Schaefer et al. 2018). To broaden the scope of this research, the subsequent investigations presented in **Papers III and IV** explore additional advanced destructive treatment technologies in collaboration with other research groups.

4.2.2 Ultraviolet treatment with and without reductants (**Paper III**)

The study in **Paper III** was conducted using a controlled laboratory system rather than real wastewater. Ultrapure water was spiked with PFOS and then treated with UV radiation, both with and without Na_2SO_3 as an additional source of hydrated electrons. It is important to note that the presence of dissolved oxygen and dissolved organic matter can reduce PFAS degradation efficiency due to competing degradation processes and UV absorption by the matrix (Mukherjee et al. 2023). The UV treatment in this study did not result in the identification of novel PFAS classes. Instead, the formation of TPs mainly resulted from two mechanisms: chain-shortening and hydrogen-substitution, occasionally in combination. These pathways are known mechanisms and are expected to occur during degradation of PFAS using UV treatment (Tan et al. 2025).

The main discovery of **Paper III** was the high formation of multiple isomers. For hydrogen-substituted PFOS (H-PFOS) there were a total of six isomers that were baseline separated. Computational chemistry calculation of bond dissociation energies suggest that only five different locations are energetically favourable for hydrogen substitution in PFOS (Bentel et al.

2019). The second key finding in this study was the identification of a previously undetected TP for this specific treatment system, namely di-hydrogen-substituted and unsaturated PFOS (H_2-UPFOS). While previous studies have reported hydrogen-substituted and unsaturated PFOS individually (Bowers et al. 2023), this is the first observation of a compound exhibiting both di-hydrogen substitution and unsaturation simultaneously. The extensive isomerisation observed has received limited attention in the literature. To evaluate whether the various isomers exhibit different toxicological properties, *in silico* toxicity predictions were performed, as discussed further in Section 4.3. Having characterised the complex isomerisation induced by UV irradiation, the focus of the PhD project was subsequently extended to plasma-based degradation techniques.

4.2.3 Plasma treatment of industrial wastewater (**Paper IV**)

The suspect and non-target screening of three industrial wastewater samples treated with plasma led to the detection of one new class of PFAS TP, which was named two-to-one fluorotelomer ether (2:1-FtE). This nomenclature indicates that the alkyl chain preceding the ether linkage consists of a C_2F_5 and CH_2 group. In total, five different 2:1-FtE compounds were detected.

An important finding was that the 2:1-FtE followed only partial homologous behaviour. While the 2:1-FtE backbone and the sulfuric acid headgroup remained consistent, the overall molecular formula did not follow a clear homologous series pattern. This suggests that 2:1-FtE compounds were not formed via simple matrix-driven reactions but rather originate from the degradation of larger precursor molecules. Furthermore, these compounds may derive from substances of unknown or variable composition, complex reaction products, or biological materials (UVCBs) (Lai et al. 2022), which could explain their variable chemical composition. In summary, the detection of the 2:1-FtE compounds suggests that it is important investigating also existing complex substances during plasma treatment, besides entirely new molecular structures. To the best of my knowledge, this is the first report of such TPs identified in plasma-treated degradation of real wastewater samples. Previous studies investigating plasma degradation pathways have largely been conducted in simplified matrices (Singh et al. 2019), highlighting the importance of applying non-target analysis to complex environmental samples.

Chain-shortening was also observed as a degradation pathway during plasma degradation. This was supported by the detection of PFOA at the initial time point (t = 0), followed by its disappearance, alongside the appearance of shorter-chain PFCAs at later time points. Other TPs identified included C_5 and C_7 hydrogen-substituted PFCAs (H-PFCA), which were hypothesised as originating from longer-chained PFCAs. The chain shortening and hydrogen substitution pathways are consistent with previous studies conducted under controlled conditions in a clean matrix (Singh et al. 2019). The only PFSA detected in **Paper IV** was perfluorobutanesulfonic acid (PFBS), for which no direct precursor was identified. Over the time of treatment, the signal intensity of PFBS increased from 0 min to a maximum at 120 min, followed by a decrease at the 180 min mark. No other PFSAs were identified, suggesting that precursors or TPs of PFBS likely remained below the LOD of the method.

A separate class of PFAS was detected, which was perfluorinated dicarboxylic acids (PFdiCA). The perfluorinated carbon chain length was three and four, namely perfluoropentane dicarboxylic acid (PFPeDiA) and perfluorohexane dicarboxylic acid (PFHxDiA), respectively. The formation of PFPeDiA may have originated either from the degradation of a larger UVCB substance or via chain-shortening of PFHxDiA, as it was present at the initial time point of treatment. This class has previously been detected in industrial wastewater and surface waters (Fu et al. 2024; Li et al. 2026).

Overall, the non-target analysis enabled the identification of numerous PFAS and TPs, many of which were identified for the very first time. As limited or no prior information is available for these compounds beyond the proposed structures, assessing their potential environmental impact is critical. Therefore, hazard estimation was conducted for the compounds identified in **Papers II, III and IV**, as discussed in the following section.

4.3 Toxicity evaluation

Two types of toxicity evaluation were included in this thesis. The toxicity evaluation in **Paper II** was originally conducted as part of a separate study (Smith et al. 2023) outside of the scope of this thesis. It involved two

bioassays to evaluate the toxicity before and after treatment. Thyroid -related toxicity was assessed through a transthretin binding assay, and the general toxicity through an *Aliivibrio fischeri* bioluminescence inhibition assay. The latter method mainly measures the difference in bioluminescence intensity and has previously demonstrated a concentration-dependent response to PFAS exposure (Fitzgerald et al. 2018). The principal outcome for these assays was that after treatment, samples overall showed lower toxicity, indicating an overall reduction of toxicity. However, it is important to note that these samples were complex mixtures containing contaminants beyond PFAS, making it difficult to attribute observed toxicity specifically to PFAS. Consequently, when focusing solely on PFAS-related effects, it was not possible to conclusively determine the contribution to PFAS and their TPs.

The second type of toxicity evaluation involved *in silico* toxicity predictions for **Papers III and IV** where endpoints for predicted effective concentrations affecting 50 % of the population for algae and fish at 96 h exposure, and for *Daphnia Magna* at 48 hours exposure. These are standardised tests recommended by the OECD (OECD 2004; 2006; 2025). These predictions were performed using the models TRIDENT (**Papers III and IV**) and VEGA (**Paper III**) (Danieli et al. 2023; Gustavsson et al. 2026). As quantitative concentration data was unavailable for the identified TPs, absolute risk assessment was not feasible. Instead, comparative toxicity evaluation approaches were used to assess the relative toxicity of TPs. For **Paper III**, predictions from both models were directly compared to PFOS and its related TPs. This comparative approach enabled the identification of TPs that may warrant prioritisation in future monitoring and treatment optimisation efforts. Additionally, all relevant isomers were evaluated individually to assess whether structural variations influenced predicted toxicity.

The overall outcome indicated that C_8 PFAS-derived TPs were generally predicted to exhibit higher toxicity compared to shorter-chain analogues. Among the evaluated compounds, H_2-UPFOS consistently showed the highest predicted toxicity across multiple endpoints and models. Although no clear relationship was observed between double-bond or hydrogen substitution site and toxicity, H_2-UPFOS was predicted to have a greater number of toxic isomers than the other TP classes. Notably, several TPs were

predicted to be more toxic than PFOS. This result highlights the need for untargeted analysis of TPs even in controlled experimental systems. The similarity scores obtained from each model were also evaluated. Overall, the TRIDENT model had greater similarity scores than the VEGA model for PFAS and was therefore selected as the primary model for subsequent analyses.

The toxicity evaluation for **Paper IV** could not be performed using the same precursor-normalised approach as in **Paper III** due to the lack of clearly defined precursor-product relationships. Instead, all identified PFAS were normalised relative to the compound with the highest predicted toxicity within each toxicity endpoint. Across all three endpoints, a 2:1-FtE compound consistently exhibited the highest predicted toxicity, suggesting that this newly identified class may pose a significant environmental hazard. As this class has not been previously reported, its combination of novelty and high predicted toxicity highlights the need for further investigation. The findings also emphasise the challenges associated with degrading substances of UVCBs. While it is generally known that natural dissolved organic matter may interfere with degradation of anthropogenic chemicals in wastewater (Marotta & Paradisi 2025), UVCB substances introduces an additional level of complexity to their heterogeneous and poorly defined composition.

4.4 Example structures of PFAS classes discussed in the thesis

Table 5. Example structures for each class of PFAS discussed in the thesis, with each paper relevant to the PFAS class listed.

PFAS Class	Example structure	Papers
2:1-FtE	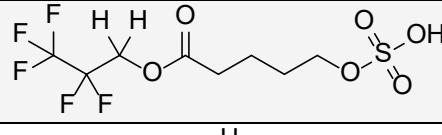	IV
Bistriflimide	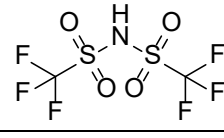	II

Cyclic-PFSA	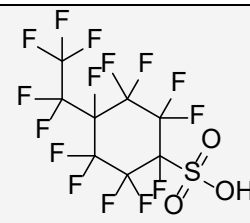	I, II
DUPFOS	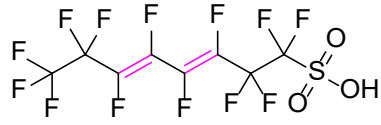	II
FASA	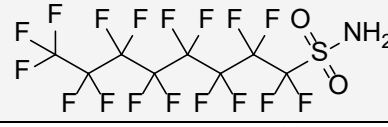	I, II
FASASA	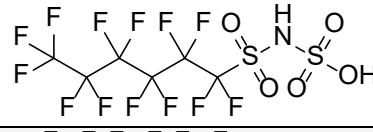	II
FASHN	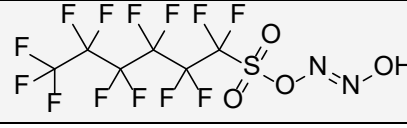	II
H_2-PFSA	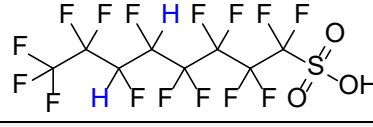	III
H_2-UPFOS	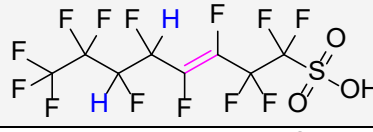	III
H-PFCA	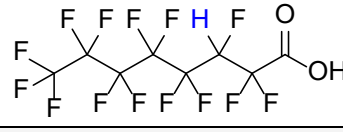	IV
H-PFSA		II, III
H-UPFOS	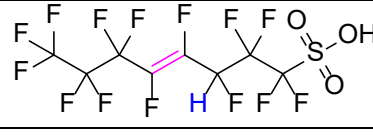	III

Keto-PFSA		II
Me-FASASi	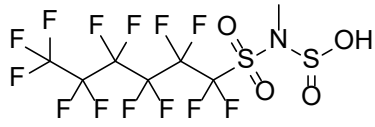	II
MeOH-FASA	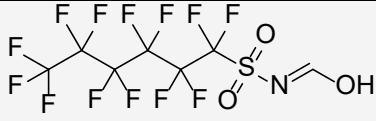	II
N-EtFASAA	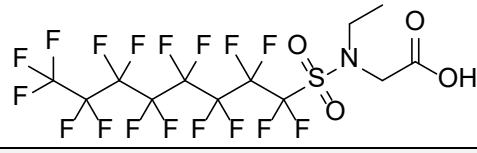	I, II
N-MeFASAA	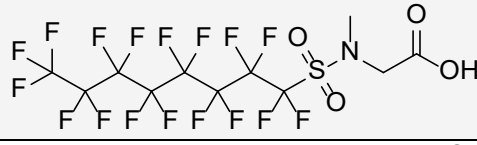	I, II
N-SPAmP-FHxSA	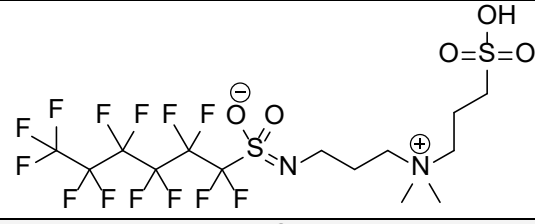	II
N-SPAmP-FHxSAA	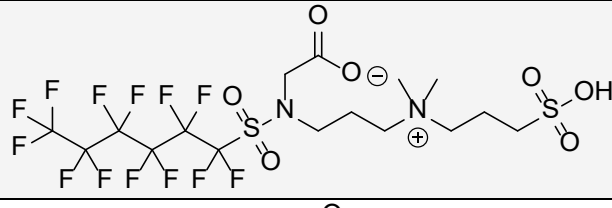	II
N-SPAmP-FHxSAPS	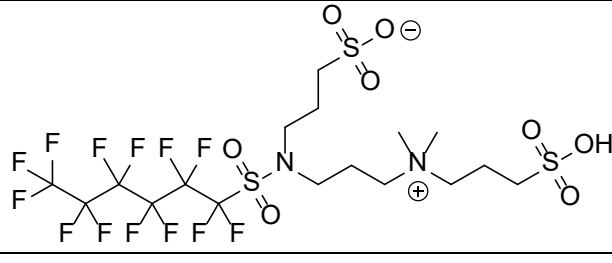	II

PFCA	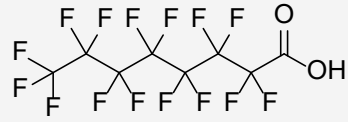	I, II, IV
PFdiCA	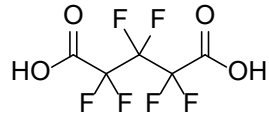	IV
PFESA	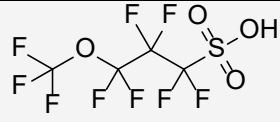	II
PFOCHS	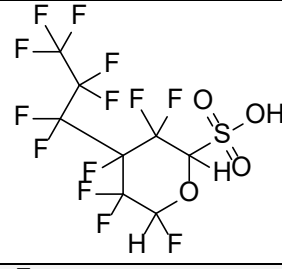	II
PFSA	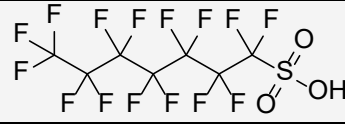	I, II, III, IV

5. Conclusions

The work presented in this thesis centres on the development and application of an untargeted analytical methodology for the identification of PFAS using suspect and non-target screening. These approaches were then used to investigate the formation of TPs for three different types of destructive treatment techniques (electrochemical oxidation, UV degradation, and plasma degradation). The results addressing the aims and sub-goals from Chapter 2 are summarised below.

I. Develop an in-house methodology for the screening and identification of PFAS using untargeted analysis techniques

    i. Create a suspect and non-target screening workflow applicable to a wide range of environmental matrices
    ii. Identify points of improvement to enable continuous methodological refinement

In **Paper I**, the developed untargeted method was compared to a conventional targeted approach. The results demonstrated that the untargeted workflow produced comparable results while also enabling the detection of additional compounds not included in the targeted method. In **Papers II, III and IV**, the method was successfully applied to detect and identify PFAS with high confidence, using both MS^1- and MS^2-based strategies. The method was also iteratively improved throughout time by implementing updated databases and features from software updates.

II. Identify TPs across different advanced destructive treatment processes

    i. Detect and identify TPs associated with specific treatment processes and degradation pathways
    ii. Propose structurally plausible candidates for newly identified compounds

Paper II identified a new class of PFAS that originated from the electrochemical oxidation treatment (FASHN). Additionally, previously unreported homologues for novel PFAS classes were detected for the first

time, originating from both the sample matrix and treatment process. **Paper III** reported for the first time the formation of H_2-UPFOS during UV treatment. While related compounds have been reported in previous literature, the combined occurrence of unsaturated carbon double bonds and two hydrogen substitutions was unique to this study. Furthermore, the formation of numerous isomeric species was elucidated, occurring mainly from hydrogen substitution at different carbon positions. **Paper IV** identified a previously undiscovered class of PFAS (2:1-FtE). The new class was inferred to originate from the degradation of a larger, undefined UVCB substance. In addition, other PFAS TPs originating from chain-shortening and hydrogen substitution pathways were identified.

III. Evaluate the toxicity and environmental hazard of identified TPs

i. Assess whether overall toxicity changes before and after treatment
ii. Evaluate the relative toxicity of individual TPs and their potential environmental impact

Due to the lack of analytical standards typically associated with untargeted techniques, no concentrations could be determined. Nevertheless, this thesis attempted to evaluate toxicity at both the sample and individual TP level. In **Papers III and IV**, toxicity was assessed using *in silico* prediction approaches. In **Paper III**, the predicted toxicity of the TPs was directly compared to that of the precursor. This revealed that several TPs may exhibit higher toxicity than the parent compound. In **Paper IV**, where no clear precursor–product relationships were established, toxicity scores were normalised relative to the most toxic compound identified in each endpoint. This approach highlighted the new class 2:1-FtE to be of high concern due to its high predicted toxicity. The combination of elevated predicted toxicity and matrix-derived origin display the need for improvement of advanced destructive treatment techniques.

Overall, this thesis demonstrates the critical importance of including untargeted methods in the development of advanced destructive treatment techniques. **Papers I** established the groundwork of method development, while **Papers II, III, and IV** showcased the diversity and complexity of TPs formed in both simple and highly complex matrices. One of the main

discoveries was that the sample matrix may have a key influence on the formation of TPs, as evidenced by the identification of matrix-dependent TPs in **Papers II and IV**. Furthermore, toxicity predictions proved useful in **Papers III and IV** for prioritising compounds and classes of concern, particularly in the absence of quantitative data. These tools provide a means to guide future research and optimisation of advanced destructive treatment techniques.

In future endeavours, untargeted analytical techniques should become the standard in the evaluation of treatment techniques. However, several challenges remain. In particular, the lack of reliable concentration estimates for TPs, largely due to variability in electrospray ionisation efficiency, which in turn limits comprehensive risk assessment. Development of new robust *in silico* toxicity prediction models would further assist in true risk assessment, as improvements in models will more closely reflect reality. Improvements to *in silico* quantification approaches would greatly improve the understanding of the formation of TPs. Such developments would also contribute to closing the mass balance of PFAS, which is often incomplete in studies of complex environmental samples, where substantial fractions of PFAS remain unexplained. There is also opportunity for improving the harmonisation of quality control, data processing, and reporting. While there are currently many in-house solutions, establishing standardised guidelines would greatly improve the reliability and trust that legislators and stakeholders place in the field of untargeted analysis.

References

Ahrens, L., Taniyasu, S., Yeung, L.W.Y., Yamashita, N., Lam, P.K.S. & Ebinghaus, R. (2010). Distribution of polyfluoroalkyl compounds in water, suspended particulate matter and sediment from Tokyo Bay, Japan. *Chemosphere*, 79 (3), 266–272. https://doi.org/10.1016/j.chemosphere.2010.01.045

Appleman, T.D., Higgins, C.P., Quiñones, O., Vanderford, B.J., Kolstad, C., Zeigler-Holady, J.C. & Dickenson, E.R.V. (2014). Treatment of poly- and perfluoroalkyl substances in U.S. full-scale water treatment systems. *Water Research*, 51, 246–255. https://doi.org/10.1016/j.watres.2013.10.067

Ateia, M., Chiang, D., Cashman, M. & Acheson, C. (2023). Total Oxidizable Precursor (TOP) Assay─Best Practices, Capabilities and Limitations for PFAS Site Investigation and Remediation. *Environmental Science & Technology Letters*, 10 (4), 292–301. https://doi.org/10.1021/acs.estlett.3c00061

Baduel, C., Mueller, J.F., Rotander, A., Corfield, J. & Gomez-Ramos, M.J. (2017). Discovery of novel per- and polyfluoroalkyl substances (PFASs) at a fire fighting training ground and preliminary investigation of their fate and mobility. *Chemosphere*, 185, 1030–1038. https://doi.org/10.1016/j.chemosphere.2017.06.096

Barzen-Hanson, K.A., Roberts, S.C., Choyke, S., Oetjen, K., McAlees, A., Riddell, N., McCrindle, R., Ferguson, P.L., Higgins, C.P. & Field, J.A. (2017). Discovery of 40 Classes of Per- and Polyfluoroalkyl Substances in Historical Aqueous Film-Forming Foams (AFFFs) and AFFF-Impacted Groundwater. *Environmental Science & Technology*, 51 (4), 2047–2057. https://doi.org/10.1021/acs.est.6b05843

Bentel, M.J., Yu, Y., Xu, L., Li, Z., Wong, B.M., Men, Y. & Liu, J. (2019). Defluorination of Per- and Polyfluoroalkyl Substances (PFASs) with Hydrated Electrons: Structural Dependence and Implications to PFAS Remediation and Management. *Environmental Science & Technology*, 53 (7), 3718–3728. https://doi.org/10.1021/acs.est.8b06648

Bowers, B.B., Lou, Z., Xu, J., De Silva, A.O., Xu, X., Lowry, G.V. & Sullivan, R.C. (2023). Nontarget analysis and fluorine atom balances of transformation products from UV/sulfite degradation of perfluoroalkyl contaminants. *Environmental Science: Processes and Impacts*, 25 (3), 472–483. https://doi.org/10.1039/d2em00425a

Bugsel, B., Zweigle, J. & Zwiener, C. (2023). Nontarget screening strategies for PFAS prioritization and identification by high resolution mass spectrometry: A review. *Trends in Environmental Analytical Chemistry*, 40, e00216. https://doi.org/10.1016/j.teac.2023.e00216

Butt, C.M., Muir, D.C.G. & Mabury, S.A. (2013). Biotransformation pathways of fluorotelomer-based polyfluoroalkyl substances: A review. *Environmental Toxicology and Chemistry*, 33 (2), 243–267. https://doi.org/10.1002/etc.2407

Cantoni, B., Turolla, A., Wellmitz, J., Ruhl, A.S. & Antonelli, M. (2021). Perfluoroalkyl substances (PFAS) adsorption in drinking water by granular activated carbon: Influence of activated carbon and PFAS characteristics. *Science of The Total Environment*, 795, 148821. https://doi.org/10.1016/j.scitotenv.2021.148821

CCTE, E. (2025). Distributed Structure-Searchable Toxicity (DSSTox) Database. The United States Environmental Protection Agency's Center for Computational Toxicology and Exposure. https://doi.org/10.23645/EPACOMPTOX.5588566

Charbonnet, J.A., McDonough, C.A., Xiao, F., Schwichtenberg, T., Cao, D., Kaserzon, S., Thomas, K.V., Dewapriya, P., Place, B.J., Schymanski, E.L., Field, J.A., Helbling, D.E. & Higgins, C.P. (2022). Communicating Confidence of Per- and Polyfluoroalkyl Substance Identification via High-Resolution Mass Spectrometry. *Environmental Science & Technology Letters*, 9 (6), 473–481. https://doi.org/10.1021/acs.estlett.2c00206

Chen, H., Qiu, W., Yang, X., Chen, F., Chen, J., Tang, L., Zhong, H., Magnuson, J.T., Zheng, C. & Xu, E.G. (2022). Perfluorooctane Sulfonamide (PFOSA) Induces Cardiotoxicity via Aryl Hydrocarbon Receptor Activation in Zebrafish. *Environmental Science & Technology*, 56 (12), 8438–8448. https://doi.org/10.1021/acs.est.1c08875

Cheng, L., Meng, P. & Knappe, D.R.U. (2025). Removal of Per- and Polyfluoroalkyl Substances (PFAS) in fixed bed anion exchange reactors: Factors determining PFAS uptake capacity and models predicting PFAS breakthrough. *Water Research*, 268, 122629. https://doi.org/10.1016/j.watres.2024.122629

Corbet, A.S. (1934). The formation of hyponitrous acid as an intermediate compound in the biological or photochemical oxidation of ammonia to nitrous acid: Chemical reactions. *The Biochemical journal*, 28 (4), 1575–1582. https://doi.org/10.1042/bj0281575

Corsini, E., Luebke, R.W., Germolec, D.R. & DeWitt, J.C. (2014). Perfluorinated compounds: Emerging POPs with potential immunotoxicity. *Toxicology Letters*, 230 (2), 263–270. https://doi.org/10.1016/j.toxlet.2014.01.038

Danieli, A., Colombo, E., Raitano, G., Lombardo, A., Roncaglioni, A., Manganaro, A., Sommovigo, A., Carnesecchi, E., Dorne, J.-L.C.M. & Benfenati, E. (2023). The VEGA Tool to Check the Applicability Domain Gives Greater Confidence in the Prediction of In Silico Models. *International journal of molecular sciences*, 24 (12). https://doi.org/10.3390/ijms24129894

De Silva, A.O., Spencer, C., Scott, B.F., Backus, S. & Muir, D.C.G. (2011). Detection of a Cyclic Perfluorinated Acid, Perfluoroethylcyclohexane Sulfonate, in the Great Lakes of North America. *Environmental Science & Technology*, 45 (19), 8060–8066. https://doi.org/10.1021/es200135c

Dewapriya, P., Nilsson, S., Ghorbani Gorji, S., O'Brien, J.W., Bräunig, J., Gómez Ramos, M.J., Donaldson, E., Samanipour, S., Martin, J.W., Mueller, J.F., Kaserzon, S.L. & Thomas, K.V. (2023). Novel Per- and Polyfluoroalkyl Substances Discovered in Cattle Exposed to AFFF-Impacted Groundwater. *Environmental Science & Technology*, 57 (36), 13635–13645. https://doi.org/10.1021/acs.est.3c03852

Dulio, V., Alygizakis, N., Ng, K., Schymanski, E.L., Andres, S., Vorkamp, K., Hollender, J., Finckh, S., Aalizadeh, R., Ahrens, L., Bouhoulle, E., Čirka, Ľ., Derksen, A., Deviller, G., Duffek, A., Esperanza, M., Fischer, S., Fu, Q., Gago-Ferrero, P., Haglund, P., Junghans, M., Kools, S.A.E., Koschorreck, J., Lopez, B., Lopez De Alda, M., Mascolo, G., Miège, C., Osté, L., O'Toole, S., Rostkowski, P., Schulze, T., Sims, K., Six, L., Slobodnik, J., Staub, P.-F., Stroomberg, G., Thomaidis, N.S., Togola, A., Tomasi, G. & Von Der Ohe, P.C. (2024). Beyond target chemicals: updating the NORMAN prioritisation scheme to support the EU chemicals strategy with semi-quantitative suspect/non-target screening data. *Environmental Sciences Europe*, 36 (1), 113. https://doi.org/10.1186/s12302-024-00936-3

Ellis, A.C., Boyer, T.H. & Strathmann, T.J. (2025). Regeneration of conventional and emerging PFAS-selective anion exchange resins used to treat PFAS-contaminated waters. *Separation and Purification Technology*, 355, 129789. https://doi.org/10.1016/j.seppur.2024.129789

Euripides & Halleran, M.R. (1988). *The Heracles of Euripides*. Focus Information Group.

Fitzgerald, N.J.M., Simcik, M.F. & Novak, P.J. (2018). Perfluoroalkyl Substances Increase the Membrane Permeability and Quorum Sensing Response in *Aliivibrio fischeri*. *Environmental Science & Technology Letters*, 5 (1), 26–31. https://doi.org/10.1021/acs.estlett.7b00518

Franke, V., Ullberg, M., McCleaf, P., Wålinder, M., Köhler, S.J. & Ahrens, L. (2021). The Price of Really Clean Water: Combining Nanofiltration with Granular Activated Carbon and Anion Exchange Resins for the Removal of Per- And Polyfluoralkyl Substances (PFASs) in Drinking Water Production. *ACS ES&T Water*, 1 (4), 782–795. https://doi.org/10.1021/acsestwater.0c00141

Fu, Y., Ji, Y., Tian, Y., Zhang, F., Sheng, N., Dai, J. & Pan, Y. (2024). Unveiling Priority Emerging PFAS in Taihu Lake Using Integrated Nontarget Screening, Target Analysis, and Risk Characterization. *Environmental Science & Technology*, 58 (42), 18980–18991. https://doi.org/10.1021/acs.est.4c06731

Gaber, N., Bero, L. & Woodruff, T.J. (2023). The Devil they Knew: Chemical Documents Analysis of Industry Influence on PFAS Science. *Annals of Global Health*, 89 (1), 37. https://doi.org/10.5334/aogh.4013

Gago-Ferrero, P., Schymanski, E.L., Bletsou, A.A., Aalizadeh, R., Hollender, J. & Thomaidis, N.S. (2015). Extended Suspect and Non-Target Strategies to Characterize Emerging Polar Organic Contaminants in Raw Wastewater with LC-HRMS/MS. *Environmental Science and Technology*, 49 (20), 12333–12341. https://doi.org/10.1021/acs.est.5b03454

Getzinger, G.J., Higgins, C.P. & Ferguson, P.L. (2021). Structure Database and in Silico Spectral Library for Comprehensive Suspect Screening of Per- And Polyfluoroalkyl Substances (PFASs) in Environmental Media by High-resolution Mass Spectrometry. *Analytical Chemistry*, 93 (5), 2820–2827. https://doi.org/10.1021/acs.analchem.0c04109

Ghorbani Gorji, S., Gómez Ramos, M.J., Dewapriya, P., Schulze, B., Mackie, R., Nguyen, T.M.H., Higgins, C.P., Bowles, K., Mueller, J.F., Thomas, K.V. & Kaserzon, S.L. (2024). New PFASs Identified in AFFF Impacted Groundwater by Passive Sampling and Nontarget Analysis. *Environmental Science & Technology*, 58 (3), 1690–1699. https://doi.org/10.1021/acs.est.3c06591

Giesy, J.P. & Kannan, K. (2001). Global distribution of perfluorooctane sulfonate in wildlife. *Environmental Science and Technology*, 35 (7), 1339–1342. https://doi.org/10.1021/es001834k

Glüge, J., Scheringer, M., Cousins, I.T., Dewitt, J.C., Goldenman, G., Herzke, D., Lohmann, R., Ng, C.A., Trier, X. & Wang, Z. (2020). An overview of the uses of per- And polyfluoroalkyl substances (PFAS). *Environmental Science: Processes and Impacts*, 22 (12), 2345–2373. https://doi.org/10.1039/d0em00291g

Gobelius, L., Hedlund, J., Dürig, W., Tröger, R., Lilja, K., Wiberg, K. & Ahrens, L. (2018). Per- and Polyfluoroalkyl Substances in Swedish Groundwater and Surface Water: Implications for Environmental Quality Standards and Drinking Water Guidelines. *Environmental Science & Technology*, 52 (7), 4340–4349. https://doi.org/10.1021/acs.est.7b05718

Graber, J.M., Alexander, C., Laumbach, R.J., Black, K., Strickland, P.O., Georgopoulos, P.G., Marshall, E.G., Shendell, D.G., Alderson, D., Mi, Z., Mascari, M. & Weisel, C.P. (2019). Per and polyfluoroalkyl substances (PFAS) blood levels after contamination of a community water supply and comparison with 2013–2014 NHANES. *Journal of Exposure Science and Environmental Epidemiology*, 29 (2), 172–182. https://doi.org/10.1038/s41370-018-0096-z

Gustavsson, M., Käll, S., Svedberg, P., Inda-Diaz, J.S., Molander, S., Coria, J., Backhaus, T. & Kristiansson, E. (2026). Transformers enable accurate prediction of acute and chronic chemical toxicity in aquatic organisms.

Science Advances, 10 (10), eadk6669. https://doi.org/10.1126/sciadv.adk6669

Hamid, N., Junaid, M., Sultan, M., Yoganandham, S.T. & Chuan, O.M. (2024). The untold story of PFAS alternatives: Insights into the occurrence, ecotoxicological impacts, and removal strategies in the aquatic environment. *Water Research*, 250, 121044. https://doi.org/10.1016/j.watres.2023.121044

Haukås, M., Berger, U., Hop, H., Gulliksen, B. & Gabrielsen, G.W. (2007). Bioaccumulation of per- and polyfluorinated alkyl substances (PFAS) in selected species from the Barents Sea food web. *Environmental Pollution*, 148 (1), 360–371. https://doi.org/10.1016/j.envpol.2006.09.021

Hensema, T.J., Berendsen, B.J.A. & Van Leeuwen, S.P.J. (2021). Non-targeted identification of per- and polyfluoroalkyl substances at trace level in surface water using fragment ion flagging. *Chemosphere*, 265, 128599. https://doi.org/10.1016/j.chemosphere.2020.128599

Hollender, J., Schymanski, E.L., Ahrens, L., Alygizakis, N., Béen, F., Bijlsma, L., Brunner, A.M., Celma, A., Fildier, A., Fu, Q., Gago-Ferrero, P., Gil-Solsona, R., Haglund, P., Hansen, M., Kaserzon, S., Kruve, A., Lamoree, M., Margoum, C., Meijer, J., Merel, S., Rauert, C., Rostkowski, P., Samanipour, S., Schulze, B., Schulze, T., Singh, R.R., Slobodnik, J., Steininger-Mairinger, T., Thomaidis, N.S., Togola, A., Vorkamp, K., Vulliet, E., Zhu, L. & Krauss, M. (2023). *NORMAN guidance on suspect and non-target screening in environmental monitoring*. *Environmental Sciences Europe* Springer Berlin Heidelberg. https://doi.org/10.1186/s12302-023-00779-4

Horst, J., McDonough, J., Ross, I. & Houtz, E. (2020). Understanding and Managing the Potential By-Products of PFAS Destruction. *Groundwater Monitoring & Remediation*, 40 (2), 17–27. https://doi.org/10.1111/gwmr.12372

Houtz, E.F., Higgins, C.P., Field, J.A. & Sedlak, D.L. (2013). Persistence of Perfluoroalkyl Acid Precursors in AFFF-Impacted Groundwater and Soil. *Environmental Science & Technology*, 47 (15), 8187–8195. https://doi.org/10.1021/es4018877

Houtz, E.F. & Sedlak, D.L. (2012). Oxidative conversion as a means of detecting precursors to perfluoroalkyl acids in urban runoff. *Environmental Science and Technology*, 46 (17), 9342–9349. https://doi.org/10.1021/es302274g

Jeong, Y., Da Silva, K.M., Iturrospe, E., Fuiji, Y., Boogaerts, T., Van Nuijs, A.L.N., Koelmel, J. & Covaci, A. (2022). Occurrence and contamination profile of legacy and emerging per- and polyfluoroalkyl substances (PFAS) in Belgian wastewater using target, suspect and non-target screening approaches. *Journal of Hazardous Materials*, 437, 129378. https://doi.org/10.1016/j.jhazmat.2022.129378

Junker, A.L., Juve, J.-M.A., Bai, L., Qvist Christensen, C.S., Ahrens, L., Cousins, I.T., Ateia, M. & Wei, Z. (2025). Best Practices for Experimental Design, Testing, and Reporting of Aqueous PFAS-Degrading Technologies. *Environmental Science & Technology*, 59 (18), 8939–8950. https://doi.org/10.1021/acs.est.4c08571

Kaiser, A.-M., Aro, R., Kärrman, A., Weiss, S., Hartmann, C., Uhl, M., Forsthuber, M., Gundacker, C. & Yeung, L.W.Y. (2021). Comparison of extraction methods for per- and polyfluoroalkyl substances (PFAS) in human serum and placenta samples—insights into extractable organic fluorine (EOF). *Analytical and Bioanalytical Chemistry*, 413 (3), 865–876. https://doi.org/10.1007/s00216-020-03041-5

Kaufmann, A., Butcher, P., Maden, K., Walker, S. & Widmer, M. (2022). Simplifying Nontargeted Analysis of PFAS in Complex Food Matrixes. *Journal of AOAC INTERNATIONAL*, 105 (5), 1280–1287. https://doi.org/10.1093/jaoacint/qsac071

Kendrick, E. (1963). A mass scale based resolution mass spectrometry of organic compounds. *Analytical Chemistry*, 35 (13), 2146–2154

Kind, T. & Fiehn, O. (2007). Seven Golden Rules for heuristic filtering of molecular formulas obtained by accurate mass spectrometry. *BMC Bioinformatics*, 8 (1), 1–20. https://doi.org/10.1186/1471-2105-8-105

Kissa, E. (2001). *Fluorinated surfactants and repellents*. 2nd ed., rev.expanded. Marcel Dekker. (Surfactant science series; v. 97)

Koelmel, J.P., Kroeger, N.M., Gill, E.L., Ulmer, C.Z., Bowden, J.A., Patterson, R.E., Yost, R.A. & Garrett, T.J. (2017). Expanding Lipidome Coverage Using LC-MS/MS Data-Dependent Acquisition with Automated Exclusion List Generation. *Journal of the American Society for Mass Spectrometry*, 28 (5), 908–917. https://doi.org/10.1007/s13361-017-1608-0

Koelmel, J.P., Paige, M.K., Aristizabal-Henao, J.J., Robey, N.M., Nason, S.L., Stelben, P.J., Li, Y., Kroeger, N.M., Napolitano, M.P., Savvaides, T., Vasiliou, V., Rostkowski, P., Garrett, T.J., Lin, E., Deigl, C., Jobst, K., Townsend, T.G., Godri Pollitt, K.J. & Bowden, J.A. (2020). Toward Comprehensive Per- A nd Polyfluoroalkyl Substances Annotation Using FluoroMatch Software and Intelligent High-Resolution Tandem Mass Spectrometry Acquisition. *Analytical Chemistry*, 92 (16), 11186–11194. https://doi.org/10.1021/acs.analchem.0c01591

Krauss, M., Singer, H. & Hollender, J. (2010). LC–high resolution MS in environmental analysis: from target screening to the identification of unknowns. *Analytical and Bioanalytical Chemistry*, 397 (3), 943–951. https://doi.org/10.1007/s00216-010-3608-9

Lai, A., Clark, A.M., Escher, B.I., Fernandez, M., McEwen, L.R., Tian, Z., Wang, Z. & Schymanski, E.L. (2022). The Next Frontier of Environmental Unknowns: Substances of Unknown or Variable Composition, Complex

Reaction Products, or Biological Materials (UVCBs). *Environmental Science & Technology*, 56 (12), 7448–7466. https://doi.org/10.1021/acs.est.2c00321

Lau, C., Anitole, K., Hodes, C., Lai, D., Pfahles-Hutchens, A. & Seed, J. (2007). Perfluoroalkyl acids: A review of monitoring and toxicological findings. *Toxicological Sciences*, 99 (2), 366–394. https://doi.org/10.1093/toxsci/kfm128

Lenka, S.P., Kah, M. & Padhye, L.P. (2021). A review of the occurrence, transformation, and removal of poly- and perfluoroalkyl substances (PFAS) in wastewater treatment plants. *Water Research*, 199. https://doi.org/10.1016/j.watres.2021.117187

Li, H., Junker, A.L., Wen, J., Ahrens, L., Sillanpää, M., Tian, J., Cui, F., Vergeynst, L. & Wei, Z. (2023a). A recent overview of per- and polyfluoroalkyl substances (PFAS) removal by functional framework materials. *Chemical Engineering Journal*, 452, 139202. https://doi.org/10.1016/j.cej.2022.139202

Li, R., Isowamwen, O.F., Ross, K.C., Holsen, T.M. & Thagard, S.M. (2023b). PFAS–CTAB Complexation and Its Role on the Removal of PFAS from a Lab-Prepared Water and a Reverse Osmosis Reject Water Using a Plasma Reactor. *Environmental Science & Technology*, 57 (34), 12901–12910. https://doi.org/10.1021/acs.est.3c03679

Li, X., Hou, M., Wu, X., Zhang, X., Ji, Z., Li, P., Zhang, Y., Ding, H., Shi, Y. & Cai, Y. (2026). Tracking PFAS across Environmental Media Surrounding Fluorochemical Industrial Park: Insights from Nontarget Analysis and Risk Assessment. *Environ. Sci. Technol.*,

Liu, Z., Bentel, M.J., Yu, Y., Ren, C., Gao, J., Pulikkal, V.F., Sun, M., Men, Y. & Liu, J. (2021). Near-Quantitative Defluorination of Perfluorinated and Fluorotelomer Carboxylates and Sulfonates with Integrated Oxidation and Reduction. *Environmental Science & Technology*, 55 (10), 7052–7062. https://doi.org/10.1021/acs.est.1c00353

Löffler, P., Rehnstam, S., Ahrens, L., Lai, F.Y. & Celma, A. (2025). Long-Term System Suitability Evaluation for Mass Accuracy in the Analysis of Small Molecules by High-Resolution Mass Spectrometry. *Journal of the American Society for Mass Spectrometry*, 36 (9), 2005–2012. https://doi.org/10.1021/jasms.5c00128

Lu, D., Sha, S., Luo, J., Huang, Z. & Zhang Jackie, X. (2020). Treatment train approaches for the remediation of per- and polyfluoroalkyl substances (PFAS): A critical review. *Journal of Hazardous Materials*, 386, 121963. https://doi.org/10.1016/j.jhazmat.2019.121963

Lu, Y., Liang, Y., Zhou, Z., Wang, Y. & Jiang, G. (2019). Possible Fluorinated Alternatives of PFOS and PFOA: Ready to Go? *Environmental Science &*

Technology, 53 (24), 14091–14092. https://doi.org/10.1021/acs.est.9b06323

Luo, Y.-S., Aly, N.A., McCord, J., Strynar, M.J., Chiu, W.A., Dodds, J.N., Baker, E.S. & Rusyn, I. (2020). Rapid Characterization of Emerging Per- and Polyfluoroalkyl Substances in Aqueous Film-Forming Foams Using Ion Mobility Spectrometry–Mass Spectrometry. *Environmental Science & Technology*, 54 (23), 15024–15034. https://doi.org/10.1021/acs.est.0c04798

Marotta, E. & Paradisi, C. (2025). The importance of mechanistic studies in the development of cold plasma-based degradation of persistent organic pollutants in water. *Current Opinion in Green and Sustainable Chemistry*, 52, 100999. https://doi.org/10.1016/j.cogsc.2025.100999

McCleaf, P., Kjellgren, Y. & Ahrens, L. (2021). Foam fractionation removal of multiple per- and polyfluoroalkyl substances from landfill leachate. *AWWA Water Science*, 3 (5), e1238. https://doi.org/10.1002/aws2.1238

McDonough, C.A., Choyke, S., Barton, K.E., Mass, S., Starling, A.P., Adgate, J.L. & Higgins, C.P. (2021). Unsaturated PFOS and Other PFASs in Human Serum and Drinking Water from an AFFF-Impacted Community. *Environmental Science & Technology*, 55 (12), 8139–8148. https://doi.org/10.1021/acs.est.1c00522

Mirabediny, M., Sun, J., Yu, T.T., Åkermark, B., Das, B. & Kumar, N. (2023). Effective PFAS degradation by electrochemical oxidation methods-recent progress and requirement. *Chemosphere*, 321, 138109. https://doi.org/10.1016/j.chemosphere.2023.138109

Mohammed Taha, H., Aalizadeh, R., Alygizakis, N., Antignac, J.-P., Arp, H.P.H., Bade, R., Baker, N., Belova, L., Bijlsma, L., Bolton, E.E., Brack, W., Celma, A., Chen, W.-L., Cheng, T., Chirsir, P., Čirka, Ľ., D'Agostino, L.A., Djoumbou Feunang, Y., Dulio, V., Fischer, S., Gago-Ferrero, P., Galani, A., Geueke, B., Głowacka, N., Glüge, J., Groh, K., Grosse, S., Haglund, P., Hakkinen, P.J., Hale, S.E., Hernandez, F., Janssen, E.M.-L., Jonkers, T., Kiefer, K., Kirchner, M., Koschorreck, J., Krauss, M., Krier, J., Lamoree, M.H., Letzel, M., Letzel, T., Li, Q., Little, J., Liu, Y., Lunderberg, D.M., Martin, J.W., McEachran, A.D., McLean, J.A., Meier, C., Meijer, J., Menger, F., Merino, C., Muncke, J., Muschket, M., Neumann, M., Neveu, V., Ng, K., Oberacher, H., O'Brien, J., Oswald, P., Oswaldova, M., Picache, J.A., Postigo, C., Ramirez, N., Reemtsma, T., Renaud, J., Rostkowski, P., Rüdel, H., Salek, R.M., Samanipour, S., Scheringer, M., Schliebner, I., Schulz, W., Schulze, T., Sengl, M., Shoemaker, B.A., Sims, K., Singer, H., Singh, R.R., Sumarah, M., Thiessen, P.A., Thomas, K.V., Torres, S., Trier, X., Van Wezel, A.P., Vermeulen, R.C.H., Vlaanderen, J.J., Von Der Ohe, P.C., Wang, Z., Williams, A.J., Willighagen, E.L., Wishart, D.S., Zhang, J., Thomaidis, N.S., Hollender, J., Slobodnik, J. & Schymanski, E.L. (2022).

The NORMAN Suspect List Exchange (NORMAN-SLE): facilitating European and worldwide collaboration on suspect screening in high resolution mass spectrometry. *Environmental Sciences Europe*, 34 (1), 104. https://doi.org/10.1186/s12302-022-00680-6

Moody, C.A. & Field, J.A. (2000). Perfluorinated Surfactants and the Environmental Implications of Their Use in Fire-Fighting Foams. *Environmental Science & Technology*, 34 (18), 3864–3870. https://doi.org/10.1021/es991359u

Mukherjee, P., Sathiyan, K., Zidki, T., Nadagouda, M.N. & Sharma, V.K. (2023). Can ultraviolet-assisted advanced reduction processes effectively destroy per- and polyfluoroalkyl substances in real water matrices? *Current Opinion in Chemical Engineering*, 42, 100971. https://doi.org/10.1016/j.coche.2023.100971

OECD (2004). *Test No. 202: Daphnia sp. Acute Immobilisation Test*. OECD. https://doi.org/10.1787/9789264069947-en

OECD (2006). *Test No. 201: Alga, Growth Inhibition Test*. OECD Publishing. https://doi.org/10.1787/9789264069923-en

OECD (2021). *Reconciling Terminology of the Universe of Per- and Polyfluoroalkyl Substances: Recommendations and Practical Guidance*. www.oecd.org/chemicalsafety/

OECD (2022). *Fact Cards of Major Groups of Per- and Polyfluoroalkyl Substances (PFASs)*. OECD. https://doi.org/10.1787/59e7ffc6-en

OECD (2025). *Test No. 203: Fish, Acute Toxicity Test*. OECD Publishing. https://doi.org/10.1787/9789264069961-en

Park, H., Vecitis, C.D., Cheng, J., Choi, W., Mader, B.T. & Hoffmann, M.R. (2009). Reductive Defluorination of Aqueous Perfluorinated Alkyl Surfactants: Effects of Ionic Headgroup and Chain Length. *The Journal of Physical Chemistry A*, 113 (4), 690–696. https://doi.org/10.1021/jp807116q

PubChem (n.d.). *PubChem: PFAS and Fluorinated Compounds in PubChem*. https://pubchem.ncbi.nlm.nih.gov/classification [2026-04-07]

Qi, Y., Fu, P. & Volmer, D.A. (2022). Analysis of natural organic matter via fourier transform ion cyclotron resonance mass spectrometry: an overview of recent non-petroleum applications. *Mass Spectrometry Reviews*, 41 (5), 647–661. https://doi.org/10.1002/mas.21634

R Core Team (2025). R: A Language and Environment for Statistical Computing. R Foundation for Statistical Computing. https://www.r-project.org/

Rehnstam, S. (2023). PFAS Homologous Series. https://github.com/SRehns/PFAS-Homologous-series

Rehnstam, S., Czeschka, M.-B. & Ahrens, L. (2023). Suspect screening and total oxidizable precursor (TOP) assay as tools for characterization of per- and polyfluoroalkyl substance (PFAS)-contaminated groundwater and treated landfill leachate. *Chemosphere*, 334, 138925. https://doi.org/10.1016/j.chemosphere.2023.138925

Rhoads, K.R., Janssen, E.M.-L., Luthy, R.G. & Criddle, C.S. (2008). Aerobic Biotransformation and Fate of *N* -Ethyl Perfluorooctane Sulfonamidoethanol (*N* -EtFOSE) in Activated Sludge. *Environmental Science & Technology*, 42 (8), 2873–2878. https://doi.org/10.1021/es702866c

Schaefer, C.E., Choyke, S., Ferguson, P.L., Andaya, C., Burant, A., Maizel, A., Strathmann, T.J. & Higgins, C.P. (2018). Electrochemical Transformations of Perfluoroalkyl Acid (PFAA) Precursors and PFAAs in Groundwater Impacted with Aqueous Film Forming Foams. *Environmental Science & Technology*, 52 (18), 10689–10697. https://doi.org/10.1021/acs.est.8b02726

Schymanski, E.L., Jeon, J., Gulde, R., Fenner, K., Ru, M., Singer, H.P. & Hollender, J. (2014). Identifying Small Molecules via High Resolution Mass Spectrometry: Communicating Confidence. 2097–2098

Schymanski, E.L., Zhang, J., Thiessen, P.A., Chirsir, P., Kondic, T. & Bolton, E.E. (2023). Per- and Polyfluoroalkyl Substances (PFAS) in PubChem: 7 Million and Growing. *Environmental Science & Technology*, 57 (44), 16918–16928. https://doi.org/10.1021/acs.est.3c04855

Singh, R.K., Brown, E., Mededovic Thagard, S. & Holsen, T.M. (2021). Treatment of PFAS-containing landfill leachate using an enhanced contact plasma reactor. *Journal of Hazardous Materials*, 408, 124452. https://doi.org/10.1016/j.jhazmat.2020.124452

Singh, R.K., Fernando, S., Baygi, S.F., Multari, N., Thagard, S.M. & Holsen, T.M. (2019). Breakdown Products from Perfluorinated Alkyl Substances (PFAS) Degradation in a Plasma-Based Water Treatment Process. *Environmental Science & Technology*, 53 (5), 2731–2738. https://doi.org/10.1021/acs.est.8b07031

Smith, S.J., Lauria, M., Ahrens, L., McCleaf, P., Hollman, P., Bjälkefur Seroka, S., Hamers, T., Arp, H.P.H. & Wiberg, K. (2023). Electrochemical Oxidation for Treatment of PFAS in Contaminated Water and Fractionated Foam─A Pilot-Scale Study. *ACS ES&T Water*,. https://doi.org/10.1021/acsestwater.2c00660

Smith, S.J., Lauria, M., Higgins, C.P., Pennell, K.D., Blotevogel, J. & Arp, H.P.H. (2024). The Need to Include a Fluorine Mass Balance in the Development of Effective Technologies for PFAS Destruction. *Environmental Science and Technology*, (Ic), 0–3. https://doi.org/10.1021/acs.est.3c10617

Smith, S.J., Wiberg, K., McCleaf, P. & Ahrens, L. (2022). Pilot-Scale Continuous Foam Fractionation for the Removal of Per- A nd Polyfluoroalkyl Substances (PFAS) from Landfill Leachate. *ACS Environmental Science and Technology Water*,. https://doi.org/10.1021/acsestwater.2c00032

Stratton, G.R., Dai, F., Bellona, C.L., Holsen, T.M., Dickenson, E.R.V. & Mededovic Thagard, S. (2017). Plasma-Based Water Treatment: Efficient

Transformation of Perfluoroalkyl Substances in Prepared Solutions and Contaminated Groundwater. *Environmental Science & Technology*, 51 (3), 1643–1648. https://doi.org/10.1021/acs.est.6b04215

Strynar, M., Dagnino, S., McMahen, R., Liang, S., Lindstrom, A., Andersen, E., McMillan, L., Thurman, M., Ferrer, I. & Ball, C. (2015). Identification of Novel Perfluoroalkyl Ether Carboxylic Acids (PFECAs) and Sulfonic Acids (PFESAs) in Natural Waters Using Accurate Mass Time-of-Flight Mass Spectrometry (TOFMS). *Environmental Science and Technology*, 49 (19), 11622–11630. https://doi.org/10.1021/acs.est.5b01215

Sun, Z., Zhang, C., Xing, L., Zhou, Q., Dong, W. & Hoffmann, M.R. (2018). UV/Nitrilotriacetic Acid Process as a Novel Strategy for Efficient Photoreductive Degradation of Perfluorooctanesulfonate. *Environmental Science and Technology*, 52 (5), 2953–2962. https://doi.org/10.1021/acs.est.7b05912

Tan, S., Wang, R., Wang, K., Yang, Z., Chen, Y. & Zhang, Y. (2025). Unravelling the structure-dependent defluorination mechanisms of per- and polyfluoroalkyl substances by hydrated electrons in UV/sulfite. *Nature Water*, 3 (6), 734–745. https://doi.org/10.1038/s44221-025-00449-0

Tautenhahn, R. (2023). Compound Discoverer 3.3 SP2 released. *My Compound Discoverer*. https://mycompounddiscoverer.com/2023/04/12/compound-discoverer-3-3-sp2-released/ [2026-04-09]

Taylor, R.B. & Sapozhnikova, Y. (2022). Comparison and validation of the QuEChERSER mega-method for determination of per- and polyfluoroalkyl substances in foods by liquid chromatography with high-resolution and triple quadrupole mass spectrometry. *Analytica Chimica Acta*, 1230, 340400. https://doi.org/10.1016/j.aca.2022.340400

UNEP (2009). SC-4/17: Listing of perfluorooctane sulfonic acid, its salts and perfluorooctane sulfonyl fluoride. Stockholm Convention on Persistent Organic Pollutants.

Vakili, M., Cagnetta, G., Deng, S., Wang, W., Gholami, Z., Gholami, F., Dastyar, W., Mojiri, A. & Blaney, L. (2024). Regeneration of exhausted adsorbents after PFAS adsorption: A critical review. *Journal of Hazardous Materials*, 471, 134429. https://doi.org/10.1016/j.jhazmat.2024.134429

Veciana, M., Bräunig, J., Farhat, A., Pype, M.-L., Freguia, S., Carvalho, G., Keller, J. & Ledezma, P. (2022). Electrochemical oxidation processes for PFAS removal from contaminated water and wastewater: fundamentals, gaps and opportunities towards practical implementation. *Journal of Hazardous Materials*, 434, 128886. https://doi.org/10.1016/j.jhazmat.2022.128886

Wang, Y., Vestergren, R., Shi, Y., Cao, D., Xu, L., Cai, Y., Zhao, X. & Wu, F. (2016). Identification, Tissue Distribution, and Bioaccumulation Potential of Cyclic Perfluorinated Sulfonic Acids Isomers in an Airport Impacted

Ecosystem. *Environmental Science & Technology*, 50 (20), 10923–10932. https://doi.org/10.1021/acs.est.6b01980

Wickham, H., Averick, M., Bryan, J., Chang, W., McGowan, L., François, R., Grolemund, G., Hayes, A., Henry, L., Hester, J., Kuhn, M., Pedersen, T., Miller, E., Bache, S., Müller, K., Ooms, J., Robinson, D., Seidel, D., Spinu, V., Takahashi, K., Vaughan, D., Wilke, C., Woo, K. & Yutani, H. (2019). Welcome to the Tidyverse. *Journal of Open Source Software*, 4 (43), 1686. https://doi.org/10.21105/joss.01686

Yin, S., Calvillo Solís, J.J., Sandoval-Pauker, C., Puerto-Diaz, D. & Villagrán, D. (2025). Advances in PFAS electrochemical reduction: Mechanisms, materials, and future perspectives. *Journal of Hazardous Materials*, 491, 137943. https://doi.org/10.1016/j.jhazmat.2025.137943

Zhang, Z., Liu, Y., Chen, Y., Qu, H., Ma, J., Pang, M., Wang, B. & Yu, G. (2026). Per- and polyfluoroalkyl substances in the environment and human tissue: A critical review of distribution, exposure pathways, and health risks. *Environmental Pollution*, 397, 127988. https://doi.org/10.1016/j.envpol.2026.127988

Zhao, S., Zhou, T., Wang, B., Zhu, L., Chen, M., Li, D. & Yang, L. (2018). Different biotransformation behaviors of perfluorooctane sulfonamide in wheat (Triticum aestivum L.) from earthworms (Eisenia fetida). *Journal of Hazardous Materials*, 346, 191–198. https://doi.org/10.1016/j.jhazmat.2017.12.018

Zhao, W. & Sun, J. (2018). Triflimide ($HNTf_2$) in Organic Synthesis. *Chemical Reviews*, 118 (20), 10349–10392. https://doi.org/10.1021/acs.chemrev.8b00279

Zweigle, J., Bugsel, B. & Zwiener, C. (2023). Efficient PFAS prioritization in non-target HRMS data: systematic evaluation of the novel MD/C-m/C approach. *Analytical and Bioanalytical Chemistry*, 415 (10), 1791–1801. https://doi.org/10.1007/s00216-023-04601-1

Popular science summary

Chemicals created by humans are generally designed for a specific purpose. Medicines have been developed to treat an illness; flavour agents have been synthesised to produce certain taste; coatings, such as on 'non-stick' pans, have been designed to prevent materials from adhering. The latter is made accessible mainly from the emergence of a new class of fully synthetic chemicals in the 20th century: per- and polyfluoroalkyl substances (PFAS). These compounds possess highly useful properties and are therefore widely used in industry.

The usefulness of PFAS can largely be summarised by two key properties. Firstly, PFAS are extremely persistent due to the presence of the carbon-fluorine bond, one of the strongest in organic chemistry. Secondly, many PFAS exhibit surfactant properties, enabling them to repel both water and oils These properties make PFAS very useful, for example in non-stick coating for frying pans (Teflon™), and waterproof textiles in outdoors clothing (GoreTex™), where durability and resistance to degradation are essential.

However, these same properties also make PFAS problematic. Since PFAS are so persistent, they will not readily degrade in the environment and instead slowly accumulate over time. Their chemical stability and widespread use have led to their global presence. PFAS have been detected in soil, water, wildlife across all levels of the food chain, and in humans. PFAS are even found in remote areas such as the Arctic region, including in water, soil, ice, and in polar bears. Although restrictions on specific PFAS have been proposed, industry can often replace one PFAS with another structurally similar compound, resulting in the presence of an estimated more than 10000 PFAS in commercial products. To address this issue, research is needed to develop technologies capable of destroying PFAS and ultimately converting them into harmless mineral products.

This PhD thesis investigates advanced destructive techniques, including electrochemical oxidation, ultraviolet degradation, and plasma-based degradation. While these methods aim to fully break down PFAS, they differ in how reactive species are generated to drive degradation.

A key finding of this work is that these treatments do not only destroy PFAS but can also generate transformation products (TPs), which are essentially unwanted byproducts of incomplete degradation or side reactions.

What's even worse is that these TPs are often difficult to detect and are not captured by conventional monitoring methods, which typically rely on known reference standards of PFAS. As a result, treatment efficiency may be overestimated if only known PFAS are measured.

In this thesis, high-resolution mass spectrometry was used to detect and identify unknown PFAS-related compounds formed during treatment. This led to the discovery of new, previously undiscovered PFAS, which were further evaluated using computational tools to estimate their potential toxicity. The main conclusion from this thesis was that surrounding water composition, known as the matrix, will heavily influence the formation of TPs. In some cases, TPs were created due to the matrix present in the samples. But there were also TPs that were created through reactions involving other substances present in the water, including previously unrecognised precursor materials.

The study also showed that simpler experimental systems can behave differently. In ultraviolet degradation experiments using pure water, fewer distinct TPs were observed based on molecular formulas. However, many of these compounds existed as different structural isomers, meaning they shared the same formula but had different arrangements of atoms. This extensive isomer formation had not been described in previous studies.

To summarise, PFAS are highly persistent environmental contaminants that continue to accumulate globally despite regulatory efforts. To reduce the amount of PFAS to enter the environment, new treatment techniques are in development, but these processes can generate previously unknown TPs. This work improves understanding of how PFAS break down under different conditions and highlights the importance of identifying not only the original compounds but also their TPs. Ultimately, this knowledge can support the development of more effective and safer PFAS treatment strategies, contributing to improved protection of human health and the environment.

Populärvetenskaplig sammanfattning

Kemikalier som människor designar tas fram för att uppfylla en särskild funktion eller ha en önskad egenskap. Mediciner är gjorda för att bota sjukdom, konstgjorda smakämnen ska smaka som något specifikt och teflonpannans yta har noggrant designats för att inget ska fastna. På 1900-talet designades en helt ny klass av syntetiska kemikalier, nämligen per- och polyfluorerade alkylsubstanser, oftast förkortat som PFAS.

PFAS unika egenskaper har lett till en mycket bred användning inom många industrisektorer. En av egenskaperna som har gjort dem så eftertraktade är deras persistens. I PFAS-molekyler finns bindningar mellan kol och fluor, den starkaste bindningen man känner till inom organisk kemi. Den är så stark att PFAS är tåliga mot både höga temperaturer och kemiska reaktioner. Den andra önskvärda egenskapen är att de kan stöta bort både fett och vatten. När dessa två egenskaper kombineras uppstår många olika användningsområden. Ett exempel är Teflon™ som finns på stekpannor som en non-stickbeläggning. Ett annat exempel är beläggningar i friluftskläder, som Gore-Tex™, som ger kläder och skor vattentäta egenskaper och bibehåller sitt skydd även efter lång användning.

Tyvärr är det de användbara egenskaperna som också skapar en problematik med PFAS. På grund av att de är så stabila bryts de inte ner på naturlig väg i miljön. På så sätt så ackumulerar mängden av PFAS i vår miljö. PFAS är så spridda att de har upptäckts nästan överallt på jorden, även i avlägsna områden, så som Arktis, där PFAS hittats i allt från både vatten, is och isbjörnar. PFAS hittas i alla delar av miljön och även i människor. Trots försök att reglera PFAS har industrin ofta kunnat ersätta förbjudna eller reglerade PFAS med andra, strukturellt liknande PFAS. Det är därför absolut nödvändigt att behandla PFAS och bryta ner dem.

Denna doktorsavhandling undersöker avancerade reningstekniker för PFAS, och då speciellt tre nedbrytningstekniker: elektrokemisk oxidering (EO), ultraviolett strålning (UV) och plasmadegradering. Avhandling handlar dock inte om själva reningsteknikerna utan om biprodukter som de oavsiktligt kan skapa. Ett av de viktigaste fynden i avhandlingen var att stabila transformationsprodukter (TP), som klassas som PFAS-ämnen, kan bildas vid rening av vatten. Problemet med dessa ämnen är att de inte är kända sedan tidigare – man har helt enkelt inte letat efter dem. Bildning av stabila TP vid vattenrening innebär att om en reningstekniks effektivitet mäts

med klassiska metoder, det vill säga man letar bara efter kända PFAS, kan PFAS-reningen överskattas då dessa metoder inte omfattar TP.

I denna avhandling användes högupplöst masspektrometri för att detektera och identifiera okända PFAS-relaterade ämnen som bildats vid behandlingsprocesserna. Detta ledde till fynd av tidigare okända PFAS, som sedan också blev analyserade med beräkningsmodeller för att uppskatta deras toxicitet. Ett av de viktigaste fynden var att vattnets kemiska sammansättning, den så kallade matrisen, har ett stort inflytande på vilka typer av TP som kan bildas. I vissa fall skapades TP direkt från matrisen. I andra fall reagerade PFAS med matrisen, med hjälp av behandlingstekniken, för att skapa nya TP.

En del av avhandlingen visade att även enkla experimentella system kan uppföra sig på ett komplext sätt. I experimenten som utfördes med UV-strålning observerades färre TP med unika summaformler. I stället hade de bildade TP strukturella skillnader; det bildades ett antal så kallade isomerer. Det betyder att trots att de har samma uppsättning av atomer så skiljer sig själva molekylstrukturen åt. Denna omfattande bildning av PFAS-isomerer som visas i avhandlingen har inte tidigare beskrivits i vetenskaplig litteratur.

För att summera, PFAS är mycket persistenta miljöföroreningar som ackumulerar globalt trots att de regleras. För att minska mängden PFAS som släpps ut i miljön så utvecklas nya reningstekniker. Dessa tekniker kan dock bilda nya, tidigare okända TP. Denna avhandling ökar vår förståelse för hur PFAS bryts ner under olika förhållanden, och understryker hur viktigt det är att inte bara mäta kända PFAS som finns i vattnet innan reningen utan även nybildade TP efter behandlingen. Slutligen kan denna kunskap stötta utvecklingen av mer effektiva och säkra reningsstrategier för PFAS, vilket i sin tur leder till bättre skydd av människors hälsa och miljön.

Acknowledgements

This thesis marks an official end to my time as a student. It has been a long road to get to where I am now. I am eternally grateful for all the opportunities that have been presented to me during my time before my PhD and during my PhD. I am especially grateful for the people I have met during my time as a PhD student. Thank you all for being such a positive force in my life.

First, I must express my most sincere gratitude to **Lutz** for wanting me to take on this project. As I have understood it, it was not an originally planned project, but something you came up with yourself. Giving me the opportunity to do this with you has been a once in a lifetime opportunity for me. This was my first real exposure to the world of PFAS, and I will never forget this abbreviation for the rest of my life. You have my sincere thanks for always pulling me back to reality after spending so much time looking at mass spectra. There is a real-life reason for looking at these spectra after all, and you always had a way of reminding me that the work is more than just drawing structures.

Foon, thank you for always being willing to support me. I hope that in the future we can work more together and make some great research. Thank you for sharing your experience in Belgium with me. Please do not hesitate to ask me to bring something back if there is anything you miss from there, I would be more than happy to get it for you.

I don't think I have ever made as many professional contacts in my life before you helped me get involved with the CRISIS project, **Karin**. For that I am extremely grateful. You have helped me put my name out there and I believe many Swedish government agencies know of me now all thanks to you presenting this opportunity to me. I hope to have represented you and your POPs group in a good light these last few years and hope to continue to do so in the future. Tack så mycket.

Thank you to my external collaborators **Zongsu Wei, Shuang Luo,** and **Selma Mededovic Thagard** for providing samples for me to analyse. Writing this thesis would not have been possible without your contributions.

Collaborations are essential for academia and for our continuous work on making our planet just a little bit better.

Thank you **Jennifer Field** for agreeing to be my opponent. I hope we will have a fruitful discussion about all the different PFAS that are out there when we meet. Hopefully Sweden will provide some good weather during your stay here.

For my lab manager **Mia,** thank you for taking care of me and the rest of the group. I know we are only slightly more organised than a preschool so please understand that I really mean it when I say thank you for your patience. Also, thanks for the cake!

To the original PFAS group that was there when I started. **Sanne** thank you for giving me your samples. I am very glad that I did not need to do any SPE for my PhD project (hahaha). Hopefully we can see each other soon at a conference, I promise I'll try to make it to the next SETAC. **Björn** thanks for the time we spent in the office together, the time in the black hole, the good times outside work as well. **Paul**, you weren't part of the PFAS group, but this trio feels natural, so you are getting grouped together. It is funny how we started almost the same week and still did not manage to finish at the same time. I am glad that we got to collaborate just before you were finished here.

(Spanish) Alberto, thank you so much for all the time you spent with me. It has been such a pleasure working with you, as well as hanging out outside of work. The conferences we went to together were highlights for me. It was always great traveling with you. You were also always a source of wisdom, for which I am eternally grateful. I must say I'm sorry for not working in the fox into my thesis, I just couldn't make it fit. Maybe look carefully during the defence to find the fox. Also, there are some samples that need running on IMS, so I have no choice but to come over some time to visit you, maybe it would be best in November or what do you say ;)

To the Italian Mafia, thank you for welcoming me when I first started here. It was so great to make friends so quickly and spend so much time outside of work with you. **Alberto**, my very dear office mate. Thank you for telling

me if there is wifi. Because of you I can immediately recognise clear cutting when I see it. Also thank you for being such a good friend, I hope we can keep in contact for many more years. Need to see Lake Como soon! **Carlotta**, the absolute no-nonsense from you was always sobering to hear. You are such a genuine person, and I have greatly appreciated our friendship, thank you for that. Congratulations on becoming a mother, I hope to see your little baby soon. **Valentina**, the shrimp queen, how many hours have we spent in the black hole? Probably too many, with not enough oxygen. Thanks for the karaoke nights, making me wake up the next morning with a sore throat from all the singing.

Kong, I almost wanted to put you in with the Italian Mafia because you were honestly one of the key members, despite not being Italian. An excellent office mate. Even though some would say you, Alberto, and I would never get any work done sharing an office. Look how we proved them wrong! At least two doctors have been produced from that office, so it can't be all that bad. Thanks for the many late nights that originally started out as "we are only having one then going home". Your friendship has been one of the highlights throughout my time as a PhD. Rise up? **Sammi**, I couldn't think of someone better to complement Kong than you. I'm so glad I got to meet you and that we can be friends. You and Kong finally living in the same country is also something I am very happy about. Wish you the best and I will come see you in Helsinki soon.

Daniel, thank you for being the one person to understand what I was talking about when referencing a video uploaded to the internet 10 years ago. I think when I started, we were the only metal heads in the group, us metalheads got to stick together. You're such a great person, I can't wait to see what the next chapter of your life will look like. Just know I will be cheering for your success.

Oscar, thank you for always being such a happy and great guy. Even when you were out working the fields in the rain, you still managed to come back with a smile. That was always so nice to see. Honourably, you were also always down to grab a beer despite living so far away. That's real dedication. You and **Vilma** are so great together and I'm glad to be friends with both of

you. I am also glad I'll be able to spend so much more time with you, as our stories don't end here. Let's make it a good one.

My current office mates **Maxi** and **Harold**. Just know that this office that we share has a very high success rate, so do not worry. You are in a good place, and I know both of you will finish your PhD with flying colours. Hopefully we can stay together as office mates just a little bit longer after I graduate. **Alina**, thank you for being such a cool researcher. You really have mastered a balance by both hanging with the PhDs and with the permanent staff. The passion and energy you bring is truly inspiring. **Georgios**, I don't know if there can exists a cooler post-doc, super nerdy and super hip at the same time, how do you do it? I am happy for your researcher position you got here, and even more happy for you for getting such a great grant. I am grateful that we will get to spend more time here at SLU together. **Patrick**, your presence here has been a greatly positive one. Thank you for organising hotpot and mahjong nights. Let's play again soon, and then I won't let you beat me. **Bent**, probably the only other person in this part of the country that knows where Vlissingen is. Thanks for all the good times, and the good jokes we've had around the lunch and coffee table. Leuk.

To the rest of the POPs group. Thank you all for the time I've had here. This group should not be taken for granted. Both for the academic achievements and for the kindness I have seen. Thank you all.

Sicong and **Jenny.** Thank you so much for being such great friends. I have never met people before that are so caring and thoughtful as you two are. You always inspire me to be as good of a person as you two are, and that I really mean. **Sicong**, I really hope we can become co-workers in the future, so get started on those grants for Formas! I miss you, but I know I will get to see you soon. Let me show you some of my new recipes when you come back. **Jenny**, we are going to take over all of SLU soon. Thanks for being my friend and let's keep supporting each other with both of our partners being in other countries! Also let's keep cooking good food for each other.

Bozhi, I don't think you know what you did to my world when you served me 辣子鸡 for the first time. Ever since I've been crazy for this recipe and that prompted me to learn a whole different world of cooking. Also, you are

one of the most kindhearted people I know. And I say that even after the massage I had in your hometown, so you know I'm being serious. Thank you for being my friend. I know you are doing so much good at your work now, but I still hope you can come back to Sweden soon.

Minli, I am glad we could bond over our love for spicy food and tasty beer. It's been great knowing you this whole time. You're so hard working, which is so inspiring, but I also think you deserve a rest soon. I am sure Reiner appreciates and recognises the hard work you put in. Let's eat more spicy food and drink many more beers soon.

To my unofficial football coach **Arief**. Thank you for being my friend. We have had so much fun together, and I'm glad I got to meet you through Gupta FC (big fan). The last couple of years here would not have been the same without you. I know you're going to do so well in Japan. **Princess**, you already know I need to say thanks for the big energy you provide. All I can say is that if you look up "girlpower" in the dictionary, your face is 100 % going to be there. Thanks for all the good times and dinners we've had. Slay Kween! **Leigh-Anna**, I am sad to not have you here for my defence, but I understand you have to slay in the USA. Thanks for all the good times and thanks for inviting me to be a member of Whiskey Nation. Hope to see you back in Sweden sometime soon.

Nick, it's been over ten years that we've known each other now. Thank you for still being my friend despite how much I annoy you all the time. Just know I do enjoy your rants very much. Always looking forward to seeing you when I visit Brussels. **Mike**, thanks for the fun banter you give, and the banter you can take too. It was really fun living together, but I never want to do it again. So happy for you, **Kamila**, and **Bruce**. **Ivan**, thanks for being so cool and always taking it easy. That can't be easy when you are hanging out with us. You, **Cate**, **Adam**, and **Jordan** are all amazing. Let's see each other soon. **Elan**, my mum's "eggboy", it's been great to get to know you. Thanks for always being such a good sport. Next time let's go to the correct restaurant in Berlin.

To my dearest **Catherine**. Thank you for being a never-ending well of knowledge. Even if it's not your field you always help and give feedback to

whatever I throw your way, and it is always incredibly good feedback that I get back. Your morals and principles are a constant source of inspiration for me, and something I strive for in everyday life. I can't say enough how happy I am to be with you and all the support you have provided me throughout the years. I love you. Also, thank you to the Johnson family who have welcomed me with open arms making me feel so incredibly welcome and part of the family. Thank you **Annie**, **John**, **Jack**, and **Ringo**.

Thank you to all my day-1's, the Viken crew. One can't ask for a better extended (unofficial) family. I look forward to seeing you all every year and hearing what goes on in your lives. Thank you all for being such a big and lovely part of my life. So, thank you **Alex**, **Fredde**, **Helen**, **Vicki**, **Micke**, **Katarina**, **Ola**, **Thina**, **Filip**, **Adam**, **Calle**, **Pia**, och **Peter**.

Thank you to my very long list of cousins and other family members. On my father's side of the family, I want to thank **Guje, Gösta, Anna, Malin, Charles, Daniel, Edward, Felix, Alma, Viggo,** och **Ebbe**. On my mother's side of the family I want to thank **Lollo, Calle kusin, Jessica, Josefin, Hanna, Daniel, Fredrik, Helmer, Axel, Philip, Nicolina, Felix, Willhelm, Filippa,** och **Ludwig**.

Finally, I must say thank you to my family. **Mamma, Pappa, Ebba,** och **Maja**. Thank you for all the years of support and love. Thank you to **Sebbe**, I finally have a real legal brother (in-law) and I am so happy it's you. Thanks to **Elias** for giving my dad some ice hockey passion again, and for being an incredibly sweet guy. I am very happy you and Maja are together. Jag älskar er.

I

Chemosphere 334 (2023) 138925

Contents lists available at ScienceDirect

Chemosphere

journal homepage: www.elsevier.com/locate/chemosphere

Suspect screening and total oxidizable precursor (TOP) assay as tools for characterization of per- and polyfluoroalkyl substance (PFAS)-contaminated groundwater and treated landfill leachate

Svante Rehnstam *, Mai-Britt Czeschka, Lutz Ahrens

Swedish University of Agricultural Sciences, Department of Aquatic Sciences and Assessment, Box 7050, 750 07 Uppsala, Sweden

HIGHLIGHTS

- Total Oxidizable Precursor assay for characterizing precursors and persistent PFAS
- Suspect screening revealed 29 persistent PFAS with High-Resolution Mass Spectrometry
- Levels of PFAS in landfill leachate and groundwater determined with MS/MS
- Semi-quantification of PFAS not commonly covered in targeted methods

GRAPHICAL ABSTRACT

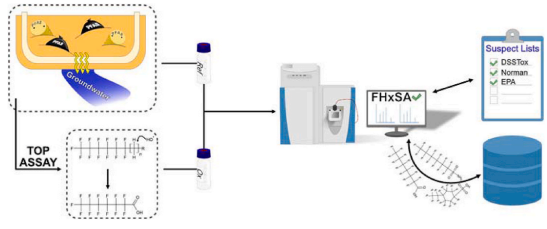

ARTICLE INFO

Handling editor: Myrto Petreas

Keywords:
Per- and polyfluoro alkyl substances
High-resolution mass spectrometry
Suspect screening
Total oxidizable precursor assay

ABSTRACT

Landfill facilities are a major source of release of per- and polyfluoroalkyl substances (PFAS) to the surrounding environment. In this study, landfill leachate treated in a conventional wastewater treatment plant and PFAS-contaminated groundwater were subjected to suspect screening analysis and semi-quantification using total oxidizable precursor (TOP) assay and liquid chromatography coupled to high-resolution mass spectrometry (LC-HRMS). TOP assays yielded expected results for legacy PFAS and their precursors, but showed no discernible evidence of degradation of perfluoroethylcyclohexane sulfonic acid. TOP assays also produced significant evidence of presence of precursors in both treated landfill leachate and groundwater, but the majority of precursors had probably degraded into legacy PFAS after many years in the landfill. Suspect screening identified a total of 28 PF AS, of which six were not included in the targeted method and were identified with confidence level (CL) $\geq$3. Semi-quantification of these six compounds showed very low concentrations, indicating that they are not as great a concern as the target PFAS.

1. Introduction

Per- and polyfluoroalkyl substances (PFAS) are a class of anthropogenic chemicals characterized by a $-CF_2-$ or $-CF_3$ moiety according to the OECD definition (OECD. Reconciling Terminology of the, 2021). PFAS are potential toxic, bioaccumulative, and typically extremely persistent (Podder et al., 2021), and display hydrophilic and hydrophobic properties (Gallen et al., 2017). They are used in many consumer

* Corresponding author. Swedish University of Agricultural Sciences, Department of Aquatic Sciences and Assessment, Box 7050, 750 07 Uppsala, Sweden.
E-mail address: svante.rehnstam@slu.se (S. Rehnstam).

https://doi.org/10.1016/j.chemosphere.2023.138925
Received 14 February 2023; Received in revised form 9 May 2023; Accepted 11 May 2023
Available online 13 May 2023

products and industrial applications, such as non-stick coating on cookware, food packaging, waterproof coating on outdoor clothes, aqueous film-forming foams (AFFF), functional fluids for machinery, and anti-corrosion agents (Sajid and Ilyas, 2017; Zabaleta et al., 2017; Kotthoff et al., 2015; Houtz et al., 2016; Glüge et al., 2020). The stability and persistence of PFAS has led to their widespread distribution in biota, sediment, soil, fresh and marine water, and groundwater (Nakayama et al., 2019). Typical sources of PFAS in the aquatic environment are municipal and industrial wastewater treatment plants (WWTPs) and landfill facilities (Letcher et al., 2015). Due to the widespread pollution and their toxic properties, PFAS are being partly phased out or increasingly regulated (Gobelius et al., 2018). Monitoring of PFAS by environmental agencies, drinking water plants, WWTPs, and other facilities typically takes the form of targeted analysis using liquid chromatography coupled with mass spectrometry (Mulabagal et al., 2018a). In such monitoring studies on water matrices, a few dozen PFAS are usually included (Mulabagal et al., 2018b), but this represents only a small fraction of the >5000 different PFAS listed by the OECD and in other recent studies (OECD. Reconciling Terminology of the, 2021; Barnabas et al., 2022). Analytical challenges include a lack of authentic standards for non-legacy PFAS and of characterization tools for identification of PFAS in water samples (Ruyle et al., 2021).

Many non-legacy PFAS, so-called PFAS precursors, are not fully fluorinated and can degrade to more persistent PFAS, such as perfluoroalkane sulfonic acids (PFSA) and perfluoroalkyl carboxylic acids (PFCA), which can be detected with target analysis methods (Taylor and Sapozhnikova, 2022). The presence of PFAS precursors can be confirmed using a total oxidizable precursor (TOP) assay, which transforms PFAS precursors into legacy PFAS that can be detected with target analysis methods (Houtz and Sedlak, 2012). However, some studies have investigated the type of PFAS precursors oxidized during TOP assays, mostly by using advanced statistical analyses on observed yields after oxidation, which vary depending on whether the PFAS precursors were produced by fluorotelomerization or electrochemical fluorination (Ruyle et al., 2021; Cortés-Francisco and Caixach, 2015). In addition, most TOP assays to date have been performed on biota, surface water, and AFFF, while studies on wastewater matrices originating from treated landfill leachate are lacking (Ruyle et al., 2021; Koch et al., 2019; Shojaei et al., 2022; Houtz et al., 2018).

A drawback of the TOP assay is that only PFAS which degrade during the oxidization process and can be detected using target analysis methods are considered, whereas for identification of PFAS molecules high-resolution mass spectrometry (HRMS) methods are needed (Krauss et al., 2010). The high resolving power (>10,000) and high mass accuracy (≤5 parts-per-million (ppm)) of HRMS allows a molecular formula to be assigned to observed *m/z* (Gross, 2017; Liu et al., 2015; Menger et al., 2020). With HRMS, it is possible to employ suspect screening, which relies on accurate masses that are matched to suspect lists containing monoisotopic masses. On the other hand, targeted analysis use reference standards to analyze the target chemicals specifically with retention times and mass spectra. Non-target screening is also a common HRMS technique, which uses prioritization and data-filtering strategies for identification of PFAS (Myers et al., 2014). A commonly used method for prioritization and characterization of PFAS is to calculate Kendrick mass defects, which are derived from the difference between the exact and nominal mass of fluorine. This allows for easy identification of homologous series of PFAS with varying chain length and commonly detected PFAS fragments (e.g., C_2F_5) (Kendrick, 1963; Strynar et al., 2015). Combined suspect and non-target screening has become a widely used method in environmental analytical chemistry, due to the sensitivity, reproducibility, and selectivity it can provide (Nakayama et al., 2019; Liu et al., 2019). However, few studies have applied suspect and non-target screening to matrices such as treated landfill leachate and the groundwater impacted by landfills (Gago-Ferrero et al., 2015).

The overall aim of this study was to identify new PFAS in two complex matrices, groundwater and WWTP-treated landfill leachate, at a landfill site in Sweden. Specific objectives were to (1) investigate degradation of PFAS precursors and legacy PFAS in TOP assays; (2) develop a simple suspect screening workflow for identification of PFAS in complex aqueous matrices; (3) perform prioritization of PFAS based on Kendrick mass defects and homologous series; and (4) identify PFAS with the highest level of confidence possible and semi-quantify their concentrations.

2. Materials and methods

2.1. Target PFAS

In total, 29 PFAS were selected for target analysis, comprising 11 (C_3–C_{13}) perfluoroalkyl carboxylic acids (PFCA) (PFBA, PFPeA, PFHxA, PFHpA, PFOA, PFNA, PFDA, PFUnDA, PFDoDA, PFTriDA, PFTeDA), eight (C_4–C_{10}) perfluoroalkane sulfonic acids (PFSA) (PFBS, PFPeS, PFHxS, PFHpS, PFOS, PFNS, PFDS, PFECHS), three *n*:2 fluorotelomer sulfonates (FTSA) (4:2 FTSA, 6:2 FTSA, 8:2 FTSA), two compounds of F–53 B (9Cl-PF3ONS, 11Cl-PF3OUdS), GenX (HFPO-DA), FOSA, MeFOSAA, EtFOSAA, and NaDONA. In addition, two n:2 fluorotelomer phosphate diesters (6:2 diPAP, 8:2 diPAP) were used for TOP assay experiments. For details, full names, and abbreviations, see Table S1 in Supporting Information (SI). For quantification, 20 internal standards (IS) from an IS mixture were added to the calibration standards and samples before extraction (Wellington Laboratories). These were: $^{13}C_4$-PFBA, $^{13}C_5$-PFPeA, $^{13}C_5$-PFHxA, $^{13}C_4$-PFHpA, $^{13}C_8$-PFOA, $^{13}C_9$-PFNA, $^{13}C_6$-PFDA, $^{13}C_7$-PFUnDA, $^{13}C_3$-PFDoDA, $^{13}C_2$-PFTeDA, $^{13}C_3$-PFBS, $^{13}C_3$-PFHxS, $^{13}C_8$-PFOS, $^{13}C_2$-4:2 FTSA, $^{13}C_2$-6:2 FTSA, $^{13}C_2$-8:2 FTSA, $^{13}C_8$FOSA, D_3-MeFOSAA, D_5-EtFOSAA, and $^{13}C_3$–HFPO-DA (for details on abbreviation names and IS purity, see Tables S1 and S2 in SI).

2.2. Sample collection

Treated landfill leachate and groundwater samples were collected at the Hovgården landfill site outside Uppsala, Sweden, in November 2021, using polypropylene bottles. The landfill has opened in 1971 and is still actively used to store mainly ashes from domestic waste incineration. All samples were filtered through Whatman® glass microfiber filters (47 mm diameter, 0.7 μm pore size) and stored at −20 °C until analysis.

2.3. Total oxidizable precursor assay

Before the TOP assay, each sample was split in two. One half was used for the TOP assay and the other was analyzed directly using a targeted PFAS method (used as reference). Both the TOP assay samples and the reference samples were analyzed in triplicate (see Section 2.4). In addition, procedural blank samples were prepared by adding equivalent volumes of Milli-Q water to sample containers. For the precursor analysis, three PFAS precursors (6:2 diPAP, 8:2 diPAP, EtFOSA) and three legacy PFAS (PFECHS, PFUnDA, PFTriDA) were spiked individually into Milli-Q water, to a final concentration of 5 ng/mL, and all samples (TOP assay and reference) were prepared and analyzed in duplicate.

The TOP assay was performed as previously described (Houtz and Sedlak, 2012). In brief, each sample and a blank for each sample were spiked with 1.6 g potassium persulfate (ACS reagent grade, Sigma-Aldrich) and 1.52 mL of 10 mol/L sodium hydroxide monohydrate solution (Suprapur, Merck). The samples were sonicated for 5 min and then placed in a water bath held at 85 °C for 5 h. To stop the reaction, the samples were placed in an ice-bath and the pH was adjusted by adding 300 μL of 30% hydrochloric acid (Suprapur, Merck).

2.4. Sample extraction

Before extraction, 100 μL of IS mixture (c = 50 ng/mL for each IS)

were added to the sample, which was then sonicated for 5 min. Extraction was performed using solid-phase extraction (SPE) with Oasis WAX cartridges (6 mL, 150 mg, 30 μm). After pre-conditioning with 4 mL 0.1% (w/w) ammonium hydroxide in methanol, 4 mL methanol, and 4 mL Milli-Q water, 100 mL of sample were loaded on the cartridge, which was eluted under vacuum at approximately one drop per second. The cartridge was then washed with 4 mL of 25 mM ammonium acetate buffer dissolved in Milli-Q water and dried under vacuum. The sample was eluted into a 15 mL polypropylene (PP) tube with 4 mL methanol, and then 4 mL 0.1% ammonium hydroxide in methanol. To concentrate the final sample, a gentle stream of nitrogen was directed above the PP tube and the sample was concentrated to just below the 1 mL mark. The extract was transferred to a 1.5 mL PP vial.

2.5. Targeted PFAS analysis

Targeted PFAS analysis was carried out using a SCIEX ExionLC Triple Quad 3500 liquid chromatograph coupled to a tandem mass spectrometer (LC-MS/MS), which was operated in negative ionization mode. Injection was performed in triplicate with 20 μL of extracted sample onto a Phenomenex Kinetex (2.0 × 4 mm, 1.7 μm) C18 pre-column, and separation on a Phenomenex Gemini 3 μm C18 (2.0 × 50 mm) analytical column at a constant temperature of 40 °C. The mobile phase consisted of 10 mM ammonium acetate in Milli-Q water and methanol, the flow rate was set 600 μL/min, and the final run time was 9 min. The initial gradient conditions were held at 5% organic modifier for 0.1 min, which was increased to 55% after another 0.1 min. The gradient was then increased to 99% over 4.4 min, held for 3.5 min, decreased to 5% over 0.5 min, and held for an additional 0.5 min (for details of the targeted analysis, see Smith et al. (2022)).

Analysis of variance (ANOVA) was used to compare PFAS concentrations before and after TOP assays for the treated landfill leachate and groundwater samples, with significance level $\alpha = 0.05$. In some cases, a compound was not detected in all 18 analyses due to being below LOQ. To not exclude too many compounds, compounds that were detected in at least 17 of the 18 samples and replicates were included in ANOVA. All compound data used were tested for normal distribution using quantile-quantile plots.

2.6. Suspect screening using high-resolution mass spectrometry

Suspect screening of PFAS on the reference samples was performed using a Vanquish Horizon UHPLC system coupled to a QExactive Focus Orbitrap mass spectrometer (Thermo Fisher Scientific, Bremen, Germany) equipped with an Ion Max heated electrospray ionization source (HESI-II) operated in negative ionization mode. Injection was performed with 10 μL of extracted sample, onto a Waters ACQUITY UPLC C18 1.7 μm (2.1 × 50 mm) analytical column equipped with a ACQUITY UPLC C18 1.7 μm guard column, at a constant temperature of 40 °C. The mobile phase consisted of 5 mM ammonium acetate in Milli-Q water and methanol, using a flow rate of 300 μL/min, with a final run time of 17 min. The initial mobile phase composition was set to 10% organic modifier, which was held for 1 min. Next, a gradient was applied, with a final composition of 95% organic modifier over 12 min, which was held for 2 min. Initial conditions were then applied over 0.1 min and held for 1.9 min. The ion source settings were as follows: sheath and auxiliary gas flow rate was set at 30 and 10 arbitrary units, respectively; spray voltage was set to 3.70 kV; capillary and auxiliary gas heater temperature were both set to 350 °C; and S-lens RF level was set at 55 arbitrary units. The instrument was run using data-dependent acquisition (top N DDA, $n = 3$) in *discovery* mode with resolution of 35,000 at 200 m/z, with a full scan ranging from 120 to 1000 m/z using resolution of 70,000 at 200 m/z. The analysis was performed in two injections on the LC-HRMS, one with stepped absolute collision energies of 20 and 60 eV, and one with stepped absolute collision energies of 10 and 20 eV.

2.7. Quality assurance and quality control

Blank samples (one for TOP assay, one for reference samples, one for the laboratory equipment) were spiked with IS prepared under the same conditions as for the TOP assay or natural samples. Procedural and instrumental blanks were analyzed with the same HRMS methods as the samples, to measure contamination and background signals. Treated leachate and groundwater samples were extracted in triplicate and PFAS precursor-spiked samples were extracted in duplicate, for reproducibility. For quantification of PFAS, the limit of detection (LOD) and limit of quantification (LOQ) were calculated by integrating the signal in the solvent blank:

$$LOD = c(Blank) + 3 \times SD$$

$$LOQ = c(Blank) + 10 \times SD$$

The quality of the TOP assay was checked in an experiment where the calibration curve was spiked into Milli-Q water. The results are shown in Table S3 in SI.

2.8. Orbitrap MS data analysis

The data obtained were processed with Compound Discoverer 3.3 (CD) using a suspect screening workflow tailored for PFAS (Table S4 in SI). Peak picking and deconvolution of the data were performed in this software, where to be considered a feature had to have a signal to noise (S/N) ratio >3 and signal intensity >10,000 counts. Blanks were included with the requirement that a feature had to be five-fold higher in the sample than in the blank. A suspect list with 4676 features was obtained from the Norman Network Substance Database and used as a mass list in Compound Discoverer 3.3. (NORMAN Substance Database) The software matched the accurate masses obtained from the HRMS data and compared these to the monoisotopic masses in the suspect list. The software also allowed use of ChemSpider for connection to various databases (EPA DSSTOx, EPA Toxcast, FDA, Massbank, Molbank, Pubmed, Royal Society of Chemistry, and Sigma-Aldrich) to compare the accurate masses obtained against the monoisotopic mass of known compounds. After the observed accurate masses were matched with monoisotopic masses from the suspect list, the annotated structures of the compounds which had MS (Podder et al., 2021) spectra were automatically evaluated with a CD algorithm running in the background, which gave a score based on how probable the annotation was estimated to be. Additionally, mzCloud, a Thermo Fisher mass spectral database, was used to compare the MS (Podder et al., 2021) spectra obtained to their own curated MS (Podder et al., 2021) spectral library, where a score was given based on the similarity of the spectra. The software was also used to calculate chemical formula when any of the previous methods of identification failed. Once compounds were annotated, the annotation was compared to the predicted isotopic pattern and given a score based on that, which was also visualized when viewing the mass spectra in the software. For all annotation methods, mass accuracy of 3 ppm in full scan was required. Kendrick mass defects (KMD) were calculated for all annotated features, in the case of CF_2 with normal rounding of the values. Fragmentation flagging was also performed with the *Compound Classes* node. CnF_{2n+1}, $CnF_{2n\text{-}1}$, $CnF_{2n\text{-}3}$, $CnF_{2n\text{-}7}$, $CnF_{2n\text{-}11}$, and $CnF_{2n+1}O$ fragments were screened, with n ranging from 1 to 7, 2 to 10, 3 to 11, 5 to 11, 7 to 12, and 1 to 3, respectively. Neutral losses were screened for in the MS (Podder et al., 2021) spectra. Losses from head groups such as carboxylic acids (CO_2), sulfinic acids (SO_2), sulfonic acids (SO_3), and HF were screened.

After data peak picking and feature detection (9668 for treated landfill leachate and 7944 for groundwater), a set of filters was applied to reduce the number of features in the samples to a more manageable level. First, a background subtraction filter was included in the workflow (see Table S4 in SI). Second, a peak rating algorithm was used to rate the shape of the peaks (from 1 to 10) annotated in each sample (version 3.3

of Compound Discoverer). The filter required a peak rating of ≥6 in the peaks for triplicate samples. Finally, a mass defect filter was used to remove all compounds which did not fall between 0.1 and −0.25 of a CF_2-adjusted KMD (Ng et al., 2022). Each identification of a compound was given a confidence level (CL) value, following Schymanski et al. (2014) as modified for PFAS by Charbonnet et al. (2022) with a more detailed level of identification.

The annotated features were screened manually after filtering to find and remove false negatives and false positives. A Kendrick mass plot was employed to identify homologous series by searching for series differing by *m/z* of ±50 (–CF_2–) or ±100 (–C_2F_4–). Features that were annotated as possible PFAS with a hit in the suspect list or online databases, but which were lacking MS (Podder et al., 2021) spectra, were added to an inclusion list. An additional analysis was performed for all samples using this newly created inclusion list, with the data-dependent MS (Podder et al., 2021) setting changed from *discovery* to *confirmation*.

3. Results and discussion

3.1. Behavior of precursor and legacy PFAS in TOP assays

Six PFAS were tested individually in spiked Milli-Q water using the TOP assay (Fig. 1). Compound concentrations not covered by the in-house targeted PFAS method were calculated from the known amount spiked into the samples. The three PFAS precursors degraded during the TOP assay, as expected and in agreement with previous studies (Houtz and Sedlak, 2012). Precursor 6:2 diPAP degraded mainly to PFPeA (40% of ∑PFAS), PFHxA (28%), PFBA (20%), and PFHpA (12%). Degradation of precursor 8:2 diPAP was slightly different, with PFHpA (38% of ∑PFAS), PFOA (26%), PFHxA (18%), PFPeA (13%), and PFBA (5%) as a minor product. Precursor EtFOSA also showed a different degradation pattern, with PFOA (90%) as the major PFAS and a low fraction of PFHxA (5%). This data aligns well with the experiments performed by Houtz and Sedlak (2012) as the major products for 6:2 diPAP and 8:2 diPAP were C_5 and a C_7 precursors, respectively (Houtz and Sedlak, 2012). Additionally, EtFOSA did, unlike the other precursors, result in a yield that was slightly lower to the concentration that was spiked into solution. The cause for this may be due to incomplete oxidation, oxidation into products not covered in the targeted method, or poor recoveries during extraction. It should be noted that PFAS degradation products which were not included in the PFAS targeted method could not be identified using LC-MS/MS.

Two of the three legacy PFAS tested, PFUnDA and PFTriDA, did not show any degradation in the TOP assay, which is in agreement with previous findings (Houtz and Sedlak, 2012). Interestingly, however, the concentration of both PFUnDA and PFTriDA decreased slightly (by 9% and 13%, respectively). The current working theory on this decrease in concentration of legacy PFAS is that the powders introduced into the samples during the TOP assay were partly sorbed. Alternatively, there may have been an analytical error and different recoveries during the extraction.

Relatively little research has been performed on the behavior of PFECHS (perfluoroethylcyclohexane sulfonic acid) in TOP assays. In a study where oilfield samples were analyzed for PFAS, PFECHS was detected in some samples, but none of the samples chosen for TOP assay contained any PFECHS (Meng et al., 2021). In other studies utilizing the TOP assay, PFECHS was not detected and thus more data are needed on this emerging contaminant (Göckener et al., 2022). The analysis performed in the present study is novel in that the TOP assay was performed on PFECHS alone, without any matrix, and the results showed that PFECHS was not affected by the TOP assay. More research on TOP assays of cyclic perfluorinated compounds is needed to explore the behavior of these compounds and determine the mass balance between PFAS precursors and final degradation products.

3.2. TOP assay on treated landfill leachate and groundwater

Triplicate samples of treated leachate and groundwater were tested

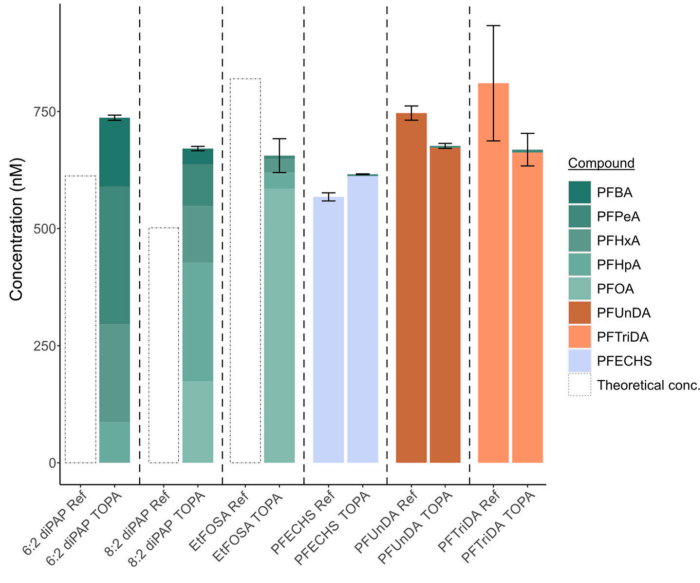

Fig. 1. Concentrations (nM) of per- and polyfluoroalkyl substance (PFAS) precursors and legacy PFAS in spiked Milli-Q water processed with a total oxidizable precursor (TOP) assay. Error bars indicate the difference between experimental replicates (n = 2). Transparent boxes with dotted lines indicate theoretical molar concentration of spiked compounds not included in the LC-MS/MS method.

in TOP assays. The overarching trend in the results was that the changes in concentration are largely negligible for PFAS (see Table S5 in SI). In treated leachate, the only compound that increased after the TOP assay was PFPeA with, on average, 11%. In groundwater, two compounds increased after the TOP assay, including PFPeA with 12% and PFHxA with 9%. There was, however, a significant difference ($p < 0.05$) in ∑PFAS before and after the TOP assay (see Table S6 in SI). The only compounds that did not show a significant difference ($p > 0.05$) were PFHxA, PFPeS, and PFOA in treated leachate and PFOA in groundwater (see Table S7 in SI). The low occurrence of PFAS precursors in samples from the selected landfill facility (see Section 2.4) may be because it is an old landfill (established 1971). Over time, any PFAS precursors originally present may have already been degraded by biotic and abiotic processes (Allred et al., 2015), during leaching through the landfill or during WWTP treatment of the leachate (Uppsala Vatten, 2021).

Overall, in this study the TOP assay was used as a prioritization strategy of samples for suspect and non-target screening, and hereby prioritize samples which contain a large proportion of unknown PFAS precursors. Although, the difference in concentration from performing the TOP assay was small in this study, the samples were further analyzed for suspect and non-target screening to verify if the TOP assay is a good prioritization strategy for suspect and non-target screening and identify PFAS precursors which are not affected by the TOP assay.

3.3. Suspect screening and non-target screening

Each sample matrix was processed separately and then subjected to the prioritization and quality control process (details of the workflow can be found in Table S4 in SI). Feature detection and peak picking by Compound Discoverer 3.3 using a modified workflow resulted in 9668 features in the treated leachate and 7944 features in the groundwater, with a threshold of S/N ratio = 3 and minimum intensity of 10000 (Fig. 2). Blank subtraction and application of the peak rating filter resulted in a total of 1152 features in the treated leachate and 747 in the groundwater. Prioritization using homologous series by applying a filter which retained features with annotated KMD between −0.25 and 0.10 resulted in 393 features in the treated leachate and 240 in the groundwater, but those figures also included false positives, which were manually screened out and not considered in the final results.

A final total of 28 PFAS were detected in the two matrices with confidence higher than CL = 3 d (Table 1), based on the new PFAS confidence levels (Charbonnet et al., 2022). Ten PFCA ($C_nF_{2n+1}CO_2H$) (C_3–C_{13}) were identified with CL = 1a based on accurate mass, mass defect, isotopic pattern match, a consistent retention time, matching MS (Podder et al., 2021) spectra with an online library, and with a reference standard. Six PFSA (C_nF_{2n+1}-SO_3H) (C_3–C_8) were identified in the matrices, all but one with CL = 1a. The only PFSA that was not confirmed with a reference standard was perfluoropropane sulfonic acid. This compound was identified with a CL = 2 b by comparing to a spectral database and having consistent retention time with related homologues. This is in agreement with previous findings that PFCA and PFSA are commonly present in landfill facilities and in the surrounding environment (Gomis et al., 2018; Arias E et al., 2015; Janousek et al., 2019).

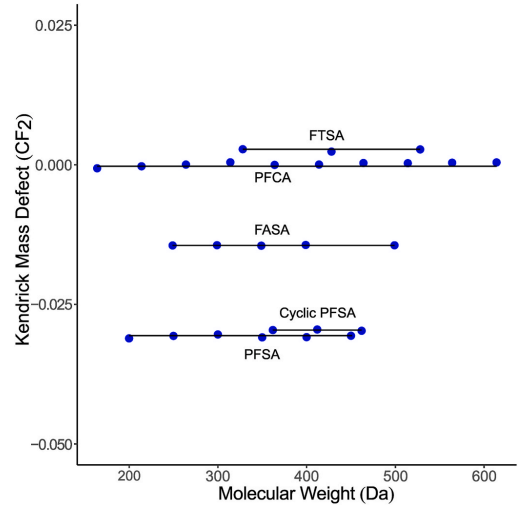

Fig. 3. CF_2-adjusted Kendrick mass defect diagram, where each dot represents a compound found in a homologous series of per- and polyfluoroalkyl substances (PFAS) in groundwater and treated landfill leachate samples. Individual compounds that did not belong to a series are excluded from the diagram.

Three isomers of PFECHS ($C_8F_{15}SO_3H$) were identified, all with the same *m/z*. One of these was identified with CL = 1a and two with CL = 3a. The mass spectra of all three isomers are displayed in Fig. S1 in SI. PFECHS has been linked to aviation-grade hydraulic fluids and has been detected at sites related to airports (Szabo et al., 2022). The isomers displayed the same diagnostic ions as the 1a confirmed compound, and thus only a tentative structure could be deduced. Additionally, the three isomers were not baseline-separated in the extracted ion chromatogram (Fig. S1 in SI), indicating that they were isomeric species. The exact position of the perfluorinated ethyl groups could not be confirmed (CL = 3a). The possibility of a perfluorodimethyl group could also not be

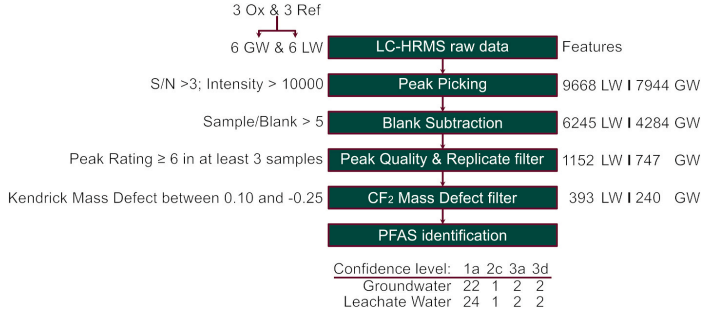

Fig. 2. Summary of the suspect screening workflow showing the prioritization strategies used and the number of features identified in groundwater (GW) and treated landfill leachate (LW) after prioritization and application of quality control filters.

Table 1
Summary of findings from suspect screening of per- and polyfluoroalkyl substances (PFAS) in treated landfill leachate and groundwater samples. Class name, structure, parameters used for identification, confidence level, in silico-determined log K_{OW} according to EPI Suite v. 4.1, United States Environmental Protection Agency, 2021 and examples of uses for the identified PFAS.

Abbreviation	Proposed structure	n	Confidence level (Charbonnet et al., 2022)	Log K_{OW}	Examples of uses
PFCA	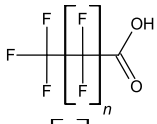	2; 3; 4; 5; 6; 7; 8; 9; 10; 11	1a; 1a; 1a; 1a; 1a; 1a; 1a; 1a; 1a; 1a	1.47; 2.14; 2.81; 3.48; 4.15; 4.81; 5.48; 6.12; 6.82; 7.49	In textiles: n = 2–11. Guo et al., 2009; Herzke et al., 2009; AFFF: n = 3–11. (Backe et al., 2013; Mumtaz et al., 2019)
PFSA	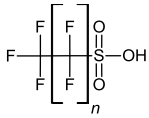	2 3; 4; 5; 6; 7	2 b; 1a; 1a; 1a; 1a 1a	0.48; 1.15; 1.82; 2.49; 3.16; 3.82; 4.49	AFFF: n = 2–7. (Backe et al., 2013; Barzen-Hanson and Field, 2015)
PFECHS	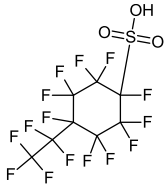	–	1a	4.42	Mist suppressant (Anich and Sierakowski, 1995); Surfactant (Tubergen and Benjamin, 1985) Aviation-grade hydraulic fluid. (Szabo et al., 2022)
PFECHS isomers	–	– –	3a	–	–
PFMeCHS	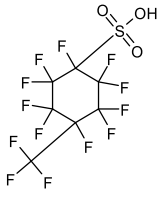	– –	3a	1.54	Surfactant (Tubergen and Benjamin, 1985)
PFCHS	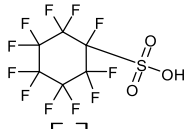	– –	2c	1.60	Etching agent for manufacturing semiconductor devices. (Hopkins et al., 1985)
FASA	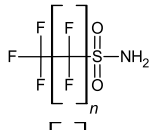	2; 3; 4; 5; 7	3 d; 1a; 3 d; 1a; 1a	2.46; 3.13; 3.79; 4.46; 5.80	Etching agent for manufacturing semiconductor devices: n = 4. (Parent et al., 2002)
FTSA	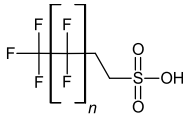	4; 6; 8 –	1a; 1a; 1a	1.32; 2.66; 4.00	Indoor carpets: n = 4, 6, 8. (Wu et al., 2020)
EtFOSAA	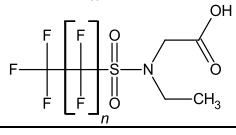	7	1a	6.22	Stain and water repellant. (Boulanger et al., 2005)

confirmed due to the lack of any such fragments in MS (Podder et al., 2021) (Fig. 4). The only fragments were $[M\text{-}HSO_3]^-$ with a mass corresponding to a C_nF_{2n-1} fragment and a FSO_3^- fragment. Considering the $[M\text{-}HSO_3]^-$ fragment, following the C_nF_{2n-1} pattern, and lack of additional C_nF_{2n-1} fragments, which would indicate a double bond, the evidence was deemed indicative of a cyclic PFAS (Charbonnet et al., 2022). Two more cyclic PFAS were identified, which also followed the C_nF_{2n-1} fragmentation pattern, indicating the same ring double bond equivalents, and which had $[M\text{-}HSO3]^-$ and FSO_3^- fragments. They also followed a homologous series, with similar mass defect and decreasing

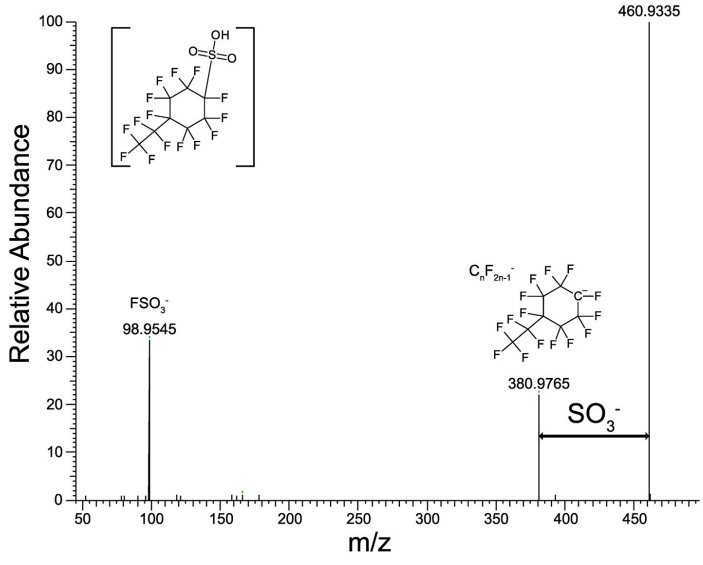

Fig. 4. MS (Podder et al., 2021) spectrum of perfluoroethylcyclohexane sulfonic acid (PFECHS) obtained from treated landfill leachate, with annotated fragments and their possible structure and formula (CL = 1a).

in nominal *m/z* by 50 in the series. They were identified as decreasing in chain length of the ethyl group to methyl group, and to without any alkyl group attached to the PFCHS. Due to the lack of any other functional groups on PFCHS apart from sulfonic acid, the structure could be identified with CL = 2c. Extracted ion chromatograms and related mass spectra of cyclic PFSAs can be seen in Fig. S2 in SI.

The only perfluoroalkane sulfonamide (FASA) initially identified in suspect screening was FOSA, but four more FASA were identified by implementing NTS strategies, in this case an inspection of the KMD plot, which showed a homologous series (Fig. 3). Authentic reference standards were only available for three FASA (FOSA, perfluorobutane sulfonamide (FBSA), and perfluorohexane sulfonamide (FHxSA)), while the other FASA were identified with CL = 3 d. The lack of diagnostic ions, which is inherent with FASA, limited the evidence to homologous series of the 1a identified compounds, accurate mass, mass defect, isotopic match, and consistent retention time (Charbonnet et al., 2022). Three FTSA were identified (4:2 FTSA, 6:2 FTSA, 8:2 FTSA), all with CL = 1a. FTSA have previously been identified as biodegradation products of fluorotelomer thioether amido sulfonic acids (FtTAoS) (Harding-Marjanovic et al., 2015). In other studies, FTSA have been found in AFFF extracts and in AFFF-contaminated waters (Mulabagal et al., 2018b; Barzen-Hanson et al., 2017). EtFOSAA was also identified through the suspect list and then confirmed with an authentic standard. EtFOSAA has previously been documented as a transformation product deriving from aerobic biotransformation of N-ethyl perfluorooctane sulfonamidoethanol. This indicates that there were several processes co-occurring in the landfill (Rhoads et al., 2008).

In a similar study conducted in Guangzhou, China, where leachate and groundwater at three landfills were sampled, many emerging PFAS were identified but, as in this study, most of these were legacy PFAS (Liu et al., 2022). In another study that analyzed PFAS in landfill (Koelmel et al., 2020), the screening results were very similar to the classes identified in this study with the exception of MeFOSAA, which was not identified using suspect screening but was detected in the targeted analysis (Koelmel et al., 2020). In another study involving targeted analysis where 70 PFAS were targeted in a simulated landfill containing PFAS products, the overall PFAS concentration was shown to increase over time (Lang et al., 2016).

3.4. Quantification and semi-quantification of PFAS in groundwater and treated landfill leachate

In total, 13 and 11 PFAS were quantified in levels above the LOQ in the treated leachate and groundwater (reference) samples, respectively (Table 2). Other PFAS were also detected, but due to their detection in blank samples they are not reported here (for details, see Table S8 in SI). Semi-quantification of compounds that were not included in the targeted LC-MS/MS method (i.e. FASA and cyclic PFSA) was performed using HRMS. For semi-quantification of FASA, the FOSA calibration curve and IS were used, while semi-quantification of the cyclic PFAS was performed using the calibration curve of PFECHS and additionally the IS $^{13}C_3$-PFHxS.

In treated landfill leachate, the dominant PFAS group was PFCA (76% of ∑PFAS), with PFOA showing the highest concentration (420 ng/L). The second largest PFAS group in treated leachate was PFSA (21% of ∑PFAS), with ~3.5 times lower concentration (400 ng/L for ∑PFSA) compared with PFCA (1400 ng/L for ∑PFCA). Dominance of PFCA and PFSA has been observed in other studies on leachate from e.g., waste-to-energy stockpiles in the UK and Spain, and from a landfill in Spain (Björklund et al., 2021; Fuertes et al., 2017). However, most previous studies have generally found higher concentrations of PFHxA than PFOA (Gallen et al., 2017; Björklund et al., 2021; Lang et al., 2017), which was not observed in this study. The other PFAS groups were generally present in lower concentrations (PFECHS 28 ng/L, ∑FASA 34 ng/L). The semi-quantified PFAS (i.e., PFMeCHS, PFCHS, FPrSA, FBSA, FPeSA, and FHxSA) had a total concentration of only 46 ng/L, which indicates lower presence of other PFAS groups than PFCA and PFSA, or lack of identification of other PFAS groups.

In groundwater, the ∑PFAS concentration was higher by a factor of ~1.5 (3420 ng/L for ∑PFAS) than in landfill water (1910 ng/L for ∑PFAS). The reasons for this difference could be that the treated landfill leachate was more diluted by precipitation and that the PFAS were

Table 2
Concentrations (ng/L ± standard deviation) of per- and polyfluoroalkyl substances (PFAS) in treated landfill leachate (LW) and groundwater (GW), sum according to targeted quantitative (Q) LC-MS/MS analysis and semi-quantitative (semiQ) LC-HRMS analysis, and overall total concentration. Compounds marked with "*" have high uncertainty due to being below method quantitation limit but above method detection limit. These compounds were not added to the concentration sum. For method limits see Table S8 in SI.

Compound	LW			GW		
PFBA	170	±	6.6	230	±	5.4
PFPeA	190	±	7.4	260	±	6.5
PFHxA	390	±	29	570	±	30
PFHpA	220	±	8.0	360	±	32
PFOA	420	±	16	940	±	68
PFBS	97	±	4.6	160	±	9.6
PFPeS	21	±	1.8	70	±	6.3
PFHxS	98	±	8.3	330	±	14
PFHpS	7.4	±	0.53	22	±	2.3
PFOS	150	±	14	250	±	17
PFECHS	28	±	2.7	39	±	3.8
EtFOSAA	19	±	1.1	<LOD		
MeFOSAA	5.1	±	0.52	<LOD		
4:2 FTSA*	<LOD			74	±	7.2
6:2 FTSA*	<LOD			59	±	3.3
Q sum	1820			3230		
PFMeCHS	2.2	±	0.14	4.1	±	0.05
PFCHS	10	±	0.45	20	±	0.97
FPrSA	4.2	±	0.28	23	±	1.7
FBSA	17	±	3.5	43	±	4.4
FPeSA	4.3	±	0.52	11	±	0.96
FHxSA	8.0	±	1.2	9.8	±	1.0
semiQ sum	46			110		
Overall total	**1860**			**3340**		

further diluted during WWTP treatment. The PFAS concentrations in groundwater were higher due to the direct impact from the waste stored in the landfill and other contributing sources. The dominant PFAS group in groundwater was PFCA (73% of ∑PFAS), followed by PFSA (26% of ∑PFAS). The other PFAS groups were generally detected in lower concentrations (PFECHS 39 ng/L, FASA 86 ng/L). The semi-quantified PFAS had a total concentration of 110 ng/L.

The composition profile of PFAS in the treated leachate and groundwater differed in terms of the dominant PFSA. In the groundwater, PFHxS (11% of ∑PFAS), followed by PFOS (7.9% of ∑PFAS) were the dominant PFSA. In the treated leachate, on the other hand, PFOS (8.4% of ∑PFAS), followed by PFHxS (5.8% of ∑PFAS) were the dominant PFSA. Furthermore, FASA and cyclic-PFSA were lower in concentration in treated leachate and higher in the groundwater, following the general trend of the other quantified PFAS. The two precursors MeFOSAA and EtFOSAA were detected above the LOQ only in the treated leachate samples and most likely these two compounds were formed either during the WWTP process or by reactions which occurred in the landfill (Allred et al., 2015; Rhoads et al., 2008; Hamid et al., 2018). This indicates that the source of PFAS was different for treated landfill leachate and groundwater, or that the composition profile changed during treatment at the WWTP or during leaching to groundwater. Semi-quantification proved useful by identifying additional PFAS which were not covered in the targeted method.

4. Conclusions

A workflow to identify and (semi)-quantify new PFAS in treated leachate and groundwater using TOP assay and suspect screening was developed and tested in this study. As expected, the PFAS precursors 6:2 diPAP and 8:2 diPAP showed almost complete degradation during the TOP assay and long-chain PFCA did not degrade significantly. The cyclic PFAS PFECHS also did not degrade during the TOP assay. Thus more studies are needed to determine the behavior of cyclic PFAS in TOP assays and their environmental persistence. In TOP assays, treated landfill leachate and groundwater showed very few PFAS with increasing concentrations, indicating that biotic and abiotic processes within the landfill over time have already degraded any PFAS precursors initially present.

Application of the suspect screening workflow to groundwater and treated landfill leachate samples resulted in identification of a total of 28 PFAS with confidence level ≥3 d. To our knowledge, this is one of the first few suspect screening study to analyze groundwater and treated landfill leachate from an active landfill site. Monitoring of PFAS in the waste sector should be continued, as PFAS are included in many household and commercial products and may be released into the environment from landfills or other waste facilities over time. The TOP assay can be useful as a method to improve and widen the scope of conventional targeted analysis and as a tool for preselecting samples although the information obtained may be limited depending on the matrix and source of PFAS. The samples discussed in this paper yielded little information regarding precursors using the TOP assay but through suspect screening precursor were detected. Semi-quantification is a useful method to estimate the concentrations of newly identified PFAS, so structured semi-quantification methods need to be developed.

Author contributions

Svante Rehnstam: Writing – Original Draft, Visualization, Formal analysis, Data Curation, Mai-Britt Czeschka: Investigation, Formal analysis, Writing – Review & Editing, Lutz Ahrens: Conceptualization, Methodology, Writing – Review & Editing, Supervision, Funding acquisition.

Declaration of competing interest

The authors declare that they have no known competing financial interests or personal relationships that could have appeared to influence the work reported in this paper.

Data availability

Data will be made available on request.

Appendix A. Supplementary data

Supplementary data to this article can be found online at https://doi.org/10.1016/j.chemosphere.2023.138925.

References

Allred, B.M.K., Lang, J.R., Barlaz, M.A., Field, J.A., 2015. Physical and biological release of poly- and perfluoroalkyl substances (PFASs) from municipal solid waste in anaerobic model landfill reactors. Environ. Sci. Technol. 49, 7648–7656.
Arias E, V.A., Mallavarapu, M., Naidu, R., 2015. Identification of the source of PFOS and PFOA contamination at a military air base site. Environ. Monit. Assess. 187.
Backe, W.J., Day, T.C., Field, J.A., 2013. Zwitterionic, cationic, and anionic fluorinated chemicals in aqueous film forming foam formulations and groundwater from U.S. military bases by nonaqueous large-volume injection HPLC-MS/MS. Environ. Sci. Technol. 47, 5226–5234.
Barnabas, S.J., et al., 2022. Extraction of chemical structures from literature and patent documents using open access chemistry toolkits: a case study with PFAS. Dig. Dis. 1, 490–501.
Barzen-Hanson, K.A., Field, J.A., 2015. Discovery and implications of C2 and C3 perfluoroalkyl sulfonates in aqueous film-forming foams and groundwater. Environ. Sci. Technol. Lett. 2, 95–99.
Barzen-Hanson, K.A., et al., 2017. Discovery of 40 classes of per- and polyfluoroalkyl substances in historical aqueous film-forming foams (AFFFs) and AFFF-impacted groundwater. Environ. Sci. Technol. 51, 2047–2057.
Björklund, S., Weidemann, E., Yeung, L.W., Jansson, S., 2021. Occurrence of per- and polyfluoroalkyl substances and unidentified organofluorine in leachate from waste-to-energy stockpile - a case study. Chemosphere 278.
Boulanger, B., Vargo, J.D., Schnoor, J.L., Hornbuckle, K.C., 2005. Evaluation of perfluorooctane surfactants in a wastewater treatment system and in a commercial surface protection product. Environ. Sci. Technol. 39, 5524–5530.

Charbonnet, J.A., et al., 2022. Communicating confidence of per- and polyfluoroalkyl substance identification via high-resolution mass spectrometry. Environ. Sci. Technol. Lett. 9, 473–481.
Cortés-Francisco, N., Caixach, J., 2015. Fragmentation studies for the structural characterization of marine dissolved organic matter. Anal. Bioanal. Chem. 407, 2455–2462.
Fuertes, I., Gómez-Lavín, S., Elizalde, M.P., Urtiaga, A., 2017. Perfluorinated alkyl substances (PFASs) in northern Spain municipal solid waste landfill leachates. Chemosphere 168, 399–407.
Gago-Ferrero, P., et al., 2015. Extended suspect and non-target strategies to characterize emerging polar organic contaminants in raw wastewater with LC-HRMS/MS. Environ. Sci. Technol. 49, 12333–12341.
Gallen, C., et al., 2017. Australia-wide assessment of perfluoroalkyl substances (PFASs) in landfill leachates. J. Hazard Mater. 331, 132–141.
Glüge, J., et al., 2020. An overview of the uses of per- and polyfluoroalkyl substances (PFAS). Environ. Sci. Process. Impacts 22, 2345–2373.
Gobelius, L., et al., 2018. Per- and polyfluoroalkyl substances in Swedish groundwater and surface water: implications for environmental quality standards and drinking water guidelines. Environ. Sci. Technol. 52, 4340–4349.
Göckener, B., Fliedner, A., Rüdel, H., Badry, A., Koschorreck, J., 2022. Long-term trends of per- and polyfluoroalkyl substances (PFAS) in suspended particular matter from German rivers using the direct total oxidizable precursor (dTOP) assay. Environ. Sci. Technol. 56, 208–217.
Gomis, M.I., Vestergren, R., Borg, D., Cousins, I.T., 2018. Comparing the toxic potency in vivo of long-chain perfluoroalkyl acids and fluorinated alternatives. Environ. Int. 113, 1–9.
Gross, Jurgen H., 2017. Mass Spectrometry, A Textbook, third ed. Springer International Publishing.
Guo, Z., Liu, X., Krebs, kenneth a., 2009. US EPA's perfluorocarboxylic acid content in 116 articles of commerce. http://books.google.com/books?hl=en&lr=&id=KoE5lJx1NjIC&oi=fnd&pg=PR7&dq=textile+finishes+and+fluorosurfactants&ots=HjGrfP9WTo&sig=Zbs6nN8UYQPkhTM4PJH6tffADn0%5Cnfile:///Users/.Jerry/Documents/Library.papers3/Articles/2009/Epa/2009 Epa.pdf%5Cnpapers3://pub.
Hamid, H., Li, L.Y., Grace, J.R., 2018. Review of the fate and transformation of per- and polyfluoroalkyl substances (PFASs) in landfills. Environ. Pollut. 235, 74–84.
Harding-Marjanovic, K.C., et al., 2015. Aerobic biotransformation of fluorotelomer thioether amido sulfonate (lodyne) in AFFF-amended microcosms. Environ. Sci. Technol. 49, 7666–7674.
Hopkins, R.J., Thomas, E.G., Kieta, H.J., 1985. Soluble Fluorinated Cycloalkane Sulfonate Surfactant Additives for NH4. US Pantent US4620934A.
Herzke, D., Posner, S., Olsson, E., 2009. Survey , screening and analyses of PFCs in consumer products. Swerea IVF Project report 09/41. Available from: https://www.miljodirektoratet.no/globalassets/publikasjoner/klif2/publikasjoner/2578/ta2578.pdf [Accessed: 25 May 2023].
Houtz, E.F., Sedlak, D.L., 2012. Oxidative conversion as a means of detecting precursors to perfluoroalkyl acids in urban runoff. Environ. Sci. Technol. 46, 9342–9349.
Houtz, E.F., Sutton, R., Park, J.S., Sedlak, M., 2016. Poly- and perfluoroalkyl substances in wastewater: significance of unknown precursors, manufacturing shifts, and likely AFFF impacts. Water Res. 95, 142–149.
Houtz, E., Wang, M., Park, J.S., 2018. Identification and fate of aqueous film forming foam derived per- and polyfluoroalkyl substances in a wastewater treatment plant. Environ. Sci. Technol. 52, 13212–13221.
Janousek, R.M., Mayer, J., Knepper, T.P., 2019. Is the phase-out of long-chain PFASs measurable as fingerprint in a defined area? Comparison of global PFAS concentrations and a monitoring study performed in Hesse, Germany from 2014 to 2018. TrAC, Trends Anal. Chem. 120, 115393.
Kendrick, E., 1963. A mass scale based resolution mass spectrometry of organic compounds. Anal. Chem. 35, 2146–2154.
Koch, A., et al., 2019. Point source characterization of per- and polyfluoroalkyl substances (PFASs) and extractable organofluorine (EOF) in freshwater and aquatic invertebrates. Environ. Sci. Process. Impacts 21, 1887–1898.
Koelmel, J.P., et al., 2020. Toward comprehensive per- A nd polyfluoroalkyl substances annotation using FluoroMatch software and intelligent high-resolution tandem mass spectrometry acquisition. Anal. Chem. 92, 11186–11194.
Kotthoff, M., Muller, J., Jürling, H., Schlummer, M., Fiedler, D., 2015. Perfluoroalkyl and polyfluoroalkyl substances in consumer products. Environ. Sci. Pollut. Res. 22, 14546–14559.
Krauss, M., Singer, H., Hollender, J., 2010. LC-high resolution MS in environmental analysis: from target screening to the identification of unknowns. Anal. Bioanal. Chem. 397, 943–951.
Lang, J.R., Allred, B.M.K., Peaslee, G.F., Field, J.A., Barlaz, M.A., 2016. Release of per- and polyfluoroalkyl substances (PFASs) from carpet and clothing in model anaerobic landfill reactors. Environ. Sci. Technol. 50, 5024–5032.
Lang, J.R., Allred, B.M.K., Field, J.A., Levis, J.W., Barlaz, M.A., 2017. National estimate of per- and polyfluoroalkyl substance (PFAS) release to U.S. Municipal landfill leachate. Environ. Sci. Technol. 51, 2197–2205.
Letcher, R.J., et al., 2015. Perfluorinated sulfonate and carboxylate compounds and precursors in herring gull eggs from across the Laurentian Great Lakes of North America: temporal and recent spatial comparisons and exposure implications. Sci. Total Environ. 538, 468–477.
Liu, Y., Pereira, A.D.S., Martin, J.W., 2015. Discovery of C5-C17 Poly- and perfluoroalkyl substances in water by in-line Spe-HPLC-Orbitrap with in-source fragmentation flagging. Anal. Chem. 87, 4260–4268.
Liu, Y., D'Agostino, L.A., Qu, G., Jiang, G., Martin, J.W., 2019. High-resolution mass spectrometry (HRMS) methods for nontarget discovery and characterization of poly- and per-fluoroalkyl substances (PFASs) in environmental and human samples. TrAC, Trends Anal. Chem. 121, 115420.
Liu, T., et al., 2022. Non-target and target screening of per- and polyfluoroalkyl substances in landfill leachate and impact on groundwater in Guangzhou, China. SSRN Electron. J. 844, 157021.
Meng, Y., Yao, Y., Chen, H., Li, Q., Sun, H., 2021. Legacy and emerging per- and polyfluoroalkyl substances (PFASs) in Dagang Oilfield: multimedia distribution and contributions of unknown precursors. J. Hazard Mater. 412, 106735.
Menger, F., Gago-Ferrero, P., Wiberg, K., Ahrens, L., 2020. Wide-scope screening of polar contaminants of concern in water: a critical review of liquid chromatography-high resolution mass spectrometry-based strategies. Trends Environ. Anal. Chem. 28, e00102.
Mulabagal, V., Liu, L., Qi, J., Wilson, C., Hayworth, J.S., 2018a. A rapid UHPLC-MS/MS method for simultaneous quantitation of 23 perfluoroalkyl substances (PFAS) in estuarine water. Talanta 190, 95–102.
Mulabagal, V., Liu, L., Qi, J., Wilson, C., Hayworth, J.S., 2018b. A rapid UHPLC-MS/MS method for simultaneous quantitation of 23 perfluoroalkyl substances (PFAS) in estuarine water. Talanta 190, 95–102.
Mumtaz, M., et al., 2019. Per- and polyfluoroalkyl substances in representative fluorocarbon surfactants used in Chinese film-forming foams: levels, profile shift, and environmental implications. Environ. Sci. Technol. Lett. 6, 259–264.
Myers, A.L., Jobst, K.J., Mabury, S.A., Reiner, E.J., 2014. Using mass defect plots as a discovery tool to identify novel fluoropolymer thermal decomposition products. J. Mass Spectrom. 49, 291–296.
Nakayama, S.F., et al., 2019. Worldwide trends in tracing poly- and perfluoroalkyl substances (PFAS) in the environment. TrAC, Trends Anal. Chem. 121.
Ng, K., et al., 2022. Target and suspect screening of 4,777 per- and polyfluoroalkyl substances (PFAS) in river water, wastewater, groundwater and biota samples in the Danube River Basin. J. Hazard Mater. 436, 129276.
Anich, A.T., Sierakowski, M.J., 1995. Mist Suppressant for solvent extraction metal electrowinning. US Patent 5,468,353.
NORMAN Substance Database. https://www.norman-network.com/nds/susdat/.
Reconciling Terminology of the Universe of Per- and Polyfluoroalkyl Substances: Recommendations and Practical Guidance, 2021. OECD. www.oecd.org/chemicalsafety/.
Parent, M., Savu, P., Flynn, R., 2002. Fluorinated Surfactants for Buffered Acid Etch Solutions.
Podder, A., Sadmani, A.H.M.A., Reinhart, D., Chang, N. Bin, Goel, R., 2021. Per and polyfluoroalkyl substances (PFAS) as a contaminant of emerging concern in surface water: a transboundary review of their occurrences and toxicity effects. J. Hazard Mater. 419, 126361.
Rhoads, K.R., Janssen, E.M.L., Luthy, R.G., Criddle, C.S., 2008. Aerobic biotransformation and fate of N-ethyl perfluorooctane sulfonamidoethanol (N-EtFOSE) in activated sludge. Environ. Sci. Technol. 42, 2873–2878.
Ruyle, B.J., et al., 2021. Isolating the AFFF signature in coastal watersheds using oxidizable PFAS precursors and unexplained organofluorine. Environ. Sci. Technol. 55, 3686–3695.
Sajid, M., Ilyas, M., 2017. PTFE-coated non-stick cookware and toxicity concerns: a perspective. Environ. Sci. Pollut. Res. 24, 23436–23440.
Schymanski, E.L., et al., 2014. Identifying small molecules via high resolution mass spectrometry: communicating confidence. Environ. Sci. Technol. 48, 2097–2098.
Shojaei, M., Joyce, A.S., Ferguson, P.L., Guelfo, J.L., 2022. Novel per- and polyfluoroalkyl substances in an active-use C6-based aqueous film forming foam. J. Hazard. Mater. Lett. 3, 100061.
Smith, S.J., Wiberg, K., McCleaf, P., Ahrens, L., 2022. Pilot-Scale continuous foam fractionation for the removal of per- A nd polyfluoroalkyl substances (PFAS) from landfill leachate. ACS Environ. Sci. Technol. Water. 2, 841–851.
Strynar, M., et al., 2015. Identification of novel perfluoroalkyl ether carboxylic acids (PFECAs) and sulfonic acids (PFESAs) in natural waters using accurate mass time-of-flight mass spectrometry (TOFMS). Environ. Sci. Technol. 49, 11622–11630.
Szabo, D., Moodie, D., Green, M.P., Mulder, R.A., Clarke, B.O., 2022. Field-based distribution and bioaccumulation factors for cyclic and aliphatic per- and polyfluoroalkyl substances (PFASs) in an urban sedentary waterbird population. Environ. Sci. Technol. 56, 8231–8244.
Taylor, R.B., Sapozhnikova, Y., 2022. Comparison and validation of the QuEChERSER mega-method for determination of per- and polyfluoroalkyl substances in foods by liquid chromatography with high-resolution and triple quadrupole mass spectrometry. Anal. Chim. Acta. 1230, 340400.
Tubergen, T.S., Benjamin, T.A., 1985. Process for Metallizing Plastics.US Patent: US4610895A.
Estimation Programs Interface SuiteTM for Microsoft® Windows, vol. 4, 2021. United States Environmental Protection Agency. US EPA, 11. (2022).
Uppsala Vatten. Hovgårdens Avfallsanläggning Hovgårdens Avfallsanläggning. https://www.uppsalavatten.se/globalassets/dokument/hushall/blanketter-och-tryckaker/anlaggningspresentation-hovgarden-2021.pdf.
Wu, Y., Romanak, K., Bruton, T., Blum, A., Venier, M., 2020. Per- and polyfluoroalkyl substances in paired dust and carpets from childcare centers. Chemosphere 251, 126771.
Zabaleta, I., et al., 2017. Screening and identification of per- and polyfluoroalkyl substances in microwave popcorn bags. Food Chem. 230, 497–506.

Supplementary Information

Suspect screening and total oxidizable precursor (TOP) assay as tools for characterization of per- and polyfluoroalkyl substance (PFAS)-contaminated groundwater and treated landfill leachate

Svante Rehnstam[a], Mai-Britt Czeschka[a], Lutz Ahrens[a]

[a] Swedish University of Agricultural Sciences, Department of Aquatic Sciences and Assessment, Box 7050, 750 07 Uppsala, Sweden

Table of Contents

Table S 1. Abbreviations of PFAS discussed in the main paper

Name	Abbreviation
Perfluorobutanoic acid	PFBA
Perfluoropentanoic acid	PFPeA
Perfluorohexanoic acid	PFHxA
Perfluoroheptanoic acid	PFHpA
Perfluorooctanoic acid	PFOA
Perfluorononanoic acid	PFNA
Perfluorodecanoic acid	PFDA
Perfluoroundecanoic acid	PFUnDA
Perfluorododecanoic acid	PFDoDA
Perfluorotridecanoic acid	PFTriDA
Perfluorotetradecanoic acid	PFTeDA
Perfluorobutane sulfonic acid	PFBS
Perfluoropentane sulfonic acid	PFPeS
Perfluorohexane sulfonic acid	PFHxS
Perfluoroheptane sulfonic acid	PFHpS
Perfluorooctane sulfonic acid	PFOS
Perfluorononane sulfonic acid	PFNS
Perfluorodecane sulfonic acid	PFDS
Perfluoroethylcyclohexane sulfonic acid	PFECHS
Perfluoromethylcyclohexane sulfonic acid	PFMCHS
Perfluorocyclohexane sulfonic acid	PFCHS
4:2 Fluorotelomer sulfonic acid	4:2 FTSA
6:2 Fluorotelomer sulfonic acid	6:2 FTSA
8:2 Fluorotelomer sulfonic acid	8:2 FTSA
6:2 Fluorotelomer phosphate diester	6:2 diPAP
8:2 Fluorotelomer phosphate diester	8:2 diPAP
9-chloro-hexadecafluoro-3-oxanonane sulfonic acid	9Cl-PF3ONS
11-chloro-eicosafluoro-3-oxaundecane-1-sulfonic acid	11Cl-PF3OUdS
hexafluoropropylene oxide dimer acid	HFPO-DA
Perfluorooctane sulfonamide	FOSA
N-methyl-perfluorooctane sulfonamido acetic acid	MeFOSAA
N-ethyl-perfluorooctane sulfonamido acetic acid	EtFOSAA
4,8-dioxa-3H-perfluorononanoic acid	NaDONA
Perfluoropentane sulfonamide	FPrSA
Perfluorobutane sulfonamide	FBSA
Perfluorohexane sulfonamide	FHxSA
Fluorotelomer thioether amido sulfonic acids	FtTAoS

Table S 2. Internal standards used for quantification and the purity of the standard

Abbreviation	IS Purity
$^{13}C_4$-PFBA	>99%
$^{13}C_5$-PFPeA	>99%
$^{13}C_5$-PFHxA	>99%
$^{13}C_4$-PFHpA	>99%
$^{13}C_8$-PFOA	>98%
$^{13}C_9$-PFNA	>99%
$^{13}C_6$-PFDA	>99%
$^{13}C_7$-PFUnDA	>99%
$^{13}C_3$-PFDoDA	>99%
$^{13}C_2$-PFTeDA	>99%
$^{13}C_3$-PFBS	>99%
$^{13}C_3$-PFHxS	>99%
$^{13}C_8$-PFOS	>99%
$^{13}C_2$-4:2 FTSA	>99%
$^{13}C_2$-6:2 FTSA	>99%
$^{13}C_2$-8:2 FTSA	>99%
$^{13}C_3$-HFPO-DA	>99%
$^{13}C_8$FOSA	>99%
D_3-MeFOSAA	98%
D_5-EtFOSAA	98%

Table S 3. Quality Assurance of Total Oxidizable Precursor assay where a calibration curve standard was used. Uncertainty expressed in average deviation of recovery

Component Name	c(blank) ng/mL	c(spiked ox A) ng/mL	c(spiked ox B) ng/mL	c(Ref A) ng/mL	c(Ref B) ng/mL	Recovery after TOP assay
PFBA	1.03	7.66	7.69	6.15	4.43	145% ± 25%
PFPeA	0	7.66	7.4	5.89	4.9	140% ± 10%
PFBS	-0.19	6.1	6.66	8.34	6.43	86% ± 15%
PFHxA	0.11	8.04	7.97	5.53	5.15	150% ± 5%
4-2FTSA	-0.71	-0.15	1.4	11.21	7.35	7% ± 10%
HFPO-DA	0	5.01	4.31	4.68	5.63	90% ± 15%
PFPeS	0	6.05	6.22	6.48	5.97	99% ± 5%
PFHpA	-0.17	8.04	7.79	6.79	5.96	124% ± 6%
NaDONA	0	0.06	0	4.72	5.76	1% ± 1%
PFHxS	0.01	6.01	6.63	9.26	6.02	83% ± 23%
PFOA	0.1	20.98	22.41	6.48	5.62	358% ± 37%
6-2 FTSA	-0.16	-0.04	0.12	6.95	6.25	1% ± 1%
PFHpS	-0.02	6.25	6.16	6.96	7.29	87% ± 3%
PFECHS	0	5.81	5.66	5.73	6.21	96% ± 5%
PFNA	0.29	5.74	6.61	6.54	5.48	103% ± 16%
FOSA	-0.16	-0.16	0.05	6.9	5.98	-1% ± 2%
PFOS	-0.56	5.93	6.3	8.41	6.14	84% ± 16%
PFDA	-0.62	6.13	5.95	7.92	6.24	85% ± 9%
8-2 FTSA	-0.29	-0.26	0.97	7.78	7.43	5% ± 8%
9Cl-PF3ONS	0	4.49	4.9	5.84	5.19	85% ± 9%
PFNS	0	5.33	4.85	5.36	5.21	96% ± 3%
PFUnDA	0.1	5.98	6.32	10.46	6.88	71% ± 17%
Me-FOSAA	0	0	0	5.97	6.23	0% ± 0%
Et-FOSAA	0	0	0	5.57	5.67	0% ± 0%
PFDS	0	4.17	3.59	5.59	4.97	74% ± 1%
PFDoDA	-0.5	5.16	6.93	7.98	5.49	90% ± 31%
11Cl-PF3OUdS	0	3.13	3.47	5.97	4.55	63% ± 12%
PFTriDA	-0.99	8.51	11.16	15.34	11.62	73% ± 20%

PFTeDA	-1.55	4.15	6.95	10.05	7.97	62% ± 23%

Table S 4. Compound Discoverer version 3.3 workflow

Detect Compounds	
1. General Settings	
Mass Tolerance [ppm]	5
Min. Peak Intensity	10000
Min. #Scans per Peak	5
Use Most Intense Isotope Only	TRUE
2. Trace Detection	
Max. Number of Gaps to Correct	2
Min. Number of Adjacent Non-Zeroes	2
3. Peak Detection	
Chromatographic S/N Threshold	3
Remove Baseline	FALSE
Gap Ratio Threshold	0.35
Max. Peak Width [min]	1
Min. Relative Valley Depth	0.1
4. Isotope Pattern Detection	
Group Isotopes for	Br; Cl
Use Peak Quality for Isotope Grouping	FALSE
Filter out Features with Bad Peaks Only	FALSE
Zig-Zag Index Threshold	0.2
Jaggedness Threshold	0.4
Modality Threshold	0.9
Remove Potentially False Positive Isotopes	FALSE
5. Compound Detection	
Ions	[M-H]-1
Base Ions	[M-H]-1
Remove Singlets	FALSE
6. Acquire X Settings	
Detect Persistent Background Ions	FALSE
Group Compounds	
1. General Settings	
Mass Tolerance	5 ppm
RT Tolerance [min]	0.2
Align Peaks	FALSE
Preferred Ions	[M-H]-1
Area Integration	Most Common Ion
2. Peak Rating Contributions	

Area Contribution	3
CV Contribution	10
FWHM to Base Contribution	5
Jaggedness Contribution	5
Modality Contribution	5
Zig-Zag Index Contribution	5
3. Peak Rating Filter	
Peak Rating Threshold	2
Number of Files	3
Mark Background Compounds	
1. General Settings	
Max. Sample/Blank	5
Max. Blank/Sample	0
Hide Background	TRUE
Calculate Mass Defect	
1. Mass Defect	
Fractional Mass Defect	FALSE
Relative Mass Defect	TRUE
Kendrick Mass Defect	TRUE
Nominal Mass Rounding	Round
2. Kendrick Formula	
Formula 1	CF2
Search Neutral Losses	
1. General Settings	
Neutral Losses	CO2; HF; SO2; SO3
High Acc. Mass Tolerance	2.5 mmu
Low Acc. Mass Tolerance	0.5 Da
S/N Threshold	3
Use DIA Scans for Search	FALSE
Assign Compound Annotations	
1. General Settings	
Mass Tolerance	3
2. Data Sources	
Data Source #1	MassList Search
Data Source #2	mzCloud Search
Data Source #3	ChemSpider Search
Data Source #4	Predicted Compositions
Data Source #5	
3. Scoring Rules	

Use mzLogic	TRUE
Use Spectral Distance	TRUE
Sfit Threshold	20
Sfit Range	20
4. Reprocessing	
Clear Names	FALSE
Search mzCloud	
1. General Settings	
Compound Classes	Industrial Chemicals; Perfluorinated Hydrocarbons; Personal Care Products/Cosmetics; Small Molecule Chemicals
Precursor Mass Tolerance	10 ppm
FT Fragment Mass Tolerance	10 ppm
IT Fragment Mass Tolerance	0.4 Da
Library	Autoprocessed; Reference
Post Processing	Recalibrated
Max. #Results	10
Annotate Matching Fragments	FALSE
Search MSn Tree	FALSE
2. DDA Search	
Identity Search	HighChem HighRes
Match Activation Type	FALSE
Match Activation Energy	Any
Activation Energy Tolerance	20
Apply Intensity Threshold	FALSE
Similarity Search	Confidence Forward
Match Factor Threshold	30
Search Mass Lists	
1. Search Settings	
Mass Lists	list.massList
Use Retention Time	FALSE
RT Tolerance [min]	10
Mass Tolerance	3 ppm
Search ChemSpider	
1. Search Settings	
Database(s)	EPA DSSTox; EPA Toxcast; FDA; MassBank; MolBank; PubMed; Royal Society of Chemistry; Sigma-Aldrich
Search Mode	By Formula or Mass
Mass Tolerance	3 ppm
Max. # of results per compound	100
Results Order	Order By Reference Count (DESC)

Max. # of Predicted Compositions to be searched per Compound	5
2. Predicted Composition Annotation	
Check All Predicted Compositions	FALSE
Apply Spectral Distance	
1. Pattern Matching	
Mass Tolerance	5 ppm
Intensity Tolerance [%]	30
Intensity Threshold [%]	1
S/N Threshold	3
Use Dynamic Recalibration	TRUE
Apply mzLogic	
1. Search Settings	
FT Fragment Mass Tolerance	10 ppm
IT Fragment Mass Tolerance	0.4 Da
Max. # Compounds	0
Max. # mzCloud Similarity Results to consider per Compound	10
Match Factor Threshold	30
Predict Compositions	
1. Prediction Settings	
Mass Tolerance	3 ppm
Min. Element Counts	C H F
Max. Element Counts	C90 H190 Br3 Cl4 F190 N10 O18 P3 S5
Min. RDBE	-1.5
Max. RDBE	120
Min. H/C	0.05
Max. H/C	3.5
Max. # Candidates	30
Max. # Internal Candidates	300
2. Pattern Matching	
Intensity Tolerance [%]	30
Intensity Threshold [%]	0.1
S/N Threshold	3
Min. Spectral Fit [%]	30
Min. Pattern Cov. [%]	90
Use Dynamic Recalibration	TRUE
3. Fragments Matching	
Use Fragments Matching	TRUE

Mass Tolerance	5 ppm
S/N Threshold	3
Compound Class Scoring	
1. General Settings	
Compound Classes	See Method section
S/N Threshold	15
High Acc. Mass Tolerance	2.5 mmu
Low Acc. Mass Tolerance	0.5 Da
Use Full MS Tree	TRUE
Allow DIA Scoring	TRUE

Table S 5. Concentrations of compounds before (Reference) and after TOP assay (Oxidized) in leachate water and groundwater.

	LW				GW			
Compound	**Reference**		**Oxidized**		**Reference**		**Oxidized**	
PFBA	170 ± 6.6		150 ± 3.6		230 ± 5.4		190 ± 4.5	
PFPeA	190 ± 7.4		210 ± 8.8		260 ± 6.5		290 ± 9.9	
PFHxA	390 ± 29		380 ± 8.9		570 ± 30		620 ± 24	
PFHpA	220 ± 8		190 ± 15		360 ± 32		320 ± 28	
PFOA	420 ± 16		400 ± 27		940 ± 68		870 ± 56	
PFBS	97 ± 4.6		91 ± 2.0		160 ± 9.6		150 ± 2.4	
PFPeS	21 ± 1.8		20 ± 1.1		70 ± 6.3		63 ± 4.1	
PFHxS	98 ± 8.3		87 ± 5.2		330 ± 14		300 ± 17	
PFHpS	7.4 ± 0.53		7.0 ± 0.38		22 ± 2.3		20 ± 1.9	
PFOS	150 ± 14		130 ± 7.0		250 ± 17		240 ± 31	
PFECHS	28 ± 2.7		20 ± 1.5		39 ± 3.8		30 ± 2.7	
EtFOSAA	19 ± 1.1		<0.10					
MeFOSAA	5.1 ± 0.52		<0.10					

Table S 6. ANOVA tables created with R for leachate water samples

Compound	term	df	sumsq	meansq	statistic	p.value
PFBA	Method	1	36.12012	36.12012	130.0833	1.79E-08
PFBA	Replicate	2	0.598772	0.299386	1.078212	0.366842
PFBA	Residuals	14	3.887367	0.277669		
PFPeA	Method	1	9.248453	9.248453	13.03574	0.002839
PFPeA	Replicate	2	0.628368	0.314184	0.442844	0.6509
PFPeA	Residuals	14	9.932566	0.709469		
PFBS	Method	1	2.620834	2.620834	15.23905	0.00159
PFBS	Replicate	2	0.211365	0.105682	0.614499	0.554877
PFBS	Residuals	14	2.40774	0.171981		
PFHxA	Method	1	9.439895	9.439895	1.841737	0.196225
PFHxA	Replicate	2	0.508331	0.254165	0.049588	0.951788
PFHxA	Residuals	14	71.75754	5.125538		
PFPeS	Method	1	0.013933	0.013933	0.480915	0.499353
PFPeS	Replicate	2	0.032727	0.016364	0.564803	0.580902
PFPeS	Residuals	14	0.405611	0.028972		
PFHpA	Method	1	46.65911	46.65911	49.21831	6.1E-06
PFHpA	Replicate	2	8.898391	4.449195	4.693228	0.027552
PFHpA	Residuals	14	13.27204	0.948003		
PFHxS	Method	1	6.560113	6.560113	10.48524	0.005952
PFHxS	Replicate	2	0.488792	0.244396	0.390626	0.683782
PFHxS	Residuals	14	8.759129	0.625652		
PFOA	Method	1	17.65875	17.65875	4.245167	0.058453
PFOA	Replicate	2	21.29374	10.64687	2.55951	0.112885
PFOA	Residuals	14	58.23622	4.15973		
PFHpS	Method	1	0.011145	0.011145	4.678342	0.048336
PFHpS	Replicate	2	0.004249	0.002124	0.891726	0.431998
PFHpS	Residuals	14	0.033352	0.002382		
PFECHS	Method	1	2.365373	2.365373	45.39936	9.5E-06
PFECHS	Replicate	2	0.058476	0.029238	0.561173	0.582857
PFECHS	Residuals	14	0.72942	0.052101		
PFOS	Method	1	19.37451	19.37451	11.83815	0.003978
PFOS	Replicate	2	1.049295	0.524648	0.320568	0.730925
PFOS	Residuals	14	22.91263	1.636617		

Table S 7. ANOVA tables created with R for ground water samples

Compound	term	df	sumsq	meansq	statistic	p.value
PFBA	Method	1	16.0072	16.0072	269.0422	1.55E-10
PFBA	Replicate	2	0.20941	0.104705	1.759834	0.208073
PFBA	Residuals	14	0.832958	0.059497		
PFPeA	Method	1	9.742093	9.742093	59.22433	2.14E-06
PFPeA	Replicate	2	0.690613	0.345307	2.099195	0.159465
PFPeA	Residuals	14	2.302927	0.164495		
PFBS	Method	1	4.235821	4.235821	13.78356	0.002319
PFBS	Replicate	2	2.93176	1.46588	4.770041	0.026317
PFBS	Residuals	14	4.302336	0.30731		
PFHxA	Method	1	13.72388	13.72388	5.819165	0.03015
PFHxA	Replicate	2	0.018039	0.009019	0.003824	0.996184
PFHxA	Residuals	14	33.0175	2.358393		
PFPeS	Method	1	0.654279	0.654279	5.061094	0.041078
PFPeS	Replicate	2	0.196855	0.098427	0.761372	0.485419
PFPeS	Residuals	14	1.809867	0.129276		
PFHpA	Method	1	10.92132	10.92132	5.45582	0.034897
PFHpA	Replicate	2	2.41653	1.208265	0.603597	0.56047
PFHpA	Residuals	14	28.02483	2.001774		
PFHxS	Method	1	15.34387	15.34387	11.54805	0.004328
PFHxS	Replicate	2	1.789316	0.894658	0.673335	0.525772
PFHxS	Residuals	14	18.60176	1.328697		
PFOA	Method	1	64.59268	64.59268	7.11099	0.01842
PFOA	Replicate	2	2.932178	1.466089	0.161401	0.852511
PFOA	Residuals	14	127.169	9.0835		
PFHpS	Method	1	0.062563	0.062563	4.94616	0.043114
PFHpS	Replicate	2	0.012232	0.006116	0.483509	0.62654
PFHpS	Residuals	14	0.177082	0.012649		
PFECHS	Method	1	0.869026	0.869026	29.75696	8.48E-05
PFECHS	Replicate	2	0.006389	0.003194	0.109384	0.897145
PFECHS	Residuals	14	0.408858	0.029204		
PFOS	Method	1	0.883706	0.883706	0.603097	0.450321
PFOS	Replicate	2	7.416562	3.708281	2.530767	0.11529
PFOS	Residuals	14	20.51392	1.46528		

Table S 8. Calculated Method Detection Limit (MDL) and Method Quantitation Limit (MQL) in the triple-quadrupole (QqQ) LC-MS/MS instrumentation; and lowest detectable concentration of PFAS in the targeted analysis using the LC-HRMS

		HRMS	QqQ	
Compound	m/z	LOD	MDL	MQL
PFBA	212.97835	0.50	3.30	8.94
PFPeA	262.97537	0.50	1.81	5.01
PFBS	298.94235	0.05	1.96	4.98
PFHxA	312.97217	0.05	1.94	5.31
4:2 FTSA	326.97363	0.50	2.15	5.11
PFPeS	348.93878	0.10	0.22	0.56
PFHpA	362.96869	0.50	2.63	6.99
NaDONA	376.96783	0.50	3.30	8.94
PFHxS	398.93542	0.05	1.84	4.57
PFOA	412.96530	0.05	2.54	6.66
6:2 FTSA	426.96664	0.50	0.05	0.10
PFHpS	448.93213	0.10	0.12	0.28
PFEtCHxS	460.93228	0.10	0.05	0.10
PFNA	462.96240	0.50	2.10	5.39
FOSA	497.94534	0.10	1.22	2.95
PFOS	498.92923	0.05	2.39	5.02
PFDA	512.95898	0.50	2.74	7.12
8:2 FTSA	526.96039	0.50	2.16	5.12
9Cl-PF3ONS	530.89471	0.50	0.05	0.10
PFNS	548.92621	0.50	0.22	0.62
PFUnDA	562.95563	1.00	2.32	5.97
MeFOSAA	569.96594	0.05	0.05	0.10
EtFOSAA	583.98350	0.50	0.05	0.10
PFDS	598.92261	0.50	0.05	0.10
PFDoDA	612.95209	1.00	2.03	5.21
11Cl-OF3OUDS	630.88776	1.00	0.05	0.10
PFTriDA	662.94928	1.00	2.11	5.49
PFTeDA	712.94580	1.00	2.89	7.72

Table S 9. Full list of compounds identified through the suspect screening

Name	Formula	Δmass [ppm] GW	Δmass [ppm] LW	MS2 ions	Calc. MW	m/z	RT [min]
Cyclohexanesulfonic acid, undecafluoro- (PFCHS)	C6 H F11 O3 S	-0.13	0.16	$[M-H]^-$ $[M-HSO_3]^-$ SO_3F^-	361.94729	360.9398	8.22
Cyclohexanesulfonic acid, decafluoro(trifluoromethyl)- (PFMeCHS)	C7 H F13 O3 S	0.02	0.61	$[M-H]^-$ $[M-HSO_3]^-$ SO_3F^-	411.94419	410.9369	9.06
Cyclohexanesulfonic acid, decafluoro(pentafluoroethyl)- (PFECHS)	C8 H F15 O3 S	0.33	0.57	$[M-H]^-$ $[M-HSO_3]^-$ SO_3F^-	461.94077	460.9335	9.77
Perfluoropropane sulfonamide (FPrSA)	C3 H2 F7 N O2 S	-0.18	0.47	$[M-H]^-$ SO_2N^-	248.96965	247.9624	5.86
Perfluorobutylsulphonamide (FBSA)	C4 H2 F9 N O2 S	0.32	0.52	$[M-H]^-$ SO_2N^-	298.9665	297.9592	7.97
Perfluoropentane sulfonamide (FPSA)	C5 H2 F11 N O2 S	-0.12	-0.14	$[M-H]^-$ SO_2N^-	348.96322	347.9559	9.21
Perfluorohexanesulfonamide (FHxSA)	C6 H2 F13 N O2 S	-0.14	0.15	$[M-H]^-$ SO_2N^-	398.96015	397.9529	10.08
Perfluorooctanesulfonamide (FOSA)	C8 H2 F17 N O2 S	0.25	0.81	$[M-H]^-$ SO_2N^-	498.95371	497.9464	11.32
4:2 Fluorotelomer sulfonic acid (4:2 FTSA)	C6 H5 F9 O3 S	0.62	0.91	SO_3^- HSO_3^- NL: HF	327.98184	326.9746	7.77
6:2 Fluorotelomer sulfonic acid (6:2 FTSA)	C8 H5 F13 O3 S	-0.58	-0.54	SO_3^- HSO_3^- NL: HF	427.97503	426.9678	9.81
8:2 Fluorotelomer sulfonic acid (8:2 FTSA)	C10 H5 F17 O3 S	0.08	0.58	SO_3^- HSO_3^- NL: HF	527.96903	526.9618	11.06
Perfluorotridecanoic acid (PFTriDA)	C13 H F25 O2	-	1.15	$C_nF_{2n+1}^-$	663.95815	662.9500	12.16
Perfluorobutanoic acid (PFBA)	C4 H F7 O2	-1.04	-2.35	$C_nF_{2n+1}^-$	213.98607	212.9788	3.04
Perfluoropentanoic acid (PFPeA)	C5 H F9 O2	0.19	-0.53	$C_nF_{2n+1}^-$	263.98318	262.9759	6.09
Perfluorohexanoic acid (PFHxA)	C6 H F11 O2	0.62	0.84	$C_nF_{2n+1}^-$	313.98039	312.9731	7.87
Perfluoroheptanoic acid (PFHpA)	C7 H F13 O2	0.20	-0.15	$C_nF_{2n+1}^-$	363.97674	362.9695	8.98
Perfluorooctanoic acid (PFOA)	C8 H F15 O2	-0.32	-0.31	$C_nF_{2n+1}^-$	413.9736	412.9663	9.78
Perfluorononanoic acid (PFNA)	C9 H F17 O2	0.39	0.89	$C_nF_{2n+1}^-$	463.97068	462.9634	10.43
Perfluorodecanoic acid (PFDA)	C10 H F19 O2	0.23	0.59	$C_nF_{2n+1}^-$	513.96745	512.9602	10.98
Perfluoroundecanoic acid (PFUdA)	C11 H F21 O2	0.18	0.69	$C_nF_{2n+1}^-$	563.96434	562.9571	11.44
Perfluorododecanoic acid (PFDoDA)	C12 H F23 O2	-0.20	0.65	$C_nF_{2n+1}^-$	613.96121	612.9539	11.82
1,1,2,2,3,3,3-Heptafluoro-1-propanesulfonic acid (PFPrS)	C3 H F7 O3 S	-2.25	-0.55	$[M-H]^-$ SO_3^-	249.95339	248.9461	4.47
Perfluorobutanesulfonic acid (PFBS)	C4 H F9 O3 S	0.52	0.76	$[M-H]^-$ SO_3^-	299.95045	298.9432	6.69
Perfluoropentanesulfonic acid (PFPeS)	C5 H F11 O3 S	-0.07	-0.23	$[M-H]^-$ SO_3^-	349.94674	348.9395	8.11
Perfluorohexanesulfonic acid (PFHxS)	C6 H F13 O3 S	-0.22	-0.38	$[M-H]^-$ SO_3^-	399.94359	398.9363	9.08
Perfluoroheptanesulfonic acid (PFHpS)	C7 H F15 O3 S	0.01	0.04	$[M-H]^-$ SO_3^-	449.94064	448.9334	9.84
Perfluorooctanesulfonic acid (PFOS)	C8 H F17 O3 S	0.52	0.71	$[M-H]^-$ SO_3^-	499.93787	498.9306	10.45
2-(N-Ethylperfluorooctanesulfonamido)acetic acid (EtFOSAA)	C12 H8 F17 N O4 S	-	0.42	-	584.9905	583.9832	11.42

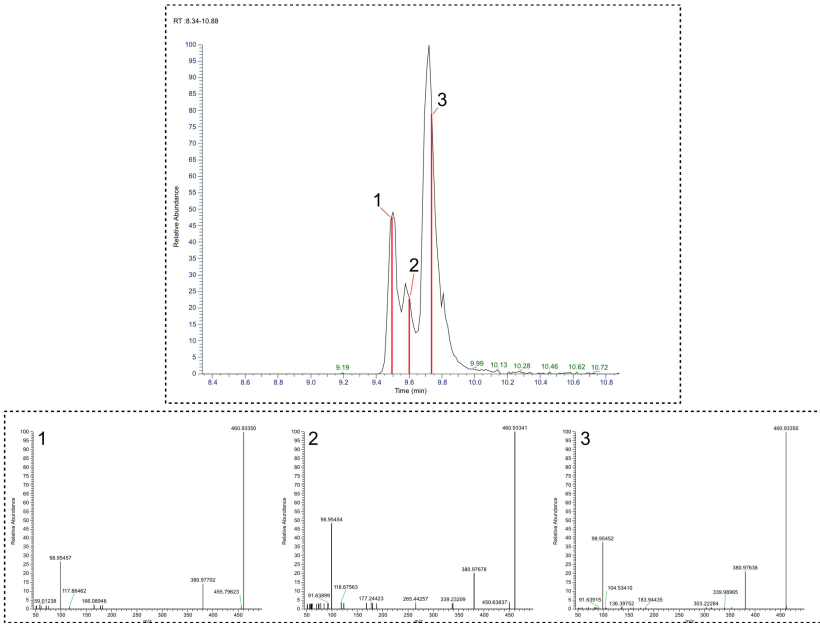

Figure S 1. Extracted ion chromatogram of PFECHS and its related isomers. Included are also MS² spectra which are annotated where in the chromatogram they were taken.

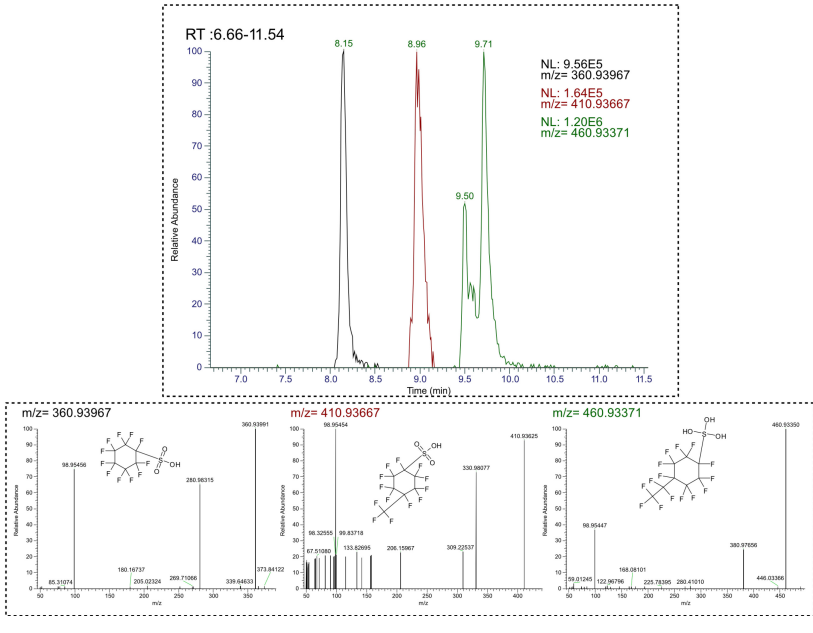

Figure S 2. Color coded extracted ion chromatograms of cyclic PFSAs. Additionally, there are the corresponding MS² spectra where the m/z is color coded from where they were taken in the chromatogram.

II

Journal of Hazardous Materials 480 (2024) 136316

Contents lists available at ScienceDirect

Journal of Hazardous Materials

journal homepage: www.elsevier.com/locate/jhazmat

Suspect and non-target screening of per- and polyfluoroalkyl substances (PFAS) and other halogenated substances in electrochemically oxidized landfill leachate and groundwater

Svante Rehnstam [a], Sanne J. Smith [a,b], Lutz Ahrens [a]

[a] Swedish University of Agricultural Sciences (SLU), Department of Aquatic Sciences and Assessment, Lennart Hjelms vag 9, 756 51 Uppsala, Sweden
[b] Delft University of Technology, Department of Water Management, Stevinweg 1, 2628 CN Delft, the Netherlands

HIGHLIGHTS

- EO as destructive treatment for PFAS-contaminated landfill leachate and groundwater.
- Identification of new halogenated substances using suspect and non-target screening.
- Transformation products identified originating from electrochemical process.
- New pathways identified for transformation of PFAS.

GRAPHICAL ABSTRACT

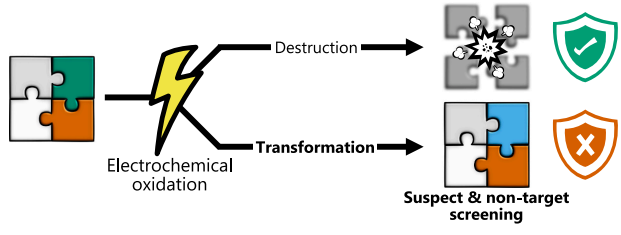

ARTICLE INFO

Keywords:
Per- and polyfluoroalkyl substances
High-resolution mass spectrometry
Electrochemical oxidation
Non-target screening
Destructive treatment
Transformation products

ABSTRACT

Release of persistent and potentially toxic per- and polyfluoroalkyl substances (PFAS) and other halogenated compounds into the aqueous environment is an emerging issue and advanced treatment methods are needed for their removal from contaminated water. Destructive treatment methods for PFAS exist, but there is a risk of incomplete degradation, resulting in creation of transformation products during treatment. This study assessed the potential of electrochemical oxidation (EO) for destruction of PFAS and other halogenated compounds, and their transformation products. Suspect and non-target screening were used to explore the chemical space of these samples and identify compounds present before and after the treatment, including transformation products. In total, 21 PFAS classes and 53 individual PFAS were identified using suspect and non-target screening, with confidence level (CL) 3d or higher. Two new classes of PFAS (FASHN and MeOH-FASA) were discovered for the first time. Suspect screening of PFAS revealed that hydro-substituted and ether PFAS could be formed during EO. A total of 12 chlorinated and two brominated compounds were also detected and confirmed with CL 1–3, with six compounds determined to be transformation products. Formation of ammonium oxidation byproducts was hypothesized as being responsible for most identified transformation products formed during EO.

E-mail address: svante.rehnstam@slu.se (S. Rehnstam).

https://doi.org/10.1016/j.jhazmat.2024.136316
Received 23 May 2024; Received in revised form 7 October 2024; Accepted 25 October 2024
Available online 28 October 2024

1. Introduction

Landfills are often considered point sources of environmental contamination [1]. Organic micropollutants in landfill leachate can have adverse effects on nearby soil, groundwater, and surface water ecosystems [2,3]. Efforts are taken to reduce the environmental impact from landfill facilities, e.g., conventional wastewater treatment techniques such as aerobic and anaerobic biological processes, chemical oxidation, and chemical precipitation are commonly utilized at such sites [4]. More advanced treatment techniques involving e.g., granular activated carbon (GAC) are sometimes included to remove organic micropollutants [5].

Per- and polyfluoroalkyl substances (PFAS), a group of halogenated organic micropollutants, are difficult to remove or degrade in water treatment processes [6]. These compounds are known for being extremely chemically and thermally persistent, potentially bioaccumulative, and toxic [7]. Due to their unique characteristics, they are widely used in products such as textiles, aqueous film-forming foams (AFFF), and non-stick coatings [8]. The most common technology for removing PFAS from water matrices is through adsorption to GAC, where PFAS are bound to a sorbent but not destroyed [9]. This creates a separate waste stream, which has to be taken care of [10]. Destructive treatment methods are typically not cost-efficient, due to the high energy intensity required to break down PFAS [11]. Combinations of different treatment methods to concentrate the waste stream and then destroy the concentrated waste have advantages over individual advanced treatment processes [12]. One example is combined foam fractionation as a concentration treatment and electrochemical oxidation (EO) as a destructive treatment [13,14].

Foam fractionation relies on the surfactant properties of many PFAS, particularly perfluoroalkyl acids (PFAA), adsorbing these compounds on rising air bubbles [15]. Presence of sufficient amphiphilic substances in water leads to formation of a foam in which PFAS are enriched. Removing this PFAS-rich foam from the water surface results in a relatively PFAS-free effluent. The PFAS in the foam fraction can be destroyed by e.g., EO, which uses anodic materials with high overpotential for the oxygen evolution reaction [16]. Direct electron transfer to the anode is the first step in oxidation of PFAS, after which the perfluoroalkyl chain is generally assumed to 'unzip', ideally ultimately achieving full defluorination. However, formation of transformation products, including PFAS, is a well-known issue [17,18].

Formation of transformation products is an unwanted process in most degradation processes, because complete PFAS mineralization is the ultimate goal [12,18]. The transformation products that may form during the EO process have not been widely investigated, since most studies rely on quantification of PFAS concentrations using targeted triple-quadrupole mass spectrometer techniques [18,19]. Advanced oxidation processes may also result in formation of harmful chlorinated and brominated transformation byproducts [13]. There is thus an urgent need for untargeted analyses to investigate how halogenated substances are (trans)formed during the EO process, to assess formation of possibly harmful degradation (by)products. Untargeted analyses are particularly important for complex matrices such as landfill leachate, because the presence of co-contaminants results in an even wider range of possible degradation (by)products.

Suspect screening and non-target screening (NTS) are analytical techniques appropriate for identifying compounds and molecules when authentic standards and surrogates are not available [20]. Suspect screening relies on databases and previously recorded data, while NTS relies instead on feature prioritization [21]. In suspect screening, efforts are made to expand the scope beyond what has already been detected, to predict transformation products through chemical transformation simulation [22]. There have also been advances in NTS specifically for PFAS, most notably the software FluoroMatch developed by Koelmel and co-workers to streamline the NTS workflow [23–25].

A previous study by our research group [13] showed that EO with boron-doped diamond anodes can successfully degrade PFAS in landfill leachate and groundwater, with or without foam fractionation as a pre-treatment step. Additional analyses performed as part of that study, most notably effect-based bioassays and extractable organofluorine (EOF) analyses, indicated the presence of unknown fluorinated and potentially toxic compounds. Those findings prompted the present study, which aimed to identify transformation products formed during EO by utilizing untargeted techniques with high-resolution mass spectrometry coupled to liquid chromatography (LC-HRMS).

2. Experimental

2.1. Samples

Four different water types were treated electrochemically: (i) groundwater and (ii) landfill leachate from a landfill facility located in Uppsala, Sweden, and foam from (iii) groundwater and (iv) landfill leachate treated using foam fractionation from our previous study [26]. For all four water types, samples representing 0 h (initial water) and 1, 3, 5, 7, and 9 h (t = 0–9) of EO treatment were analyzed. The foam fractionation setup used a 10 cm diameter column, into which a peristaltic pump was pumping groundwater and leachate water. The foam generated from the air introduced through the air inlet was collected in foam collection vessels. Electrochemical oxidation was performed with a feed tank and a 20 L flow-through cell which was equipped with a boron-doped diamond anode and stainless steel cathode. For details of the experimental set-up and sample extraction, see [13].

2.2. Instrumental analysis

Liquid chromatography (LC) was performed using a Vanquish Horizon UPLC system. It was coupled to a QExactive Focus Orbitrap mass spectrometer (Thermo Fisher Scientific, Bremen, Germany), with a heated electrospray ionization source (HESI-II) run in negative ionization mode. Samples (10 μL) were injected using a LC TriPlus RSH autosampler. The chromatographic system used a gradient mobile phase program consisting of an aqueous solvent with 5 mM of ammonium acetate and an organic solvent with 5 mM ammonium acetate, all run with a flow rate of 0.3 mL min^{-1}. For details of the gradient program, see Table S1 in Supplementary Information (SI). The Orbitrap was run in negative polarity mode, set to perform a full scan over the range 100–1000 *m/z*. For collection of MS^2 data, the instrument used data-dependent acquisition (DDA) in *discovery mode* (loop count set to n = 3). The ion source settings were as follows: sheath gas flow rate 45 a.u., auxiliary gas flow rate 10 a.u., sweep gas flow rate 0 a.u., spray voltage 4.1 kV, capillary temperature 350 °C, S-lens RF level 25 a.u., and auxiliary gas heater temperature 400 °C.

2.3. Data processing

The raw data obtained in LC-HRMS were processed using Compound Discoverer (version 3.3), in two separate tailored modular workflows (for details, see Table S2 in SI). One workflow was tailored for PFAS analysis and the other for compounds containing bromine and chlorine. For a peak to be considered a feature, it needed to have signal to noise ratio (S/N) greater than 3 and signal intensity greater than 10,000 counts. The use of a low S/N is to avoid false negatives (type II errors) in the early stages of processing, which is common practice in untargeted analyses [20,27]. The PFAS plugin from ThermoFisher [28], which is based on the work of Kaufmann et al. [29] and Koelmel et al. [24], was used to determine mass over carbon (m/C) and mass defect over carbon (md/C) ratios, for initial screening of potential peaks [29,24,25]. The plugin also contained a list of known PFAS fragments recorded in MS/MS measurements.

For PFAS, peak picking resulted in a total number of 144,387 features being detected (Fig. 1). Blank subtraction was performed to

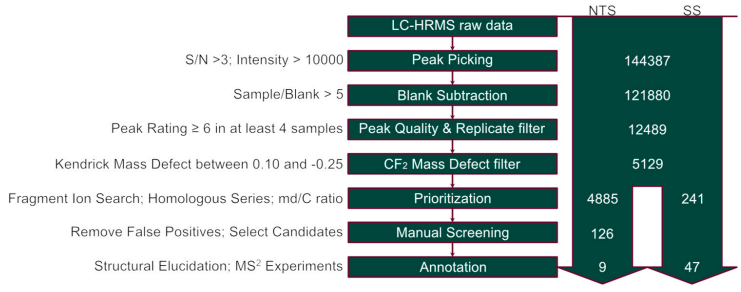

Fig. 1. Flow chart summarizing the non-target (NTS) and suspect screening (SS) process.

remove any contaminants introduced from sample preparation and laboratory equipment, which reduced the number of features to 121,880. After blank subtraction, quality control of the detected features was performed by utilizing the peak rating algorithm in Compound Discoverer, where a peak need to be present in all four replicates and have a peak rating greater than 6 to be considered a real feature, resulting in a total of 12,489 features. Peak rating is calculated based on four main factors, namely full-width half maxima to base (FWHM2Base), Jaggedness, Modality, and Zig-Zag. FWHM2Base is calculated based on a ratio of the peak width at half height divided by the peak. The peak rating is reversely proportional to the value of FWHM2Base. Jaggedness measures how many times the intensity of a peak alternate between going up and down in a row, where a low Jaggedness value will result in a higher peak rating. Modality will look for unexpected valleys in a peak that may occur before reaching baseline. Once again a low value for Modality will increase the peak rating. The final factor, Zig-Zag, calculates the mean number of valleys in one peak and divide it by the peak height from baseline. A high Zig-Zag value will result in a low peak rating. For more details on how the peak rating calculations are performed see the Compound Discoverer User Guide for LC Studies [30]. Details of data processing are provided in Table S2 in SI.

For brominated and chlorinated compounds, peak picking resulted in 146,007 features, which were reduced through blank subtraction (123,280 features) and peak quality and replicate filter (12,711 features) (Fig. S1 in SI).

2.4. Suspect screening for identification of PFAS

After peak rating, all peaks which did not fall within a CF_2-adjusted Kendrick mass defect (KMD) of −0.25 and 0.10 were filtered out, which resulted in 5129 final features, although this step was only performed in the PFAS analysis (Fig. 1). Suspect screening for PFAS was performed using a suspect list obtained from the NORMAN Network's substance database, which was filtered for PFAS [31] ($n = 1291$), Chemical List PFASSTRUCT-2022–04-20 ($n = 10737$) and PFAS_NIST obtained from the ThermoFisher PFAS plugin ($n = 4951$) [28], and the *in-silico* generated suspect list ($n = 36604$) from Getzinger et al. [22] (in total $n = 53{,}643$, with compound overlapping between the suspect lists) [22]. Prioritization was performed using the suspect screening lists by filtering out all features without a hit, which resulted in 241 features. After further manual annotation, mainly to remove false positives, 44 features were identified.

2.5. Suspect screening for identification of brominated and chlorinated compounds

For brominated and chlorinated compounds, only the NORMAN Network's substance database was used [32]. The database was first filtered to include only drinking water chemicals and then further filtered for disinfection by-products. Finally, one suspect list for chlorinated compounds was made by filtering for compounds containing "Cl" ($n = 6313$) and one was made for brominated compounds by filtering for compounds containing "Br" ($n = 1909$) (Fig. S1 in SI).

All compounds with hits from ChemSpider or the suspect lists were subjected to the fragment ion search (FISh) function in Compound Discoverer. This feature created *in-silico* fragments of the proposed structures and produced a match factor based on the number of peaks from the MS^2 data that matched the *in-silico* generated fragments. The proposed structures were ranked and prioritized based on the number of matching FISh fragments. Compounds which had a FISh score higher than zero were controlled for false positives (23 features) and then further manually annotated (14 features).

2.6. Non-target screening for identification of PFAS

Non-targeted screening comprised four parts: (i) iterative-DDA using the IE-Omics R script developed by Koelmel et al. (2017); (ii) fragment flagging, which is referred to as 'compound classes' in Compound Discoverer; (iii) a mass defect vs carbon number approach, as described by Kaufmann et al. [29]; and (iv) homologous series identification, which was performed by an in-house written R-script [33].

The iterative-DDA strategy was developed to generate as many MS^2 spectra as possible in the shortest possible time (Koelmel et al., 2017). Using iterative DDA made other strategies such as fragment flagging more powerful, as they depend on the presence of MS^2 data.

The mass defect vs carbon number approach was used as a first step in feature prioritization [29]. Features with m/C ratio greater than 35 and less than −0.0007 were investigated. When all fragment ion search potential hits, homologous series hits, and md/C ratio hits were combined, a total of 4885 features was obtained. These features were further categorized manually as false positives or potential hits, resulting in a final total of 126 features, which were then further annotated. The final total of nine annotated compounds was obtained from non-target screening.

Fragment flagging was enabled by integration of the FluoroMatch fragment library into Compound Discoverer. The fragment library contained over 800 curated diagnostic fragments, which were used as prioritization tools. If a feature which contained MS2 data had a fragment that matched any fragment in the library, it was given a Compound Class Score greater than zero. The feature list was then sorted in terms of abundance of fragments matching the library, and false positives and potential hits were categorized.

In homologous series identification, the final prioritization strategy used in non-target screening, the feature list was first curated based on quality control from peak ratings and no false positives from previous investigations. Features that remained were exported to an Excel file, which was then imported into R and subjected to the in-house R script for identifying homologous series. The homologous series scripts can be

found on GitHub [33].

For both suspect and non-target screening results, confidence level (CL) was determined based on a modified version, where the modifications were adjusted to better reflect CL in PFAS [34,35].

2.7. Quality control

Quality control was performed before and after the instrumental analysis. The mass spectrometer was first calibrated with the standard Pierce Mix for negative mode calibration on an QExactive Focus Orbitrap and then a mixture of chemicals was injected five times into the instrument with a fast gradient. The mass accuracy of the injected standards was determined, and in all cases fell well within the 3 ppm limit set in the laboratory. After analysis, the mass accuracy was once again measured by injecting the standard mixture five more times. If the value fell within the 3 ppm limit, the quality of the analysis was deemed acceptable.

2.8. Numerical data analysis

The Compound Discoverer software used for feature detection and evaluation also calculates the average area of each feature in every sample matrix and time point based on the median value. These median values were used to calculate the relative area of each compound of interest to evaluate how they were affected by the water treatment process.

The data were processed in R, using the *tidyverse* and *stringr* packages for data wrangling and creating graphics [36-38]. Relative areas for compounds and features obtained from Compound Discoverer were first processed by normalizing all values, that meaning both PFAS results and Br & Cl results, to the area of an internal standard present in all samples ($^{13}C_8$-PFOA internal standard (IS)). Each compound featured in any of the heatmap plots had its area normalized as a percentage total area summed. The relative area was then plotted as a color, with the time point with the greatest area given the darkest hue.

3. Results and discussion

3.1. Suspect screening of PFAS

In total, 17 PFAS classes and 47 individual PFAS were identified using suspect screening at CL 1–3 in treated and untreated samples (Table 1). Five individual PFAS (perfluorononane sulfonic acid, perfluoroundecanoic acid, perfluorododecanoic acid, perfluorotridecanoic acid, and perfluorotetradecanoic acid) identified in concentrations close to the limit of quantitation using the targeted method in our original study [13] were not identified here.

All perfluoroalkyl carboxylic acids (PFCA, ID 1 f) and all perfluoroalkyl sulfonic acids (PFSA, ID 2 f) except perfluoropropane sulfonic acid (PFPrS) were identified at CL 1a and confirmed with reference standards. PFPrS was identified at CL 2a, due to co-occurrence of many homologues with higher retention times and similar fragmentation patterns in the MS^2 data. The fragments observed in the MS^2 data matched other PFSA. PFPrS was the only PFAA detected here that was not included in the targeted method developed in our previous study [13].

Three fluorotelomer sulfonates, 4:2 FTSA, 6:2 FTSA, and 8:2 FTSA, were detected and confirmed at CL 1a. Three cyclic PFSA were identified (ID 4 f, 5 f, and 6 f), of which perfluoroethylcyclohexane sulfonic acid (PFECHS, level 1a) was the only one confirmed with a standard. Additionally, two isomers of PFECHS were present, but they could only be determined at CL 3a, due to uncertainty of the position of the perfluorinated ethyl group. Two homologues of PFECHS with identical fragmentation patterns were also detected. These were perfluoromethylcyclohexane sulfonic acid (PFMCHS) and perfluorocyclohexane sulfonic acid, which were identified at CL 3a and 2b, respectively. Cyclic PFSA have been detected previously in various environmental matrices, such as lakes and other surface water bodies [39]. We also want to acknowledge the difficulty with differentiating cyclic PFAS and unsaturated linear PFAS, but we do believe in this work that these were indeed cyclic in structure [34].

Perfluoroalkyl sulfonamides (FASA, ID 7 f) were detected with chain length of C_{3-6}, in addition to the previously quantified C_8 homologue. The C_4, C_6, and C_8 FASA were identified at CL 1a with reference standards. The C_3 and C_5 FASA were identified at CL 2c with the aid of homologue evidence and partly due to the low amount of diagnostic fragments inherent to FASA. FASA have been detected previously in matrices such as wastewater originating from 3M factories [40]. It is also known to occur at AFFF impacted sites where it believed to be an intermediate transformation product originating from a more complex structure but has been left with a sulfonamide head group [41,42].

Another AFFF derived PFAS is the group of N-methyl perfluoroalkane sulfonamidoacetic acids (Me-FASAA, ID 17 f), where only the C_8 N-methyl Me-FOSAA was previously included. It was identified here at CL 1a using a reference standard (Fig. S2 in SI). The C_3, C_4, C_5, and C_6 Me-FOSAA homologues were identified at CL 2b, due to the amount of diagnostic ions found in the MS^2 data (Fig. S2 in SI). The group N-ethyl (Et-FASAA, ID 18 f) had a similar spread of carbon chain lengths (C_4, C_5, C_6, C_8 Et-FASAA). Once again, only the C_8 form was previously included and was identified here at CL 1a using a reference standard. The homologues were confirmed at the same CL as the Me-FASAA (CL 2b), due to the strong diagnostic evidence found in the MS^2 data (Fig. S3 in SI). Me- and Et-FASAA have been detected previously in matrices such as urban runoff water, groundwater, and soil ([43]; T. V. [44]).

Of the remaining six PFAS classes identified with suspect screening, none was included in the targeted method used in the previous study [13].

First, two hydro-substituted perfluoroalkane sulfonic acids (H-PFSA, ID 9 f) were detected in the samples (Fig. S4 in SI). C_4 H-PFSA was confirmed at CL 2a by comparing the mass spectra against data found in the literature (T. [45]), whereas C_6 H-PFSA was confirmed at CL 3a. The most notable fragment was the $C_3F_5^-$ ion and the fragmentation did not follow the repeated loss of CF_2/CFH pattern but instead created a perfluoroalkene fragment, as reported previously [45]. There was also no observable HF loss in the spectra, contradicting previous findings [46], most likely due to the low abundance of ions acquired from samples. H-PFSA has been reported previously in groundwater, surface water, and sediment (T. [45,46]).

Second, three perfluoroalkyl ether sulfonic acids (PFESA, ID 10 f) were detected in the samples (Fig. S5 in SI). Two of these contained three perfluorocarbons, but with the ether group located at different positions. The two isomers were not baseline-separated, but the chromatograph clearly showed that these were two separate isomers and this was confirmed using MS^2 data. The first eluting peak had the ether group separated to the terminal CF_3 and the rest of the perfluorocarbon chain, which was highlighted by the lone fragment matching in accurate mass of CF_3O^-. The second eluting peak gave a match with the accurate mass of the fragment matching $C_2F_5O^-$. The third PFESA contained five fluorine saturated carbons, with the ether located before the terminal CF_3 group. Both PFESA with an ether group located next to the terminal CF3 showed the same fragment (CF_3O^-). PFESA have been detected previously [47,48].

Third, three AFFF-derived PFAA precursors, N-SPAmP-FHxSA, N-SPAmP-FHxSAA, and N-SPAmP-FHxSAPS (ID 19 f, 20 f, and 21 f), were detected (Fig. S6, S7 and S8 in SI). All spectra were compared with literature values to confirm the structure [49], which made it possible to identify them at CL 2a.

Fourth, keto-PFSA (ID 14 f) were detected with a perfluorocarbon chain of C_6, C_7, and C_8, at CL 3a for all three homologues (Fig. S9 in SI). Perfluoroalkene anions ($C_5F_9^-$ and $C_3F_5^-$) were observed in the mass spectrum, indicating a double bond formed at the terminal carbon. One

Table 1
Summary of results of suspect and non-target screening of PFAS: ID, class name, structure, number of CF_2 moieties (where applicable), and confidence level (CL).

ID	Class name	Structure	n	CL
1 f	PFCA	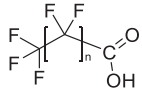	3 – 9	1a; 1a; 1a; 1a; 1a; 1a; 1a
2 f	PFSA	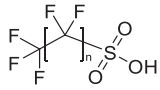	2 – 7	2a; 1a; 1a; 1a; 1a; 1a
3 f	n:2 FTSA	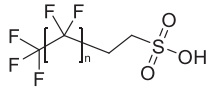	3; 5; 7	1a; 1a; 1a
4 f	PFECHS	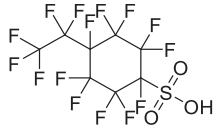	-	1a; 3a; 3a
5 f	PFMCHS	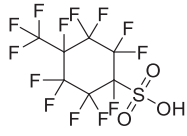	-	3a
6 f	PFCHS	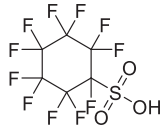	-	2b
7 f	FASA	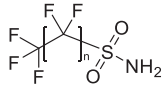	2 – 5; 7	3c; 1a; 3c; 1a;1a
8 f	FASHN	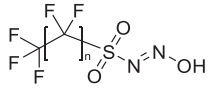	3 - 5	2b; 2b; 2b
9 f	H-PFSA	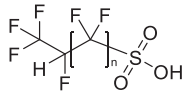	2; 4	2a; 3a; 3a
10 f	PFESA	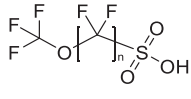	2 - 4	2a; 2a; 2a
11 f	MeOH-FHxSA	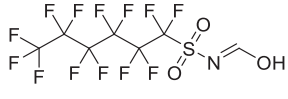	-	2b

(*continued on next page*)

Table 1 (*continued*)

ID	Class name	Structure	n	CL
12 f	PFOCHS	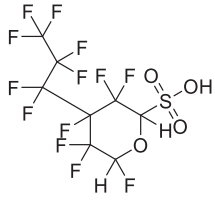	-	3a
13 f	Me-FASASiA	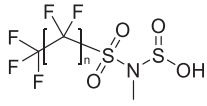	3 – 5	3b; 3b; 3b
14 f	Keto-PFSA	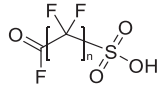	5 - 7	3a; 3a; 3a
15 f	DUPFOS	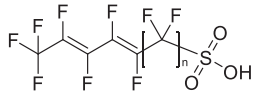	3	3b
16 f	FASASA	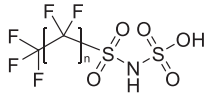	5; 7	2c; 2c
17 f	Me-FASAA	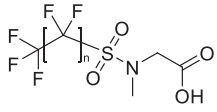	2 – 5; 7	2b; 2b; 2b; 2b; 1a
18 f	Et-FASAA	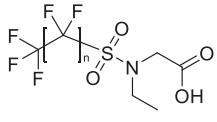	3—5; 7	2b; 2b; 2b; 1a
19 f	N-SPAmP-FHxSA	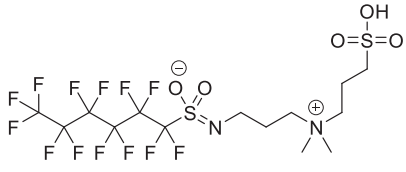	-	2a
20 f	N-SPAmP-FHxSAA	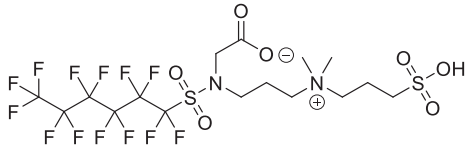	-	2a

(*continued on next page*)

Table 1 (*continued*)

ID	Class name	Structure	n	CL
21 f	N-SPAmP-FHxSAPS	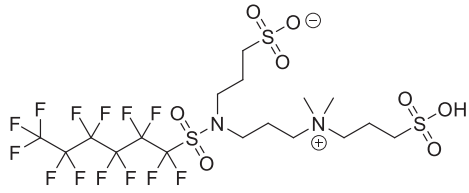	-	2a
22 f	Bistriflimide	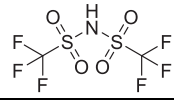	-	2b

FASHN
FHxHSN

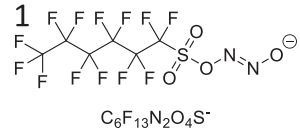

No.	Found m/z	Expected m/z	Error (ppm)	Error (mDa)
1	442.93768	442.93767	0.02	0.01
2	398.93661	398.9366	0.03	0.01
3	98.95615	98.95577	3.84	0.38
4	82.96086	82.96085	0.12	0.01
5	79.95742	79.95736	0.75	0.06
6	77.96558	77.96552	0.77	0.06

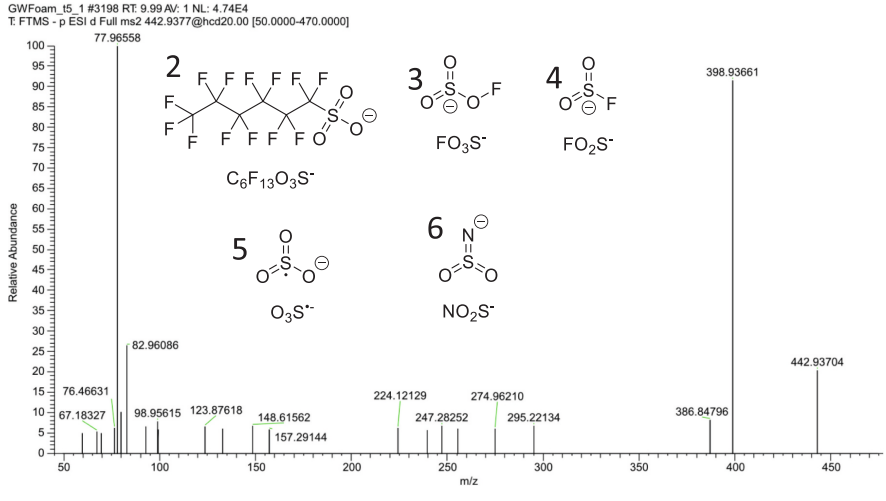

Fig. 2. Annotated mass spectrum of perfluorohexane sulfonhyponitrite (FHxHSN) showing the potential structure of the parent ion and the resulting fragments.

peak in particular implied that the functional group in question was an aldehyde with a neutral loss corresponding to loss of CF_2O. However, this peak was close to the noise level and only appeared in one of the homologues. Low-intensity and irregular mass spectra have been reported previously for this compound group [50,51].

The remaining two classes each only included one single compound. Perfluoroctane dienoic sulfonic acid (DUPFOS, ID 15 f) was detected (Fig. S10 in SI), but due to lack of diagnostic ions the exact positions of the double bonds could not be determined. A fragment consisting of C_8F_{13}, giving more information than MS1 alone, indicated that the compound was at the very least unsaturated in two places. Due to this lack of information, the CL was 3b. Only one previous study has detected this compound, in an AFFF formulation [52].

Another compound, known commercially as Bistriflimide (ID 22 f), was identified (Fig. S11 in SI). The compound is characterized by a central amide with SO_2 groups on each side, which is bonded to terminal CF_3. Although the molecule is small, the fragments obtained through MS2 data can be considered diagnostic, and as such it was identified at CL 2b. Bistriflimide is used as a reagent and catalyst in organic synthesis [53].

3.2. Structural and prioritization results from non-target screening

Non-target screening yielded two new classes of PFAS and four individual PFAS which, to the best of our knowledge, have never been reported previously, are not included in any suspect list, and have not been proposed in any previous study. These completely new and unreported compounds were in fact transformation products which developed during EO, indicating that entirely new structures can be created in remediation technologies.

In total, the non-target screening process yielded nine individual PFAS which were not present in any of the suspect lists used in the study. These included FASHN (ID 8 f), MeOH-FASA (ID 11 f), Me-FASASiA (ID 13 f), and FASASA (ID 16 f), where the classes FASHN and MeOH-FASA have not been reported previously. The other classes discovered in non-target screening prioritization have been reported previously [41,54], but new homologues were discovered in these classes, extending previous findings.

The first class of new compounds discovered (CL 2b) comprised perfluoroalkyl sulfonate hyponitrites (FASHN, ID 8 f) with perfluorocarbon chain length ranging from C_4 to C_6. The annotated spectrum of the C_6 homologue, perfluorohexane sulfonhyponitrite (FHxSHN), is shown in Fig. 2. Some fragments in the fragment library were the parent ions of the various chain lengths of PFSA, which were formed on neutral loss of N_2O^- as a transformation product created in the EO process (see Section 3.4.1).

The second new class of compounds, which also was determined to be formed during EO, was N-methanol perfluoroalkyl sulfonamide (MeOH-FASA) with C_6 chain length (MeOH-FHxSA; Fig. S12 in SI). The two pieces of evidence which led to derivation of this structure were the mass of the neutral loss and the fragment at ~107 *m/z*, indicating $CHNO_3S$ as the functional head group. The most likely configuration in this case is a sulfonamide with an unsaturated carbon bonded to an alcohol, hence the name MeOH-FASA. No homologues were detected and only C_6 MeOH-FASA was identified at CL 2b.

Other compound groups detected are better classified as emerging classes of environmental pollutants rather than completely new PFAS, as they have been reported previously [41,54,55]. However, the complementary information provided here demonstrates that additional isomers and homologues should be included in future studies. Therefore, information about the characteristic fragments is provided here to confirm and expand current knowledge.

The first class of emerging PFAS discovered was named perfluoroalkyl sulfonamide sulfonic acid (FASASA, 16 f) with two homologues in this class, namely C_6 and C_8, at CL 2c (Fig. S13 in SI). The most stable and intense peak in the mass spectrum was a *m/z* corresponding to FHxSA, which resulted from a neutral loss determined to be SO_3^-. This resulted in an observed *m/z* of a FHxSA and FOSA for C_6 and C_8, respectively. Additional evidence that the feature contained nitrogen was the peak at 77.96552 *m/z*, which corresponds to a molecular formula of SO_2N^- and is commonly found in FASA and other PFAS containing sulfonamide functional groups. The data obtained with collision energies at 10 and 30 eV did not yield any peaks with only the perfluoroalkyl backbone. However, when the collision energy was increased to 50 eV, $C_2F_5^-$ and $C_3F_7^-$ peaks were observed, further confirming the annotation. Although the head group of this class seems unorthodox, it has previously been synthesized in production of Zinc-Enzyme inhibitors [56]. It was detected in a recent study analyzing AFFF-impacted groundwater [54], which was the first to report the C_6 homologue, a finding now complemented by our discovery of the C_8 homologue.

Another class of emerging compounds with *m/z* of 475.93005 was discovered (Fig. S14 in SI). On elucidating the structure of this compound, it was determined to be an n-methyl perfluoroalkyl sulfonamide sulfinic acid (Me-FASASi) previously described in the literature as "methyl((perfluorohexyl)sulfonyl)sulfuramidous acid" [41]. However, Dewapriya et al. [41] discovered only two homologues, namely C_6 and C_8, whereas we identified C_4, C_5, and C_6 homologues. Additionally, this class of PFAS has only previously been detected in blood serum samples obtained from cattle [41], and our study is the first to detect it in aqueous samples.

The third class of emerging compounds discovered had a theoretical *m/z* of 440.94717 (Fig. S15 *in SI*). It has been reported in a previous publication as a type of fluorotelomer [55]. However, our results indicated that this feature is in fact a cyclic isomer (see compound ID 11 f in Table 1). The main evidence indicating a cyclic structure was the low amount of CF_2 losses and the fact that the longest perfluoroalkyl chain detected was a $C_3F_5^-$ peak. Additionally, most of the peaks detected by Hensema et al. (2020) were not detected in any MS^2 data in our study. However, the ring opening is not well described by the detected fragments (Fig. S15 in SI) and the compound of concern has not been confirmed with authentic reference standards.

3.3. Suspect screening of chlorinated and brominated compounds

A total of 12 chlorinated and two brominated compounds were detected and confirmed at CL 3 or above using the conventional Schymanski scale for assigning CL [35]. All compounds with CL 2a were confirmed using the Massbank mass spectrum record, which includes aromatic chlorinated transformation products, brominated transformation products, ordinary chlorinated micropollutants, and ordinary brominated micropollutants. No compounds which contained both chlorine and bromine in the same structure were detected. One compound detected (1,2,2-trichloroethanesulfonic acid) was not present in any of the suspect lists, so it had to be manually annotated. Mass spectrometry evidence and a discussion of compounds not identified as EO transformation products are provided in SI.

1,2,2-Trichloroethane sulfonic acid (ID 1c) is a highly chlorinated compound which was not present in any suspect list, but the fragments gave enough information to confirm it at CL 2b (Fig. S16 in SI). This compound has not been reported previously, to the best of our knowledge. The structure was determined based on the fragment observed at 114.92658 *m/z*, which with the aid of an elemental composition calculator was calculated to be an SO_3Cl^- ion. Based on this, the elemental composition of the compound was calculated to be $C_2Cl_3SO_3H$.

3,5-Dichlorosalicylic (ID 3c) acid was detected using the suspect list from Massbank (Fig. S17 in SI). There were many different isomers, but only one matched the spectral library obtained from Massbank at CL 2a. 3,5-Dichlorosalicylic acid is a bioactive compound used as a primer to start a defensive reaction in plants [57]. It has also been detected previously as a byproduct after EO treatment [58], as further discussed in

Section 3.4.2 below.

Three nitro-substituted phenyl compounds were detected, all of which were determined to be transformation products. This class of compounds was not well defined due to the absence of any Massbank records for the proposed structures. 2,6-Dichloro-4-nitrophenol (ID 4c) was detected through the suspect list (Fig. S18 in SI). This compound was not available in any spectral library that we accessed and could only be confirmed at CL 3. 2,6-Dichloro-4-nitrophenol is an intermediate in chemical synthesis and a disinfection byproduct [59]. It has been reported previously in various matrices such as seawater and drinking water ([60]; J. [61]). 2-Chloro-4,6-dinitrophenol (ID 7c) was determined at CL 3 (Fig. S19 in SI). It is a supplement used in culture medium for growth of microorganisms and has been reported previously in wastewater [62,63]. 4-Chloro-3-nitrobenzenesulfonic acid (10c) was identified at CL 3 (Fig. S20 in SI). It is a reagent used for preparation of 2-chloro-3-bromoaniline [64]. It is included in a suspect list made through *in-silico* predictions of phase 1 human metabolites [65].

3-[(2-Chlorophenyl)amino]−3-oxopropanoic acid (ID 6c), which was detected with the suspect list, did not have any spectral record in Massbank with CL 3 (Fig. S21 in SI). This compound has a data quality level of 5 on the CompTox Chemicals Dashboard, which is "programmatically curated from ACToR or PubChem, unique chemical identifiers with low confidence, single public source" with no reliable source available [66].

Only two brominated compounds were identified in suspect screening and both were determined to be transformation products. One of these, 2,4-dinitro-6-bromophenol (ID 1b), had very few fragments that could be considered diagnostic and the exact positions of the functional groups on the benzene could not be determined, so it was given CL 3 (Fig. S22 in SI). It is a precursor to brominated aniline derivatives and is hypothesized to be a potential breakdown product of tetrabromobisphenol A [67,68]. The other brominated compound detected in suspect screening was 3,5-dibromo-4-hydroxybenzoic acid (ID 2b), at CL 3 (Fig. S23 in SI). It is a secondary plant metabolite and has been reported previously in rivers downstream of industrial waste water effluents ([69]; H. H. [70])..

3.4. Transformation products

3.4.1. PFAS transformation products

Three different groups of PFAS were detected during EO and classified as (i) detected at all or almost all time points during EO at the same intensity, (ii) decreasing normalized area during EO, indicating mineralization or transformation of the compound into transformation products, or (iii) PFAS transformation products not detected at t = 0 and formed during EO (Fig. 3). The PFAS classes detected at all time points were PFESA (only the shortest homologue, ID 10 f, with some exceptions), Keto-PFSA (ID 14 f), and DUPFOS (ID 15 f), indicating that these persistent PFAS were resistant to the EO process applied in this study. The PFAS classes which showed decreasing levels were PFOCHS (ID 12 f), Me-FASASi (ID 13 f), FASASA (ID 16 f), Me-FASAA (ID 17 f), Et-FASAA (ID 18 f), N-SPAmP-FHxSA (ID 19 f), N-SPAmP-FHxSAA (ID 20 f), N-SPAmP-FHxSAPS (ID 21 f), and Bistriflimide (ID 22 f). The decreasing concentrations indicate that these compounds were either changed into transformation products or mineralized, as shown previously for PFCA and PFSA [71,72]. The third class of PFAS created during the EO process included FASHN (ID 8 f), H-PFSA (ID 9 f), and PFPrES in the PFESA (ID 10 f).

An increase in nitrate, originating from oxidation of ammonia during EO, may explain the formation of FASHN (Fig. 4). The hyponitrous acid group (N_2O_2H-group) of FASHN could be explained by the high concentration of nitrate, which in groundwater samples increased from below 1 mg L^{-1} to 6–8 mg L^{-1} after EO treatment in our previous study [13]. The high oxidation potential of the boron-doped diamond may have resulted in formation of hyponitrous acid, as an intermediate in ammonia oxidation that can be nucleophilically substituted on the

Table 2
Summary of results of suspect screening of chlorinated and brominated compounds: ID, class name, structure, and confidence level (CL).

ID	Name	Structure	CL
1c	1,2,2-Trichloroethane-sulfonic acid	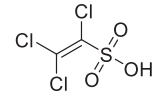	2b
2c	Chlorprop	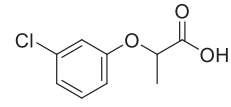	2a
3c	3,5-Dichlorosalicylic acid	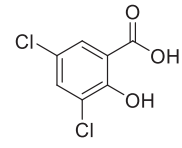	3
4c	2,6-Dichloro−4-nitrophenol	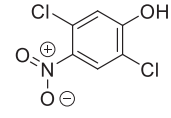	3
5c	Mecoprop	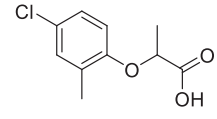	2a
6c	3-[(2-Chlorophenyl)amino]−3-oxopropanoic acid	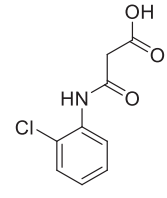	3
7c	2-Chloro−4,6-dinitrophenol	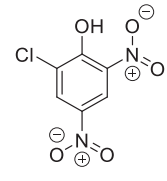	3
8c	2-Chloro−4-aminotoluene−5-sulfonic acid	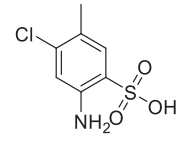	3
9c	2,5-Dichlorobenzene-sulfonic acid	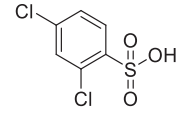	3

(*continued on next page*)

Table 2 (*continued*)

10c	4-Chloro−3-nitrobenzene-sulfonic acid	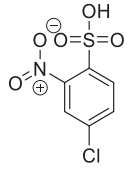	3
11c	2,3,4-Trichlorobenzene-sulfonic acid	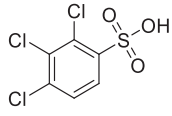	2b
12c	2-(2-Amino−4-chlorophenoxy)−5-chlorobenzene-sulfonic acid	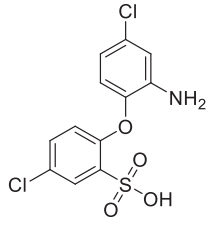	3
1b	2,4-dinitro−6-bromophenol	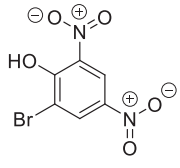	3
2b	3,5-Dibromo−4-hydroxybenzoic acid	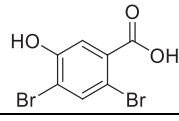	3

sulfonic acid head-group. We base this hypothesis on fundamental data on ammonia oxidation showing that one of the intermediate oxidation products is hyponitrous acid [73].

Although FASASA was not identified as a transformation product in EO treatment, we highlight it as a compound of emerging concern. A previous study showed that compounds with the FASASA head group ($C_6F_5SO_2NHSO_3H$ & 3-CF_3-C_6H_4 SO_2NHSO_3H) can be synthesized from alkylsulfonyl halides and sulfamic acid, in the presence of 1 N NaOH [74]. We hypothesize that the presence of sulfamic acid, which has been detected in wastewater treatment plant effluent around Europe at concentrations up to 1.6 ppm [75], led to the formation of FASASA-type compounds in the landfill from which our leachate samples originated. Sulfamic acid has also been detected in Candian municipal landfill sites and we believe that it is likely then to also be present in this landfill [76].

MeOH-FHxSA (ID 11 f) was detected after one hour of EO treatment, but not after 3 h or at any other time point. The most likely reason, based on the structure determined for this compound, was incomplete degradation of e.g., N-SPAmP-FHxSAA, Et-FASAA, or Me-FASAA. Common transformation products that occur normally during natural degradation are N-ethyl (Et-FOSE) and N-methyl perfluoroalkyl sulfonamido ethanols (Me-FOSE), which are very close in structure to MeOH-FHxSA (J. [77]). A carboxylic acid functional group is located on the amide for N-SPAmP-FHxSAA, as also observed for Et-FHxSAA and Me-FHxSAA. These could be converted to alcohols through a hydroxyl substitution on the carbon bonded to the amide combined with alkyl cleavages (Fig. 4).

H-PFSA were also determined to be a transformation product, as they were only detected in treated samples. However, the branched isomer of H-PFHxS was detected at t = 0 in every sample matrix. This class of PFAS is known to occur in biota and other environmental matrices such as groundwater, wastewater, and AFFF impacted soils. ([41,55]; T. [78, 79]). Detection of H-PFSA in our samples may indicate a new pathway for formation of hydrogen-substituted PFAS in aqueous samples. Only H-PFSA were detected here, but other terminal PFAS products such as H-PFCA should not be ignored and may be detected in other EO studies.

PFESA were not detected at t = 0 of EO treatment in one of the four matrices analyzed (leachate water), while in the other three matrices PFPeES and PFBES were detected at t = 0. On the other hand, PFPrES was never detected at t = 0, but at the earliest after 3 h of EO treatment. It is possible that chain shortening of longer-chain PFESA occurred, since the intensity of shorter-chain PFESA increased from 0 to 3 h of EO treatment. This is consistent with the mechanism of EO treatment, which results in chain shortening [16].

Me-FASASiA was detected in groundwater sample at t = 0, whereas it was not detected in leachate water at t = 0, but appeared after 1 h of EO treatment. It is possible that this class was simply not detected at t = 0 in the leachate samples due to low concentrations or matrix effects, rather than being formed during EO. This class of PFAS has been detected in biota [41], but was detected in aqueous samples for the first time in this study.

3.4.2. *Chlorinated and brominated transformation products*

There was a clear trend for all transformation products, except 3,5-dibromo-4-hydroxybenzoic acid and 3-[(2-chlorophenyl)amino]−3-oxopropanoic acid, to contain nitro groups, due to the increase of nitrate after EO (see Section 3.4.1). Introduction of nitrate radicals into a system has previously been shown to produce nitrate-containing organics, with nitro-substitution as a transformation pathway [80]. Another interesting finding was that these transformation products were often created, but then began breaking down. This indicates that nitrate was not the limiting reagent for their formation, since it was still present after the treatment.

In the EO-treated groundwater foam, nitro-phenols (2,6-dichloro-4-nitrophenol, 2-chloro-4,6-dinitrophenol, and 2,4-dinitro-6-bromophenol; ID 4c, 7c, and 1b) were not detected until after t = 5 h, whereas these compounds were detected at t = 3 h in the EO-treated groundwater (Fig. 5). The time of highest intensity for these transformation products also differed between the EO-treated groundwater and groundwater foam (Fig. 5). Two out of three transformation products were present in their highest concentration in the EO-treated groundwater at t = 5 h, but in the EO-treated groundwater foam at t = 7. Thus either the foam fractionation pre-treatment did not efficiently concentrate the precursors needed for formation of these transformation products, or the foam matrix limited the rate of reaction. This slower formation means that the foam fractionation step could create a rate-limiting matrix, where pre-concentration of PFAS causes some chlorinated and brominated compounds to be less efficiently oxidized. 3,5-dichlorosalicylic acid has been reported previously as a byproduct of EO [58], but in our study it was detected before treatment and the concentration increased as more was formed during EO treatment.

This study demonstrated formation of transformation products during EO treatment, which occurred as a direct result of the treatment. The toxicity of the newly formed compounds need to be investigated in the future. However, in our previous study [13] we included effect-based analyses, namely transthyretin (TTR)-binding assays and *A. fischeri* bioluminescence assays. The TTR binding assay uses endocrine disruption as its endpoint, while the bioluminescence assay is a measure of general toxic potency. The activity (toxicity) of the water decreased strongly (~ 90 %) after electrochemical treatment for both assays [13],

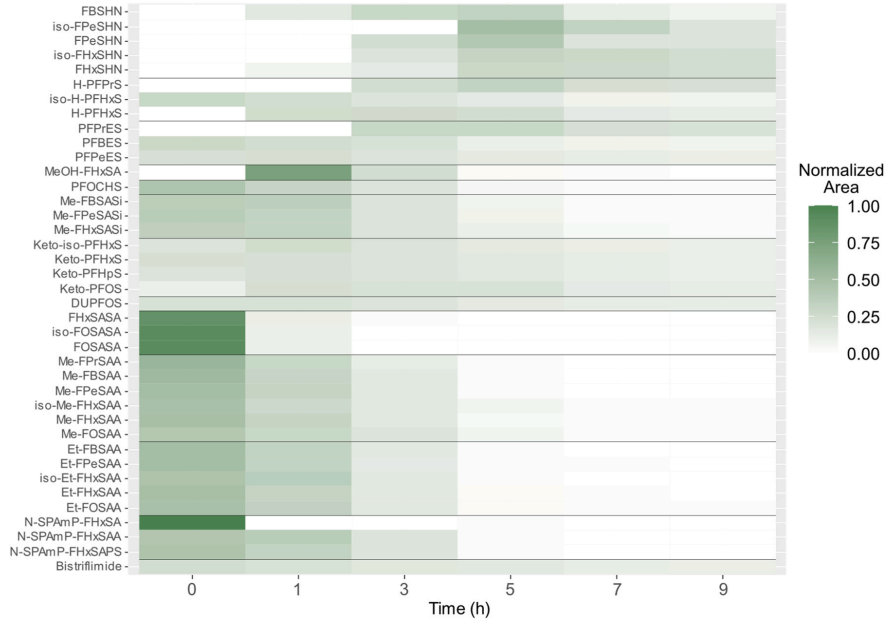

Fig. 3. Heat map of per- and polyfluoroalkyl substances (PFAS) detected in suspect and non-target screening of enriched foam obtained from groundwater after 0, 1, 3, 5, 7, and 9 h of electrochemical oxidation (EO) treatment. A compound with an "iso-"prefix is a branched isomer which eluted before the linear isomer.

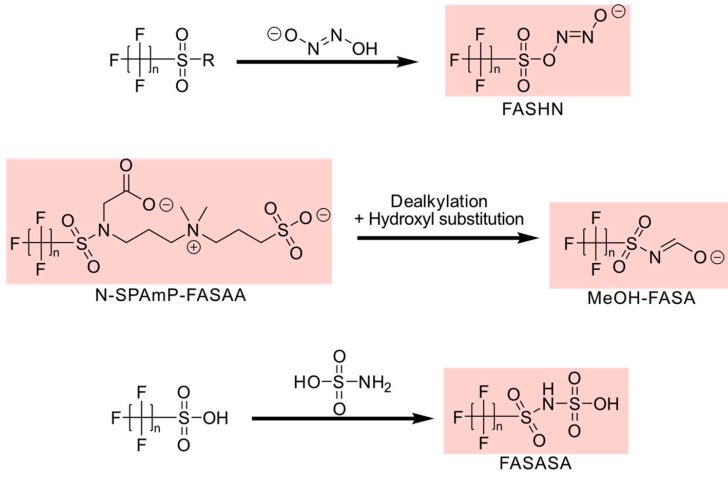

Fig. 4. Proposed formation pathway of (top to bottom) FASHN, FASASA, and MeOH-FASA, three new classes of per- and polyfluoroalkyl substances (PFAS) discovered in this study. Compound structures marked in pink boxes were detected and structure was determined at confidence level (CL) 3d or above.

indicating that the activity of the transformation products was negligible compared with that of the original pollutants. However, the toxicity of the untreated water could not be explained solely by the originally measured target PFAS, and hence the compounds identified here may have partly caused the bioassay activity at time zero.

In addition to contamination of the aqueous environment, there may be a risk of emitting unknown transformation products (products of incomplete destruction, reactions occurring with the matrix, etc.) to the air. Little is known about this, necessitating further research on the water treatment techniques currently used. What is known is currently is the risk of producing short chain PFAS which although not as bio-accumulative, might still be toxic due to their ubiquity in the

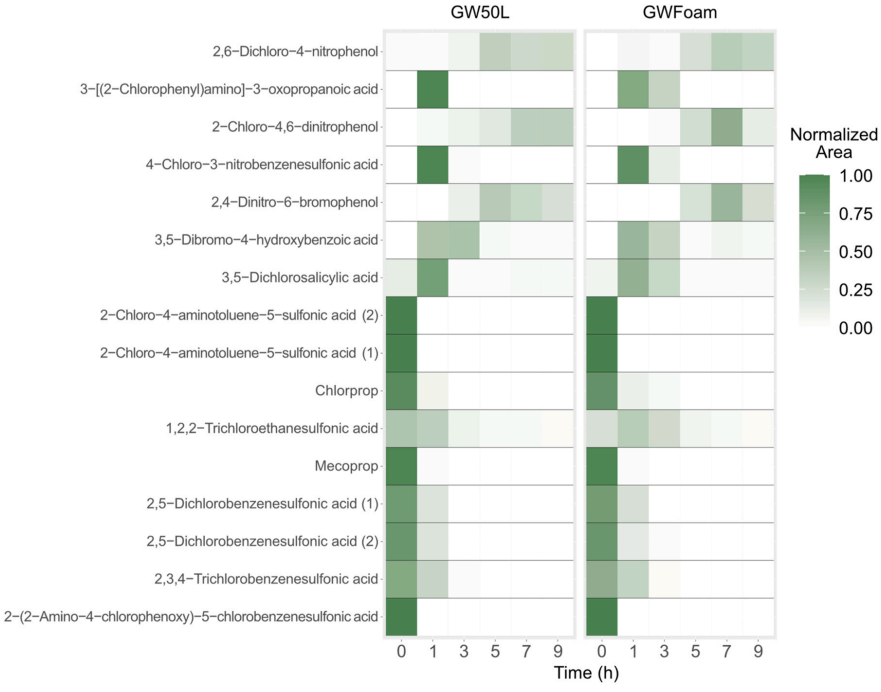

Fig. 5. Heat map of chlorinated and brominated compounds identified during suspect screening after 0, 1, 3, 5, 7, and 9 h of electrochemical oxidation (EO) treatment in (left) 50 L of groundwater (GW50L) treated with EO and (right) groundwater foam (GWFoam) pre-treated with foam fractionation and then treated with EO.

environment. Furthermore, techniques such as GAC and foam fractionation are less effective at removing short chain PFAS [16,26]. The risk of emitting airborne contaminants should also be investigated. Effect-directed analyses could be used for identification of such toxic compounds [81], by combining appropriate bioassays with non-targeted screening techniques.

4. Conclusions

PFAS, chlorinated and brominated compounds, and their transformation products were identified in landfill leachate and groundwater treated with EO, with or without foam fractionation as a preconcentration step. Thus while EO treatment may have the potential to destroy PFAS, there is an associated risk of formation of transformation products. More studies are needed to determine their concentrations and their toxicity. This study revealed that ammonia is oxidized during EO, so formation of nitrate and nitrate radicals might be one of the contributing factors to formation of N-containing transformation products. Literature has found that halogenated nitrogenous disinfection byproducts are more toxic disinfection byproducts that are only halogenated [82].

Suspect and non-target screening proved to be appropriate techniques for exploring the chemical space created by destructive treatment of PFAS. Two new classes of PFAS (FASHN and MeOH-FASA) were discovered for the first time, one of which included transformation products (FASHN). These transformation products were possibly formed through a substitution reaction of hyponitrous acid, with this functional group becoming the new head group of a PFAS. Detection of H-PFSA revealed a potential new pathway for its formation during EO treatment. Six chlorinated or brominated compounds formed during EO treatment were detected, and pre-treatment with foam fractionation seemed to affect formation and/or degradation of these compounds.

These findings highlight the need to monitor transformation products during EO treatment and the importance of suspect and non-targeted screening tools. Further studies are needed to identify transformation products arising in novel destructive treatment technologies being developed in response to stricter PFAS regulations in drinking water and other aqueous matrices. Previous bioassays indicate that the transformation products identified here are unlikely to be significantly biologically active, but it is possible that previously unidentified PFAS present before treatment modified the biological effect in the matrices tested.

Environmental implication

This study focuses on the identification of PFAS and other halogenated compounds, and their transformation products using electrochemical oxidation (EO) on landfill leachate and groundwater. The development of advanced treatment methods can reduce the potential thread of these compounds to environmental and human health. In this study potentially toxic transformation products are formed during the EO treatment process, which can be potential environmental hazards. Additionally, we could show that the water matrix plays an important role in the types of chemicals that can be formed. This study contributes to a better evaluation of advanced treatment method for removal of hazardous pollutants.

CRediT authorship contribution statement

Sanne J Smith: Writing – review & editing, Validation, Supervision, Resources, Investigation. **Lutz Ahrens:** Writing – review & editing, Supervision, Resources, Funding acquisition. **Svante Rehnstam:** Writing – original draft, Visualization, Software, Investigation, Formal analysis.

Declaration of Competing Interest

The authors declare that they have no known competing financial interests or personal relationships that could have appeared to influence the work reported in this paper.

Appendix A. Supporting information

Supplementary data associated with this article can be found in the online version at doi:10.1016/j.jhazmat.2024.136316.

Data Availability

Data will be made available on request.

References

[1] Baderna, D., Maggioni, S., Boriani, E., Gemma, S., Molteni, M., Lombardo, A., et al., 2011. A combined approach to investigate the toxicity of an industrial landfill's leachate: chemical analyses, risk assessment and in vitro assays. Environ Res 111 (4), 603–613. https://doi.org/10.1016/j.envres.2011.01.015.

[2] Bakare, A.A., Mosuro, A.A., Osibanjo, O., 2000. Effect of simulated leachate on chromosomes and mitosis in roots of Allium cepa (L.). J Environ Biol 21 (3), 263–271 https://www.scopus.com/inward/record.uri?eid=2-s2.0-0033896486&partnerID=40&md5=323f013eee02e0daf12e351ebde0510a.

[3] El-Fadel, M., Findikakis, A.N., Leckie, J.O., 1997. Environmental impacts of solid waste landfilling. J Environ Manag 50 (1), 1–25. https://doi.org/10.1006/jema.1995.0131.

[4] Renou, S., Givaudan, J.G., Poulain, S., Dirassouyan, F., Moulin, P., 2008. Landfill leachate treatment: review and opportunity. J Hazard Mater 150 (3), 468–493. https://doi.org/10.1016/j.jhazmat.2007.09.077.

[5] Mohammad-pajooh, E., Turcios, A.E., Cuff, G., Weichgrebe, D., Rosenwinkel, K.H., Vedenyapina, M.D., et al., 2018. Removal of inert COD and trace metals from stabilized landfill leachate by granular activated carbon (GAC) adsorption. J Environ Manag 228 (September)), 189–196. https://doi.org/10.1016/j.jenvman.2018.09.020.

[6] Hamid, H., Li, L.Y., Grace, J.R., 2018. Review of the fate and transformation of per- and polyfluoroalkyl substances (PFASs) in landfills. Environ Pollut 235, 74–84. https://doi.org/10.1016/j.envpol.2017.12.030.

[7] Bell, E.M., De Guise, S., McCutcheon, J.R., Lei, Y., Levin, M., Li, B., et al., 2021. Exposure, health effects, sensing, and remediation of the emerging PFAS contaminants – Scientific challenges and potential research directions. Sci Total Environ 780, 146399. https://doi.org/10.1016/j.scitotenv.2021.146399.

[8] Glüge, J., Scheringer, M., Cousins, I.T., Dewitt, J.C., Goldenman, G., Herzke, D., et al., 2020. An overview of the uses of per- And polyfluoroalkyl substances (PFAS). Environ Sci: Process Impacts 22 (12), 2345–2373. https://doi.org/10.1039/d0em00291g.

[9] Gagliano, E., Sgroi, M., Falciglia, P.P., Vagliasindi, F.G.A., Roccaro, P., 2020. Removal of poly- and perfluoroalkyl substances (PFAS) from water by adsorption: Role of PFAS chain length, effect of organic matter and challenges in adsorbent regeneration. Water Res 171, 115381. https://doi.org/10.1016/j.watres.2019.115381.

[10] Veciana, M., Bräunig, J., Farhat, A., Pype, M.L., Freguia, S., Carvalho, G., et al., 2022. Electrochemical oxidation processes for PFAS removal from contaminated water and wastewater: fundamentals, gaps and opportunities towards practical implementation. J Hazard Mater 434 (December 2021). https://doi.org/10.1016/j.jhazmat.2022.128886.

[11] Xu, B., Liu, S., Zhou, J.L., Zheng, C., Weifeng, J., Chen, B., et al., 2021. PFAS and their substitutes in groundwater: Occurrence, transformation and remediation. J Hazard Mater 412, 125159. https://doi.org/10.1016/j.jhazmat.2021.125159.

[12] Kucharzyk, K.H., Darlington, R., Benotti, M., Deeb, R., Hawley, E., 2017. Novel treatment technologies for PFAS compounds: a critical review. J Environ Manag 204, 757–764. https://doi.org/10.1016/j.jenvman.2017.08.016.

[13] Smith, S.J., Lauria, M., Ahrens, L., McCleaf, P., Hollman, P., Bjälkefur Seroka, S., et al., 2023. Electrochemical oxidation for treatment of PFAS in contaminated water and fractionated foam—a pilot-scale study. ACS EST Water. https://doi.org/10.1021/acsestwater.2c00660.

[14] Wang, Y., Ji, Y., Li, K., Huang, Q., 2023. Foam fractionation and electrochemical oxidation for the treatment of per- and polyfluoroalkyl substances (PFAS) in environmental water samples. Chemosphere 339 (May). https://doi.org/10.1016/j.chemosphere.2023.139615.

[15] We, A.C.E., Zamyadi, A., Stickland, A.D., Clarke, B.O., Freguia, S., 2024. A review of foam fractionation for the removal of per- and polyfluoroalkyl substances (PFAS) from aqueous matrices. J Hazard Mater 465 (ember 2023)), 133182. https://doi.org/10.1016/j.jhazmat.2023.133182.

[16] Radjenovic, J., Duinslaeger, N., Avval, S.S., Chaplin, B.P., 2020. Facing the challenge of poly- and perfluoroalkyl substances in water: is electrochemical oxidation the answer? Environ Sci Technol 54 (23), 14815–14829. https://doi.org/10.1021/acs.est.0c06212.

[17] Horst, J., McDonough, J., Ross, I., Houtz, E., 2020. Understanding and managing the potential by-products of PFAS destruction. Groundw Monit Remediat 40 (2), 17–27. https://doi.org/10.1111/gwmr.12372.

[18] Smith, S.J., Lauria, M., Higgins, C.P., Pennell, K.D., Blotevogel, J., Arp, H.P.H., 2024. The need to include a fluorine mass balance in the development of effective technologies for PFAS destruction. Environ Sci Technol Ic. https://doi.org/10.1021/acs.est.3c10617.

[19] Gar Alalm, M., Boffito, D.C., 2022. Mechanisms and pathways of PFAS degradation by advanced oxidation and reduction processes: A critical review. Chem Eng J 450 (P4)), 138352. https://doi.org/10.1016/j.cej.2022.138352.

[20] Hollender, J., Schymanski, E.L., Ahrens, L., Alygizakis, N., Béen, F., Bijlsma, L., et al., 2023. NORMAN guidance on suspect and non-target screening in environmental monitoring. In: In *Environmental Sciences Europe*, 35. Springer Berlin Heidelberg,. https://doi.org/10.1186/s12302-023-00779-4.

[21] Menger, F., Gago-Ferrero, P., Wiberg, K., Ahrens, L., 2020. Wide-scope screening of polar contaminants of concern in water: A critical review of liquid chromatography-high resolution mass spectrometry-based strategies. Trends Environ Anal Chem 28, e00102. https://doi.org/10.1016/j.teac.2020.e00102.

[22] Getzinger, G.J., Higgins, C.P., Ferguson, P.L., 2021. Structure database and in silico spectral library for comprehensive suspect screening of per- and polyfluoroalkyl substances (PFASs) in environmental media by high-resolution mass spectrometry. Anal Chem 93 (5), 2820–2827. https://doi.org/10.1021/acs.analchem.0c04109.

[23] Koelmel, J.P., Paige, M.K., Aristizabal-Henao, J.J., Robey, N.M., Nason, S.L., Stelben, P.J., et al., 2020. Toward comprehensive per- A nd polyfluoroalkyl substances annotation using fluoromatch software and intelligent high-resolution tandem mass spectrometry acquisition. Anal Chem 92 (16), 11186–11194. https://doi.org/10.1021/acs.analchem.0c01591.

[24] Koelmel, J.P., Stelben, P., Godri, D., Qi, J., McDonough, C.A., Dukes, D.A., et al., 2022. Interactive software for visualization of nontargeted mass spectrometry data—FluoroMatch visualizer. Exposome 2 (1), 35–37. https://doi.org/10.1093/exposome/osac006.

[25] Koelmel, J.P., Stelben, P., McDonough, C.A., Dukes, D.A., Aristizabal-Henao, J.J., Nason, S.L., et al., 2022. FluoroMatch 2.0—making automated and comprehensive non-targeted PFAS annotation a reality. Anal Bioanal Chem 414 (3), 1201–1215. https://doi.org/10.1007/s00216-021-03392-7.

[26] Smith, S.J., Wiberg, K., McCleaf, P., Ahrens, L., 2022. Pilot-scale continuous foam fractionation for the removal of per- a nd polyfluoroalkyl substances (PFAS) from landfill leachate. ACS Environ Sci Technol Water. https://doi.org/10.1021/acsestwater.2c00032.

[27] Schulz, W., Landeswasserversorgung, Z., Lucke, T., Oberleitner, D., Balsaa, P., 2019. Use Non-Target Screen LC-ESI-HRMS Water Anal (Guidel-Ed 1, *0* https://www.researchgate.net/publication/338357752.

[28] Sanchez, J.M., Tautenhahn, R., 2023. A comprehensive software workflow for non-targeted analysis of per- and polyfluoroalkyl substances (PFAS) by high-resolution mass spectrometry (HRMS). In. Thermo Fischer Scientific,.

[29] Kaufmann, A., Butcher, P., Maden, K., Walker, S., Widmer, M., 2022. Simplifying nontargeted analysis of PFAS in complex food matrixes. J AOAC Int 105 (5), 1280–1287. https://doi.org/10.1093/jaoacint/qsac071.

[30] Thermo Fisher Scientific, 2023. User Guide for LC Studies Software Version 3.3 SP2 (Issue March). https://assets.thermofisher.com/TFS-Assets/CMD/manuals/XCALI-98478-Compound-Discoverer-User-Guide-LC-Studies-XCALI98478-en.pdf.

[31] NORMAN Network, 2021. NORMAN Substance Database - NORMAN SusDat (https://www.norman-network.com/nds/susdat/).

[32] NORMAN Network, 2023. NORMAN Substace Database - NORMAN SusDat (https://www.norman-network.com/nds/susdat/).

[33] Rehnstam, S., 2023. PFAS Homol Ser (https://github.com/SRehns/PFAS-Homologous-series).

[34] Charbonnet, J.A., McDonough, C.A., Xiao, F., Schwichtenberg, T., Cao, D., Kaserzon, S., et al., 2022. Communicating confidence of per- and polyfluoroalkyl substance identification via high-resolution mass spectrometry. Environ Sci Technol Lett. https://doi.org/10.1021/acs.estlett.2c00206.

[35] Schymanski, E.L., Jeon, J., Gulde, R., Fenner, K., Ruff, M., Singer, H.P., et al., 2014. Identifying small molecules via high resolution mass spectrometry: Communicating confidence. Environ Sci Technol 48 (4), 2097–2098. https://doi.org/10.1021/es5002105.

[36] R Core Team, 2022. R: A Lang Environ Stat Comput (https://www.r-project.org/).

[37] Wickham, H., 2022. String: Simple, Consistent Wrappers Common String Oper (https://cran.r-project.org/package=stringr).

[38] Wickham, H., Averick, M., Bryan, J., Chang, W., McGowan, L., François, R., et al., 2019. Welcome to the Tidyverse. J Open Source Softw 4 (43), 1686. https://doi.org/10.21105/joss.01686.

[39] De Silva, A.O., Spencer, C., Scott, B.F., Backus, S., Muir, D.C.G., 2011. Detection of a cyclic perfluorinated acid, perfluoroethylcyclohexane sulfonate, in the great lakes of North America. Environ Sci Technol 45 (19), 8060–8066. https://doi.org/10.1021/es200135c.

[40] Boulanger, B., Vargo, J.D., Schnoor, J.L., Hornbuckle, K.C., 2005. Evaluation of perfluorooctane surfactants in a wastewater treatment system and in a commercial surface protection product. Environ Sci Technol 39 (15), 5524–5530. https://doi.org/10.1021/es050213u.
[41] Dewapriya, P., Nilsson, S., Ghorbani Gorji, S., O'Brien, J.W., Bräunig, J., Gómez Ramos, M.J., et al., 2023. Novel Per- and Polyfluoroalkyl Substances Discovered in Cattle Exposed to AFFF-Impacted Groundwater. Environ Sci Technol 57 (36), 13635–13645. https://doi.org/10.1021/acs.est.3c03852.
[42] Rhoads, K.R., Janssen, E.M.L., Luthy, R.G., Criddle, C.S., 2008. Aerobic biotransformation and fate of N-ethyl perfluorooctane sulfonamidoethanol (N-EtFOSE) in activated sludge. Environ Sci Technol 42 (8), 2873–2878. https://doi.org/10.1021/es702866c.
[43] Houtz, E.F., Higgins, C.P., Field, J.A., Sedlak, D.L., 2013. Persistence of perfluoroalkyl acid precursors in AFFF-impacted groundwater and soil. Environ Sci Technol 47 (15), 8187–8195. https://doi.org/10.1021/es4018877.
[44] Nguyen, T.V., Reinhard, M., Chen, H., Gin, K.Y.H., 2016. Fate and transport of perfluoro- and polyfluoroalkyl substances including perfluorooctane sulfonamides in a managed urban water body. Environ Sci Pollut Res 23 (11), 10382–10392. https://doi.org/10.1007/s11356-016-6788-9.
[45] Liu, T., Hu, li-X., Han, Y., Dong, L.-L., Wang, Y.-Q., Zhao, J.-H., et al., 2022. Non-target and target screening of per- and polyfluoroalkyl substances in landfill leachate and impact on groundwater in Guangzhou, China. SSRN Electron J 844 (April), 157021. https://doi.org/10.2139/ssrn.4092427.
[46] Newton, S., McMahen, R., Stoeckel, J.A., Chislock, M., Lindstrom, A., Strynar, M., 2017. Novel polyfluorinated compounds identified using high resolution mass spectrometry downstream of manufacturing facilities near decatur, Alabama. Environ Sci Technol 51 (3), 1544–1552. https://doi.org/10.1021/acs.est.6b05330.
[47] Fernandez, N.A., Rodriguez-Freire, L., Keswani, M., Sierra-Alvarez, R., 2016. Effect of chemical structure on the sonochemical degradation of perfluoroalkyl and polyfluoroalkyl substances (PFASs). Environ Sci: Water Res Technol 2 (6), 975–983. https://doi.org/10.1039/c6ew00150e.
[48] McCord, J., Strynar, M., 2019. Identification of per- and polyfluoroalkyl substances in the cape fear river by high resolution mass spectrometry and nontargeted screening. Environ Sci Technol 53 (9), 4717–4727. https://doi.org/10.1021/acs.est.8b06017.
[49] Barzen-Hanson, K.A., Roberts, S.C., Choyke, S., Oetjen, K., McAlees, A., Riddell, N., et al., 2017. Discovery of 40 classes of per- and polyfluoroalkyl substances in historical aqueous film-forming foams (AFFFs) and AFFF-impacted groundwater. Environ Sci Technol 51 (4), 2047–2057. https://doi.org/10.1021/acs.est.6b05843.
[50] Baduel, C., Mueller, J.F., Rotander, A., Corfield, J., Gomez-Ramos, M.J., 2017. Discovery of novel per- and polyfluoroalkyl substances (PFASs) at a fire fighting training ground and preliminary investigation of their fate and mobility. Chemosphere 185, 1030–1038. https://doi.org/10.1016/j.chemosphere.2017.06.096.
[51] McDonough, C.A., Higgins, C.P., Choyke, S., Barton, K.E., Mass, S., Starling, A.P., et al., 2021. Unsaturated PFOS and other PFASs in human serum and drinking water from an afff-impacted community. Environ Sci Technol 55 (12), 8139–8148. https://doi.org/10.1021/acs.est.1c00522.
[52] Luo, Y.S., Aly, N.A., McCord, J., Strynar, M.J., Chiu, W.A., Dodds, J.N., et al., 2020. Rapid characterization of emerging per- and polyfluoroalkyl substances in aqueous film-forming foams using ion mobility spectrometry-mass spectrometry. Environ Sci Technol 54 (23), 15024–15034. https://doi.org/10.1021/acs.est.0c04798.
[53] Zhao, W., Sun, J., 2018. Triflimide (HNTf2) in organic synthesis. Chem Rev 118 (20), 10349–10392. https://doi.org/10.1021/acs.chemrev.8b00279.
[54] Ghorbani Gorji, S., Gómez Ramos, M.J., Dewapriya, P., Schulze, B., Mackie, R., Nguyen, T.M.H., et al., 2023. New PFASs Identified in AFFF impacted groundwater by passive sampling and nontarget analysis. Environ Sci Technol. https://doi.org/10.1021/acs.est.3c06591.
[55] Hensema, T.J., Berendsen, B.J.A., van Leeuwen, S.P.J., 2021. Non-targeted identification of per- and polyfluoroalkyl substances at trace level in surface water using fragment ion flagging. Chemosphere 265, 128599. https://doi.org/10.1016/j.chemosphere.2020.128599.
[56] Supuran, C.T., Winum, J.-Y., Wang, B., 2009. DRug Design Of Zinc-enzyme Inhibitors, 14. John Wiley & Sons, Incorporated,, pp. 58–59.
[57] Hamany Djande, C.Y., Steenkamp, P.A., Piater, L.A., Tugizimana, F., Dubery, I.A., 2023. Metabolic reprogramming of barley in response to foliar application of dichlorinated functional analogues of salicylic acid as priming agents and inducers of plant defence. Metabolites 13 (5). https://doi.org/10.3390/metabo13050666.
[58] Ambauen, N., Muff, J., Mai, N.L., Hallé, C., Trinh, T.T., Meyn, T., 2019. Insights into the kinetics of intermediate formation during electrochemical oxidation of the organic model pollutant salicylic acid in chloride electrolyte. Water 11 (7). https://doi.org/10.3390/w11071322.
[59] Arora, P.K., Srivastava, A., Garg, S.K., Singh, V.P., 2018. Recent advances in degradation of chloronitrophenols. Bioresour Technol 250, 902–909. https://doi.org/10.1016/j.biortech.2017.12.007.
[60] Jiang, J., Zhang, X., Zhu, X., Li, Y., 2017. Removal of intermediate aromatic halogenated dbps by activated carbon adsorption: a new approach to controlling halogenated dbps in chlorinated drinking water. Environ Sci Technol 51 (6), 3435–3444. https://doi.org/10.1021/acs.est.6b06161.
[61] Liu, J., Zhang, X., Li, Y., Li, W., Hang, C., Sharma, V.K., 2019. Phototransformation of halophenolic disinfection byproducts in receiving seawater: Kinetics, products, and toxicity. Water Res 150, 68–76. https://doi.org/10.1016/j.watres.2018.11.059.
[62] Hughes, B.M., McKenzie, D.E., Duffin, K.L., 1993. Identification of components in waste streams by electrospray and tandem mass spectrometry. J Am Soc Mass Spectrom 4 (7), 604–610. https://doi.org/10.1016/1044-0305(93)85022-P.
[63] Lenke, H., Knackmuss, H.J., 1996. Initial hydrogenation and extensive reduction of substituted 2,4-dinitrophenols. Appl Environ Microbiol 62 (3), 784–790. https://doi.org/10.1128/aem.62.3.784-790.1996.
[64] National Center for Biotechnology Information, 2024. [Translated] A kind of preparation method of 2-chloro-3-bromoaniline https://pubchem.ncbi.nlm.nih.gov/patent/CN-113461538-A.
[65] Meijer, J., Lamoree, M., Hamers, T., Antignac, J.P., Hutinet, S., Debrauwer, L., et al., 2021. An annotation database for chemicals of emerging concern in exposome research. Environ Int 152. https://doi.org/10.1016/j.envint.2021.106511.
[66] United States Environmental Protection Agency, 2024. 3-(2-chloroanilino)-3-oxopropanoic Acid - Chem Details https://comptox.epa.gov/dashboard/chemical/details/DTXCID10314322.
[67] National Center for Biotechnology Information, 2024. Process for preparing 2-bromo-4.6-dinitroaniline. https://pubchem.ncbi.nlm.nih.gov/patent/CS-759089-A3.
[68] Zhong, Y., Li, D., Mao, Z., Huang, W., Peng, P., Chen, P., et al., 2014. Kinetics of tetrabromobisphenol A (TBBPA) reactions with H2SO4, HNO3 and HCl: Implication for hydrometallurgy of electronic wastes. J Hazard Mater 270, 196–201. https://doi.org/10.1016/j.jhazmat.2014.01.032.
[69] Dehkordi, S.K., Paknejad, H., Blaha, L., Svecova, H., Grabic, R., Simek, Z., et al., 2022. Instrumental and bioanalytical assessment of pharmaceuticals and hormone-like compounds in a major drinking water source—wastewater receiving Zayandeh Rood river, Iran. Environ Sci Pollut Res 29 (6), 9023–9037. https://doi.org/10.1007/s11356-021-15943-7.
[70] Nguyen, H.H., Ha, K.N., Huynh, D.L., Pham, D.D., Tran, T.M.D., Vo, V.G., et al., 2023. Secondary metabolites from leaves of bouea macrophylla. Chem Nat Compd 59 (3), 540–542. https://doi.org/10.1007/s10600-023-04046-z.
[71] Gomez-Ruiz, B., Gómez-Lavín, S., Diban, N., Boiteux, V., Colin, A., Dauchy, X., et al., 2017. Efficient electrochemical degradation of poly- and perfluoroalkyl substances (PFASs) from the effluents of an industrial wastewater treatment plant. Chem Eng J 322, 196–204. https://doi.org/10.1016/j.cej.2017.04.040.
[72] Schaefer, C.E., Choyke, S., Ferguson, P.L., Andaya, C., Burant, A., Maizel, A., et al., 2018. Electrochemical Transformations of Perfluoroalkyl Acid (PFAA) Precursors and PFAAs in Groundwater Impacted with Aqueous Film Forming Foams. Environ Sci Technol 52 (18), 10689–10697. https://doi.org/10.1021/acs.est.8b02726.
[73] Corbet, A.S., 1935. The formation of hyponitrous acid as an intermediate compound in the biological or photochemical oxidation of ammonia to nitrous acid. Biochem J 29 (5), 1086–1096. https://doi.org/10.1042/bj0291086.
[74] Scozzafava, A., Briganti, F., Supuran, C.T., 1998. Carbonic anhydrase inhibitors. Part 59 inhibition of carbonic anhydrase isozymes I, II and IV with arsanilic acid derivatives. Main Group Met Chem 21 (6), 357–364.
[75] Freeling, F., Scheurer, M., Sandholzer, A., Armbruster, D., Nödler, K., Schulz, M., et al., 2020. Under the radar – Exceptionally high environmental concentrations of the high production volume chemical sulfamic acid in the urban water cycle. Water Res 175. https://doi.org/10.1016/j.watres.2020.115706.
[76] Propp, V.R., De Silva, A.O., Spencer, C., Brown, S.J., Catingan, S.D., Smith, J.E., et al., 2021. Organic contaminants of emerging concern in leachate of historic municipal landfills. Environ Pollut 276, 116474. https://doi.org/10.1016/j.envpol.2021.116474.
[77] Liu, J., Mejia Avendaño, S., 2013. Microbial degradation of polyfluoroalkyl chemicals in the environment: a review. Environ Int 61, 98–114. https://doi.org/10.1016/j.envint.2013.08.022.
[78] Liu, T., Hu, L.X., Han, Y., Xiao, S., Dong, L.L., Yang, Y.Y., et al., 2024. Non-target discovery and risk prediction of per- and polyfluoroalkyl substances (PFAS) and transformation products in wastewater treatment systems. J Hazard Mater 476 (March), 135081. https://doi.org/10.1016/j.jhazmat.2024.135081.
[79] Shojaei, M., Kumar, N., Guelfo, J.L., 2022. An integrated approach for determination of total per- and polyfluoroalkyl substances (PFAS). Environ Sci Technol 56 (20), 14517–14527. https://doi.org/10.1021/acs.est.2c05143.
[80] Sun, W., Zhang, P., Yang, B., Shu, J., Wang, Y., Li, Y., 2015. Products and mechanisms of the heterogeneous reaction of three suspended herbicide particles with NO3 radicals. Sci Total Environ 514, 185–191. https://doi.org/10.1016/j.scitotenv.2015.02.003.
[81] Jonkers, T.J.H., Meijer, J., Vlaanderen, J.J., Vermeulen, R.C.H., Houtman, C.J., Hamers, T., et al., 2022. High-performance data processing workflow incorporating effect-directed analysis for feature prioritization in suspect and nontarget screening. Environ Sci Technol 56 (3), 1639–1651. https://doi.org/10.1021/acs.est.1c04168.
[82] Bond, T., Huang, J., Templeton, M.R., Graham, N., 2011. Occurrence and control of nitrogenous disinfection by-products in drinking water - A review. Water Res 45 (15), 4341–4354. https://doi.org/10.1016/j.watres.2011.05.034.

SI- Suspect and non-target screening of per- and polyfluoroalkyl substances (PFAS) and other halogenated substances in electrochemically oxidized landfill leachate and groundwater

Contents

Table S1. The gradient program used in the liquid chromatography. The organic modifier consisted of Methanol with an added 5mM of ammonium acetate.

Time	Organic modifier (%)
0.0	10
1.0	10
13.0	95
15.0	95
15.1	10
17.0	10

Table S2. Settings used for data processing in Compound Discoverer. Each setting is listed for each node

Detected compounds	
1. General Settings	
Mass Tolerance [ppm]	5
Min. Peak Intensity	10000
Min. #Scans per Peak	5
Use Most Intense Isotope Only	TRUE
2. Trace Detection	
Max. Number of Gaps to Correct	2
Min. Number of Adjacent Non-Zeroes	2
3. Peak Detection	
Chromatographic S/N Threshold	1.5
Remove Baseline	FALSE
Gap Ratio Threshold	0.35
Max. Peak Width [min]	1
Min. Relative Valley Depth	0.1
4. Isotope Pattern Detection	
Group Isotopes for	Br; Cl
Use Peak Quality for Isotope Grouping	TRUE
Filter out Features with Bad Peaks Only	True
Zig-Zag Index Threshold	0.2
Jaggedness Threshold	0.4
Modality Threshold	0.9
Remove Potentially False Positive Isotopes	TRUE
5. Compound Detection	

Ions	[2M+FA-H]-1; [2M-H]-1; [2M-H+HAc]-1; [M+Cl]-1; [M+FA-H]-1; [M-2H+K]-1; [M-CF2COOH]+1; [M-CO]-1; [M-COH]-1; [M-COOH]-1; [M-H]-1; [M-H+HAc]-1; [M-H-H2O]-1
Base Ions	[M-H]-1
Remove Singlets	FALSE
6. Acquire X Settings	
Detect Persistent Background Ions	FALSE
Group Compounds	
1. General Settings	
Mass Tolerance	5 ppm
RT Tolerance [min]	0.2
Align Peaks	FALSE
Preferred Ions	[M-H]-1
Area Integration	Most Common Ion
2. Peak Rating Contributions	
Area Contribution	3
CV Contribution	10
FWHM to Base Contribution	5
Jaggedness Contribution	5
Modality Contribution	5
Zig-Zag Index Contribution	5
3. Peak Rating Filter	
Peak Rating Threshold	5
Number of Files	3
Mark Background Compounds	
1. General Settings	
Max. Sample/Blank	5
Max. Blank/Sample	0
Hide Background	TRUE
Calculate Mass Defect	
1. Mass Defect	
Fractional Mass Defect	FALSE
Relative Mass Defect	TRUE
Kendrick Mass Defect	TRUE
Nominal Mass Rounding	Round
2. Kendrick Formula	
Formula 1	CF2
Search Neutral Losses	
1. General Settings	

Neutral Losses	CO2; HF; SO2; SO3; CF2
High Acc. Mass Tolerance	2.5 mmu
Low Acc. Mass Tolerance	0.5 Da
S/N Threshold	3
Use DIA Scans for Search	FALSE
Assign Compound Annotations	
1. General Settings	
Mass Tolerance	5
2. Data Sources	
Data Source #1	MzCloud Search
Data Source #2	ChemSpider Search
Data Source #3	MassList Search
Data Source #4	Predicted Compositions
Data Source #5	
3. Scoring Rules	
Use mzLogic	TRUE
Use Spectral Distance	TRUE
Sfit Threshold	20
Sfit Range	20
4. Reprocessing	
Clear Names	TRUE
Search mzCloud	
1. General Settings	
Compound Classes	Perfluorinated Hydrocarbons
Precursor Mass Tolerance	10 ppm
FT Fragment Mass Tolerance	10 ppm
IT Fragment Mass Tolerance	0.4 Da
Library	Autoprocessed; Reference
Post Processing	Recalibrated
Max. #Results	10
Annotate Matching Fragments	TRUE
Search MSn Tree	TRUE
2. DDA Search	
Identity Search	Cosine
Match Activation Type	FALSE
Match Activation Energy	Any
Activation Energy Tolerance	20
Apply Intensity Threshold	TRUE
Similarity Search	Similarity Forward
Match Factor Threshold	40

Search Mass Lists	
1. Search Settings	
Mass Lists	list.massList
Use Retention Time	FALSE
RT Tolerance [min]	2
Mass Tolerance	5 ppm
Search ChemSpider	
1. Search Settings	
Database(s)	EPA DSSTox
Search Mode	By Formula or Mass
Mass Tolerance	5 ppm
Max. # of results per compound	100
Results Order	Order By Reference Count (DESC)
Max. # of Predicted Compositions to be searched per Compound	3
2. Predicted Composition Annotation	
Check All Predicted Compositions	T
Predict Compositions	
1. Prediction Settings	
Mass Tolerance	5 ppm
Min. Element Counts	C H F
Max. Element Counts	C90 H190 Br3 Cl4 F50 N10 O18 P3 S5
Min. RDBE	0
Max. RDBE	40
Min. H/C	0.1
Max. H/C	3.5
Max. # Candidates	15
Max. # Internal Candidates	500
2. Pattern Matching	
Intensity Tolerance [%]	30
Intensity Threshold [%]	0.1
S/N Threshold	3
Min. Spectral Fit [%]	30
Min. Pattern Cov. [%]	90
Use Dynamic Recalibration	TRUE
3. Fragment Matching	
Use Fragment Matching	TRUE
Mass Tolerance	5 ppm
S/N Threshold	3

Compound Class Scoring	
1. General Settings	
Compound Classes	See Method section
S/N Threshold	1
High Acc. Mass Tolerance	5 ppm
Low Acc. Mass Tolerance	10 ppm
Use Full MS Tree	FALSE
Allow DIA Scoring	FALSE

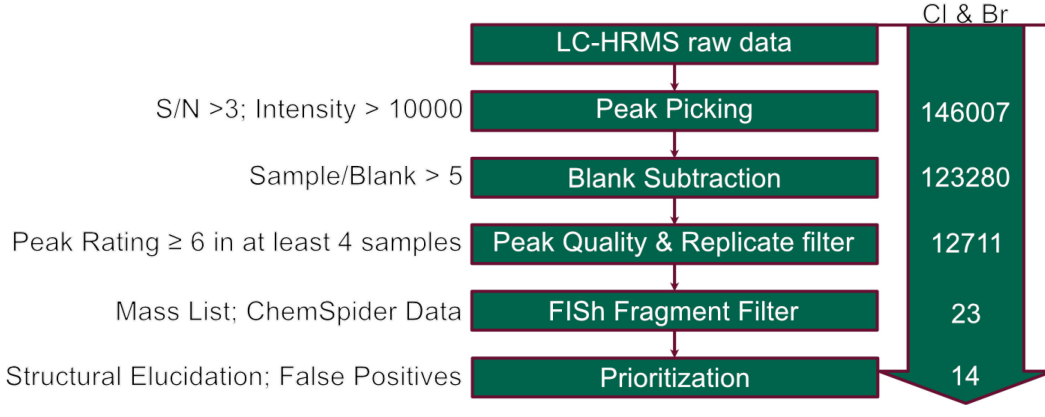

Figure S1. Flowchart summarizing the suspect screening process for brominated and chlorinated compounds.

1. Mass spectrometry

1.1. Annotation of PFAS compounds identified through suspect and non-target screening

Me-FASAA
Me-FBSAA

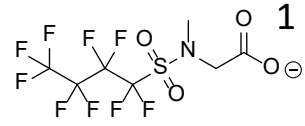

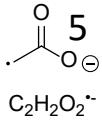

Nr	Found m/z	Expected m/z	Error (ppm)	Error (mDa)
1	369.97925	369.98011	-2.32	-0.86
2	311.97476	311.97463	0.42	0.13
3	218.98631	218.98618	0.59	0.13
4	82.96099	82.96085	1.69	0.14
5	58.00449(NL)	58.00548	-17.07	-0.99

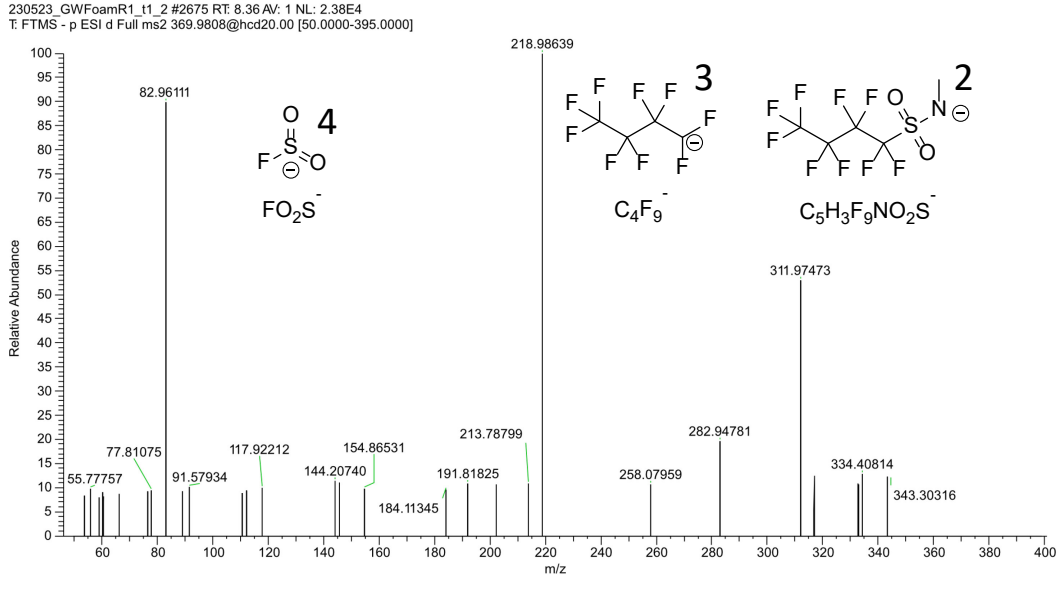

Figure S2. Annotation of compound class Me-FOSAA compound Me-FBSAA.

Et-FASAA
Et-FBSAA

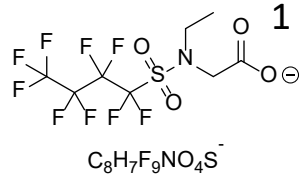

Nr	Found m/z	Expected m/z	Error (ppm)	Error (mDa)
1	383.99518	383.99576	-1.51	-0.58
2	325.9903	325.99028	0.06	0.02
3	282.94812	282.94808	0.14	0.04
4	218.98615	218.98618	-0.14	-0.03
5	82.96098	82.96085	1.57	0.13

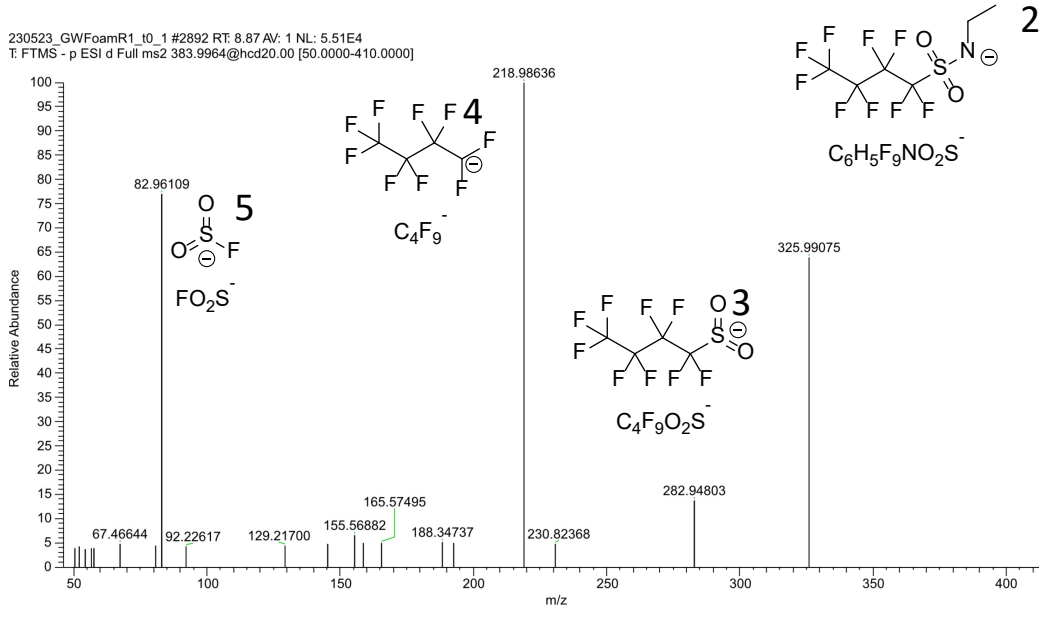

Figure S3. Annotation of compound class Et-FASAA compound Et-FBSAA.

H-PFSA
H-PFBS

Nr	Found m/z	Expected m/z	Error (ppm)	Error (mDa)
1	280.95209	280.95241	-1.14	-0.32
2	130.99272	130.99256	1.22	0.16
3	98.95593	98.95577	1.62	0.16
4	79.95744	79.95736	1.00	0.08

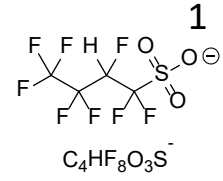

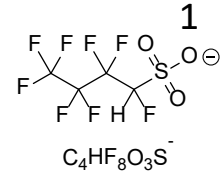

Figure S4. Annotation of compound class H-PFSA compound H-PFBS.

PFESA
PBESA

Nr	Found m/z	Expected m/z	Error (ppm)	Error (mDa)
1	314.93854	314.93791	2.00	0.63
2	134.98756	134.98748	0.59	0.08
3	84.99072	84.99067	0.59	0.05

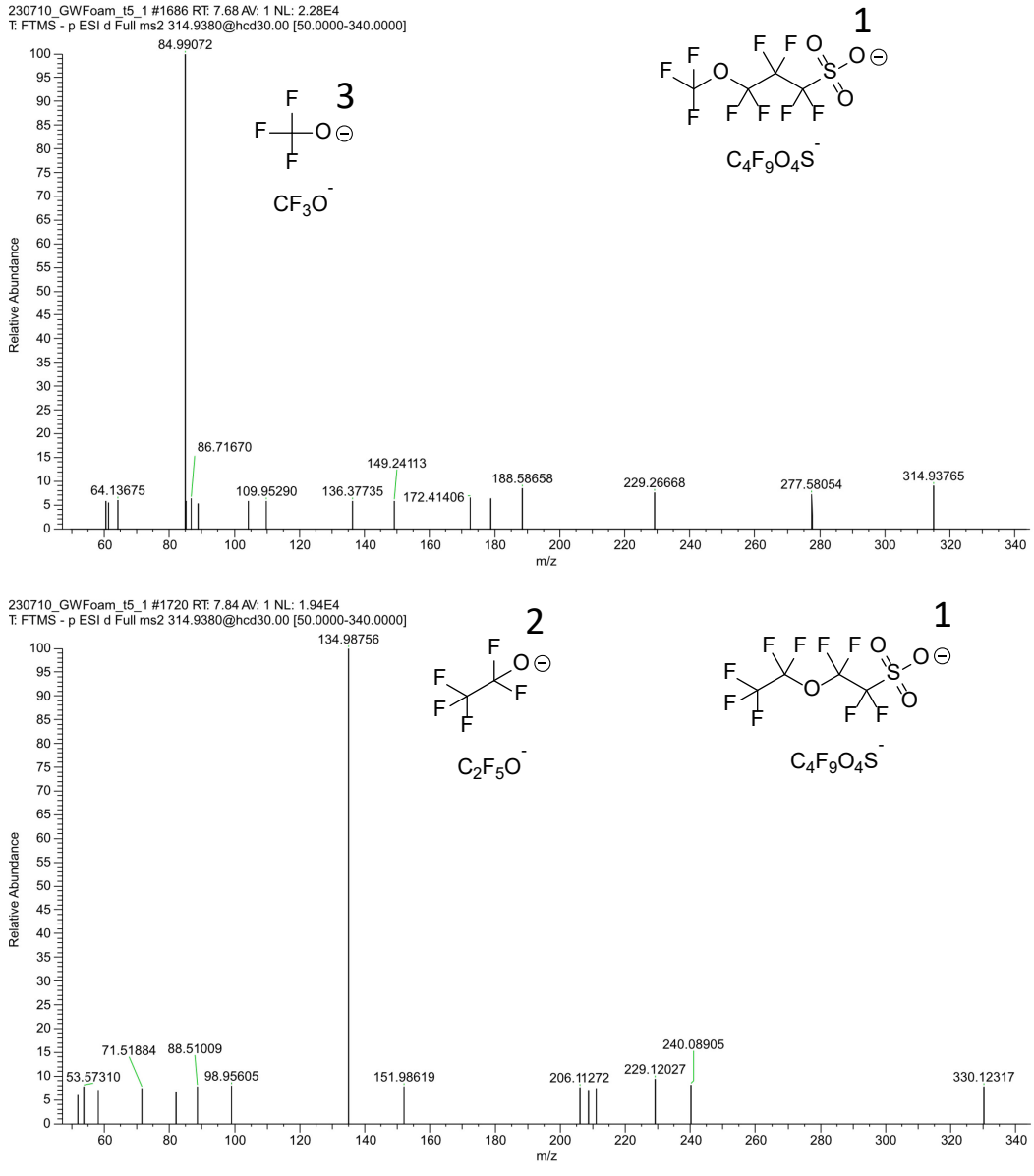

Figure S5. Annotation of compound class PFESA compound PBESA.

N-SPAmP-FHxSA

Nr	Found m/z	Expected m/z	Error (ppm)	Error (mDa)
1	605.04650	605.04550	1.65	1.00
2	483.04221	483.04174	0.97	0.47
3	168.98950	168.98937	0.77	0.13
4	166.05467	166.05434	1.99	0.33
5	118.99265	118.99256	0.76	0.09

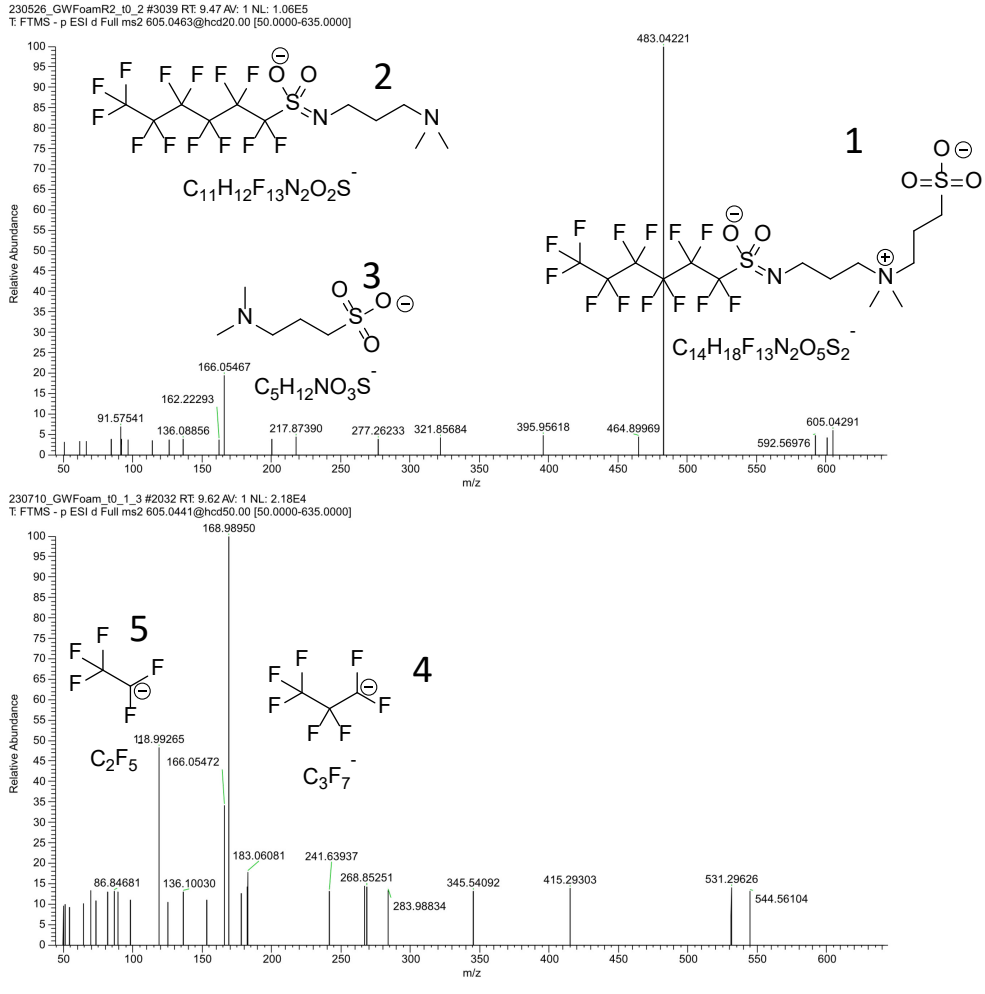

Figure S6. Annotation of the compound N-SPAmP-FHxSA.

N-SPAmP-FHxSAA

Nr	Found m/z	Expected m/z	Error (ppm)	Error (mDa)
1	663.0525	663.05098	2.29	1.52
2	166.05447	166.05434	0.78	0.13

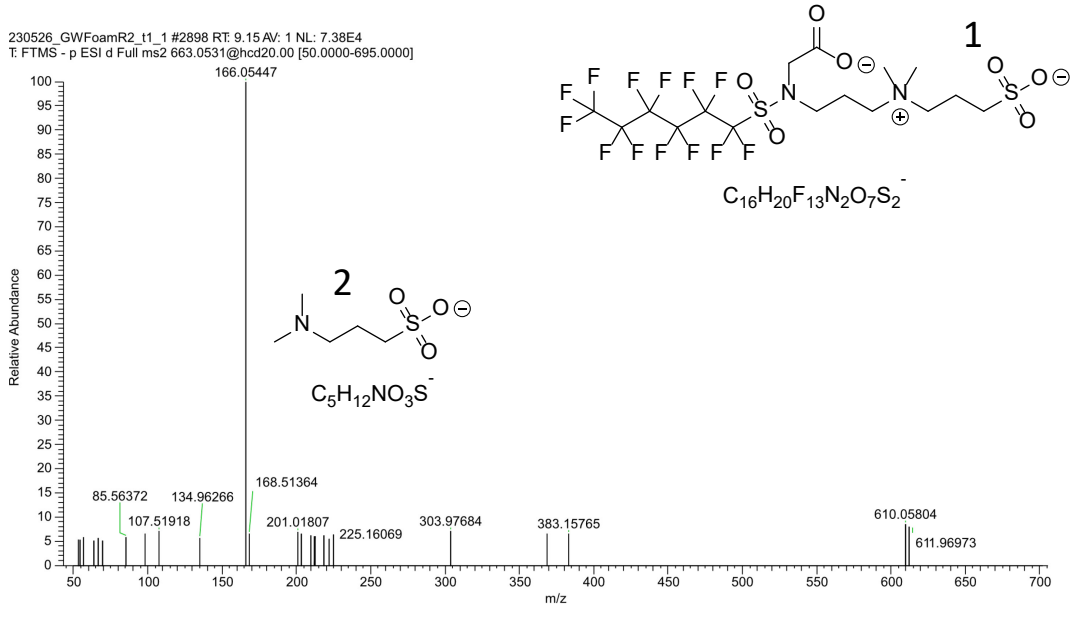

Figure S7. Annotation of the compound N-SPAmP-FHxSAA.

N-SPAmP-FHxSAPS

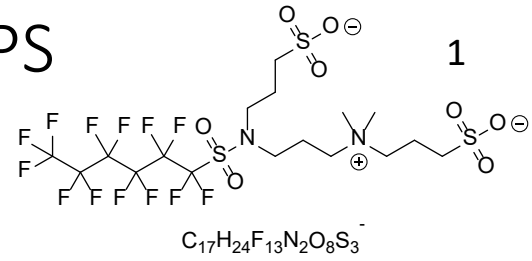

Nr	Found m/z	Expected m/z	Error (ppm)	Error (mDa)
1	727.04938	727.04927	0.15	0.11
2	605.04547	605.0455	-0.05	-0.03
3	483.04205	483.04174	0.64	0.31

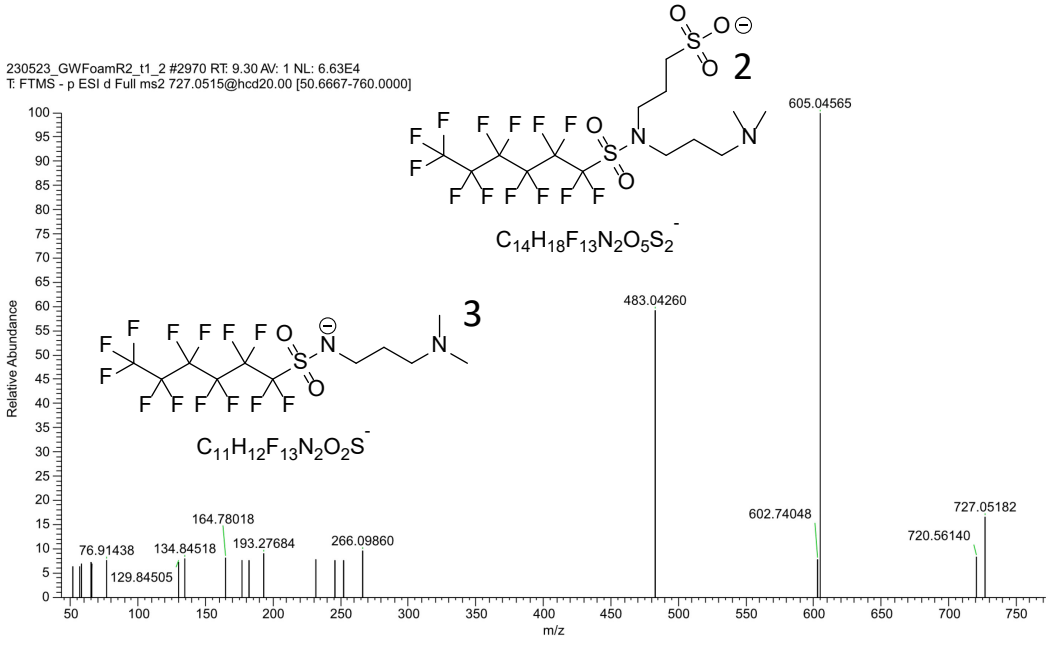

Figure S8. Annotation of the compound N-SPAmP-FHxSAPS.

Keto-PFSA
Keto-PFHxS

Nr	Found m/z	Expected m/z	Error (ppm)	Error (mDa)
1	376.93509	376.93471	1.01	0.38
2	310.94287	310.94299	-0.39	-0.12
3	230.98608	230.98618	-0.43	-0.1
4	130.99294	130.99256	2.90	0.38
5	98.95609	98.95577	3.23	0.32
6	79.9575	79.95736	1.75	0.14

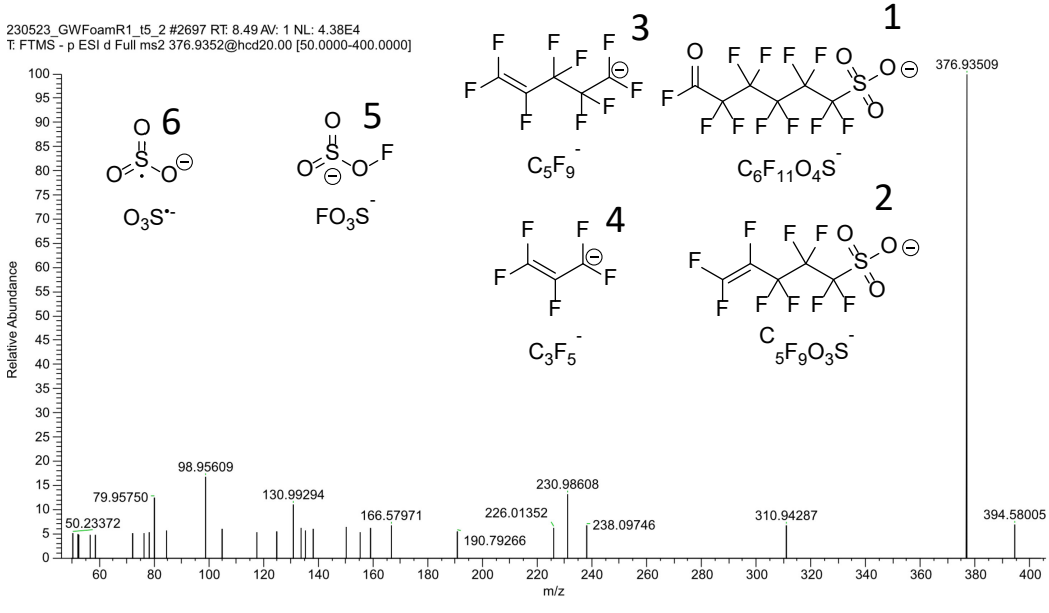

Figure S9. Annotation of compound class Keto-PFSA compound Keto-PFHxS.

DUPFSA
DUPFOS

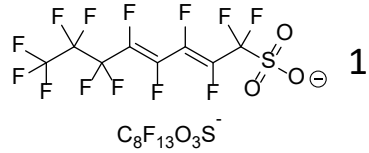

Nr	Found m/z	Expected m/z	Error (ppm)	Error (mDa)
1	422.93734	422.9366	1.75	0.74
2	342.97989	342.97979	0.29	0.10
3	98.95573	98.95577	-0.40	-0.04
4	82.96091	82.96085	0.72	0.06
5	79.95745(NL)	79.95682	7.88	0.63

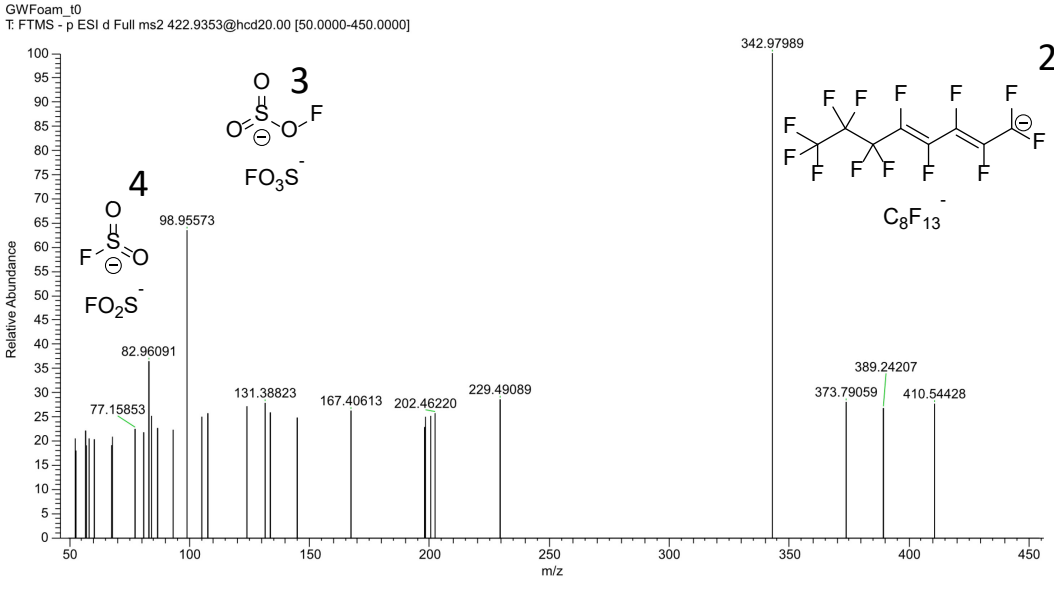

Figure S10. Annotation of compound class DUPFSA compound DUPFOS.

Bistriflimide

Nr	Found m/z	Expected m/z	Error (ppm)	Error (mDa)
1	279.91818	279.91784	1.21	0.34
2	146.96095	146.96073	1.50	0.22
3	82.96104	82.96085	2.29	0.19
4	77.96562	77.96552	1.28	0.10

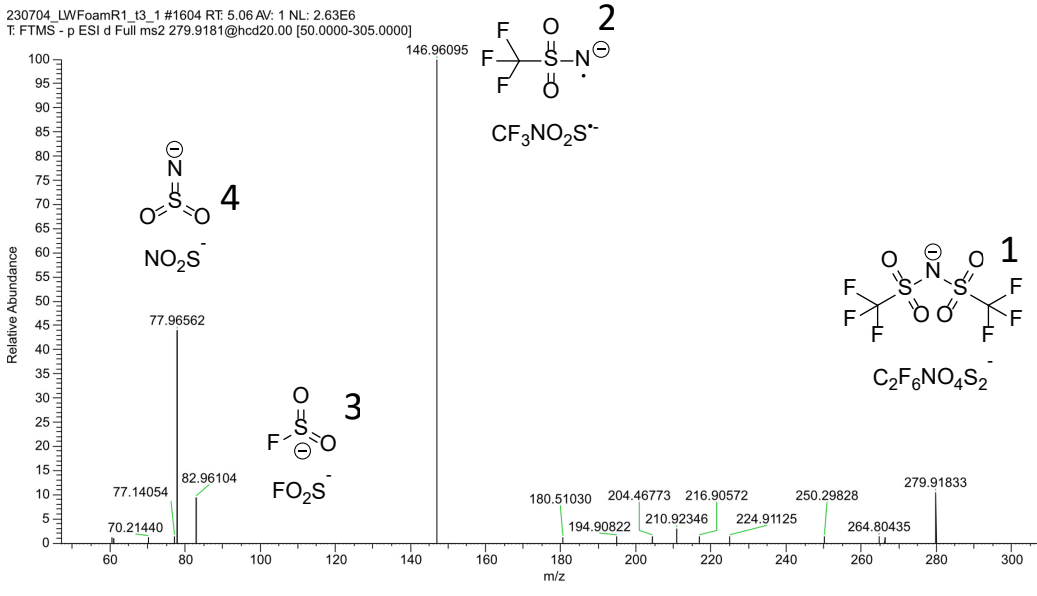

Figure S11. Annotation of the compound Bistriflimide.

MeOH-FASA
MeOH-FHxSA

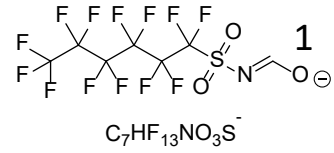

Nr	Found m/z	Expected m/z	Error (ppm)	Error (mDa)
1	425.94827	425.94750	1.81	0.77
2	318.98074	318.97979	2.98	0.95
3	168.99005	168.98937	4.02	0.68
4	106.9685	106.96826	2.24	0.24
5	63.96255	63.96245	1.56	0.10

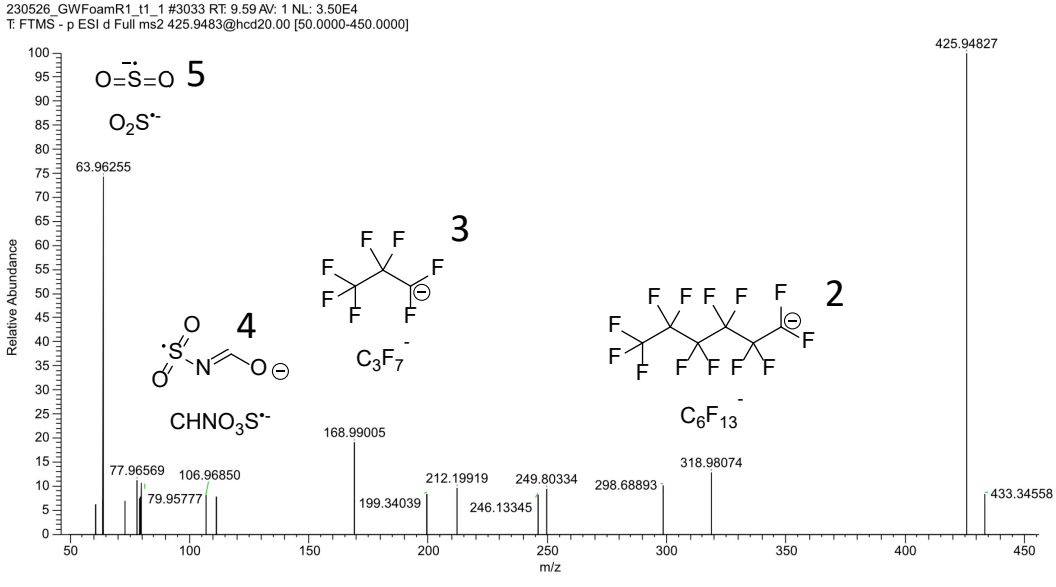

Figure S12. Annotation of compound class MeOH-FASA compound MeOH-FHxSA.

FASASA

FOSASA

Nr	Found m/z	Expected m/z	Error (ppm)	Error (mDa)
1	577.9032	577.90302	0.31	0.18
2	497.94623	497.9462	0.06	0.03
3	168.98918	168.98937	-1.12	-0.19
4	118.99244	118.99256	-1.01	-0.12
5	77.96552	77.96552	0.00	0.00

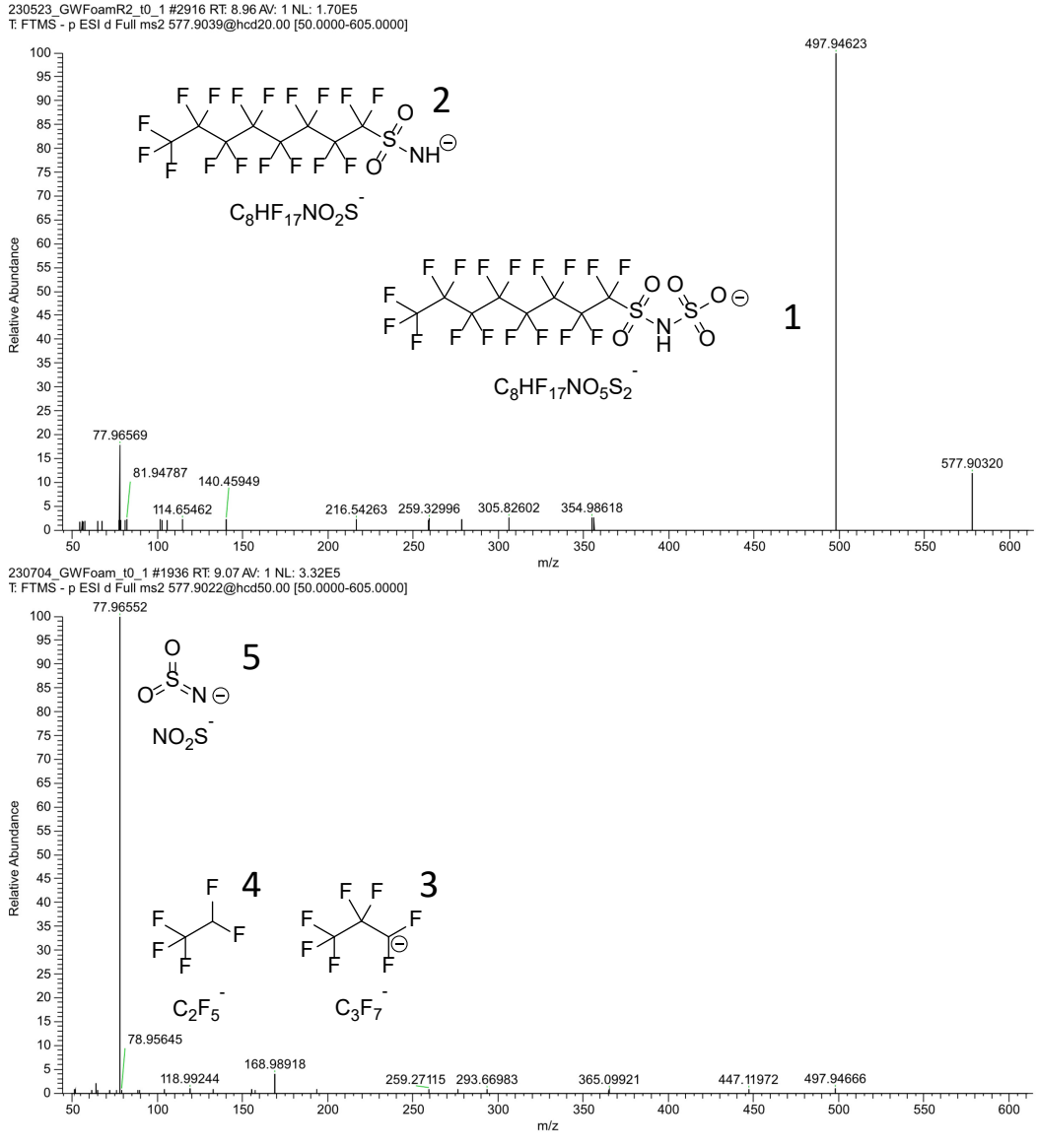

Figure S13. Annotation of compound class FASASA compound FOSASA.

Me-FASASi
Me-FHxSASi

Nr	Found Mass (Da)	Expected Mass (Da)	Error (ppm)	Error (mDa)
1	475.93005	475.93014	-0.19	-0.09
2	156.95094	156.9509	0.25	0.04
3	92.98906	92.989	0.65	0.06
4	318.97893 (NL)	318.97924	-0.41	-0.13

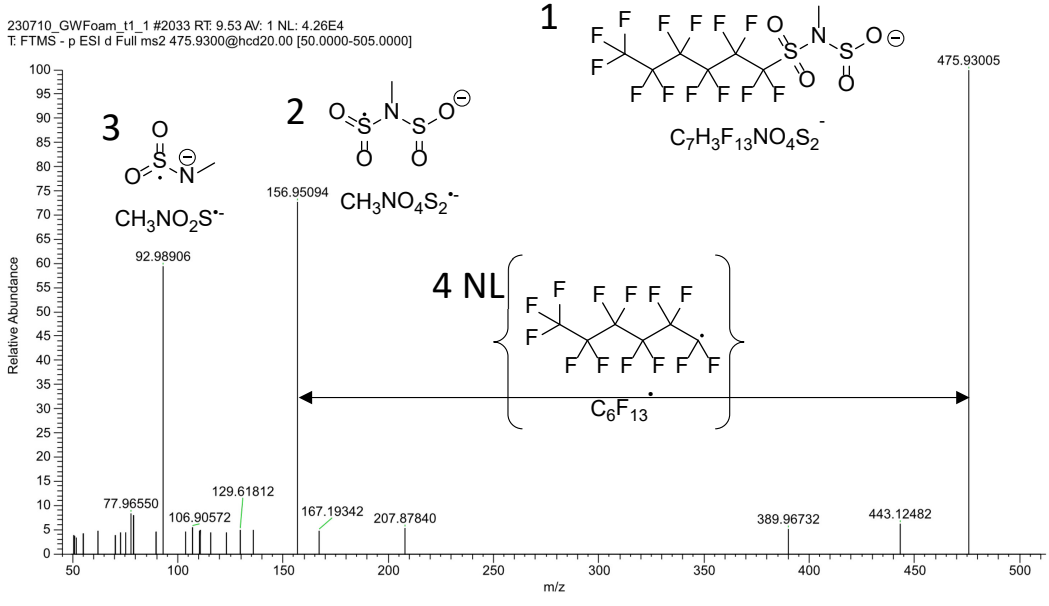

Figure S14. Annotation of compound class Me-FASASi compound Me-FHxSASi.

PFOCHS

Nr	Found m/z	Expected m/z	Error (ppm)	Error (mDa)
1	440.94720	440.94717	0.07	0.03
2	292.98318	292.98298	0.68	0.20
3	168.98947	168.98937	0.59	0.10
4	98.95599	98.95577	2.22	0.22
5	80.96535	80.96519	1.98	0.16

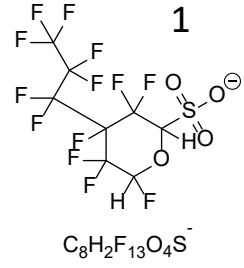

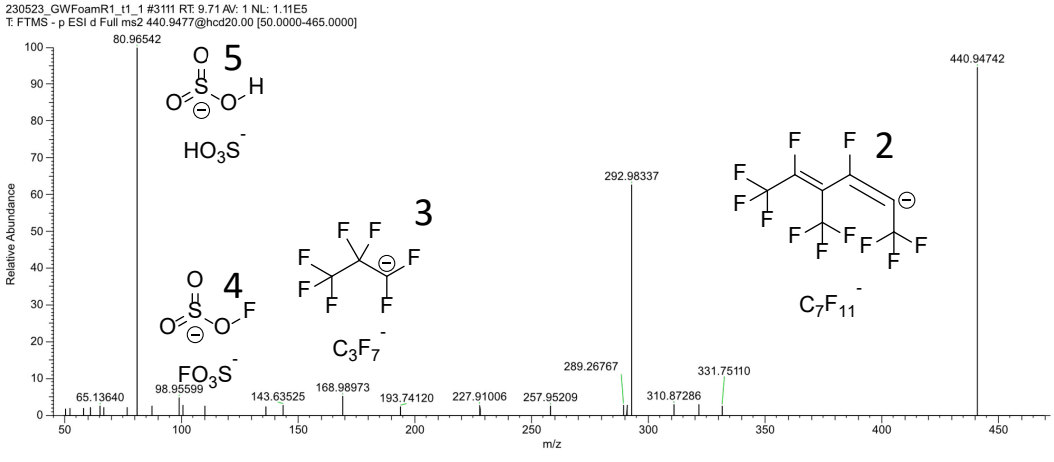

Figure S15. Annotation of the compound PFOCHS.

1.2. Annotation of Cl & Br compounds identified through suspect screening

1,2,2-trichloroethanesulfonic

No.	Found m/z	Expected m/z	Error (ppm)	Error (mDa)
1	208.86383	208.86392	-0.43	-0.09
2	114.92658	114.92622	3.13	0.36

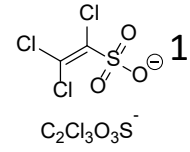

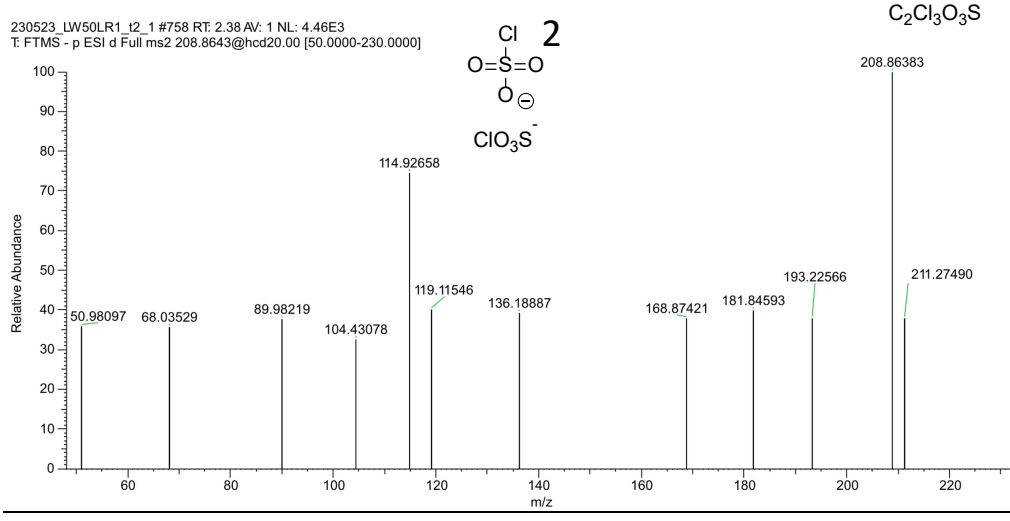

Figure S16. Annotation of the compound 1,2,2-trichloroethanesulfonic acid

3,5-Dichlorosalicylic acid

Nr	Found m/z	Expected m/z	Error (ppm)	Error (mDa)
1	204.94684	204.94647	1.81	0.37
2	160.95689	160.95664	1.55	0.25
3	124.98036	124.97997	3.12	0.39

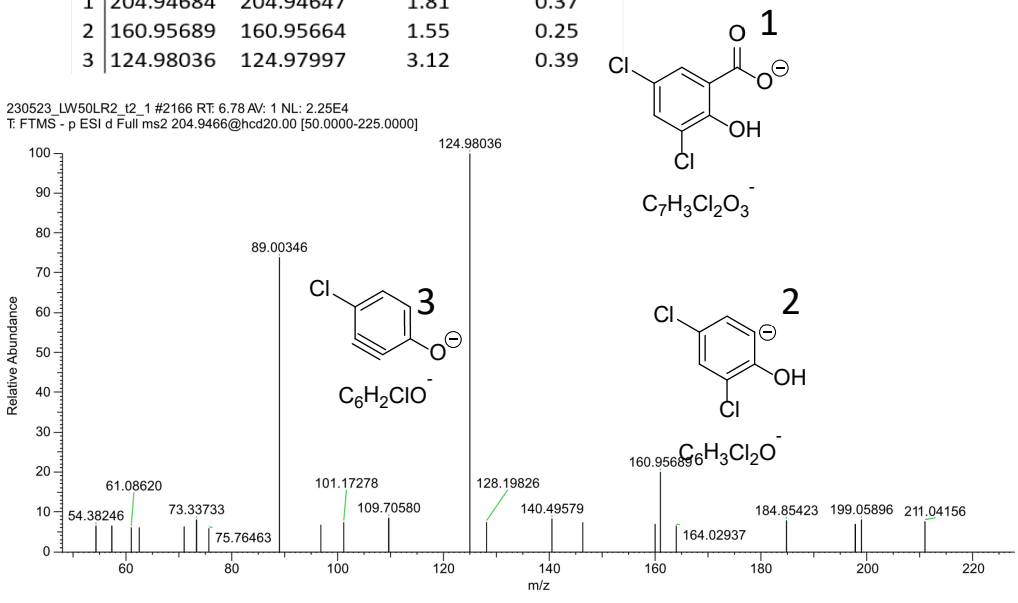

Figure S17. Annotation of 3,5-dichlorosalicylic acid

2,6-Dichloro-4-nitrophenol

Nr	Found m/z	Expected m/z	Error (ppm)	Error (mDa)
1	205.94130	205.94172	-2.04	-0.42
2	175.94392	175.94373	1.08	0.19
3	139.96727	139.96706	1.50	0.21

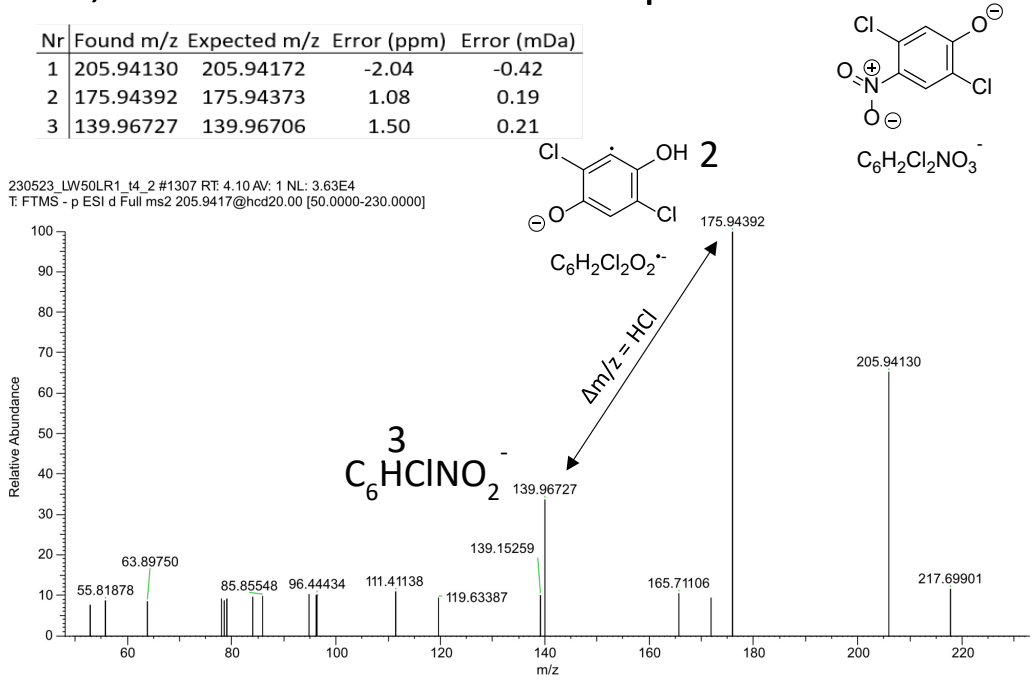

Figure S18. Annotation of 2,6-dichloro-4-nitrophenol

2-Chloro-4,6-dinitrophenol

Nr	Found m/z	Expected m/z	Error (ppm)	Error (mDa)
1	216.96619	216.96577	1.94	0.42
2	158.97308	158.97287	1.32	0.21
3	92.99842	92.99820	2.37	0.22
4	59.01387	59.01385	0.34	0.02

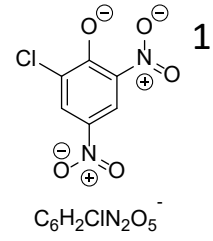

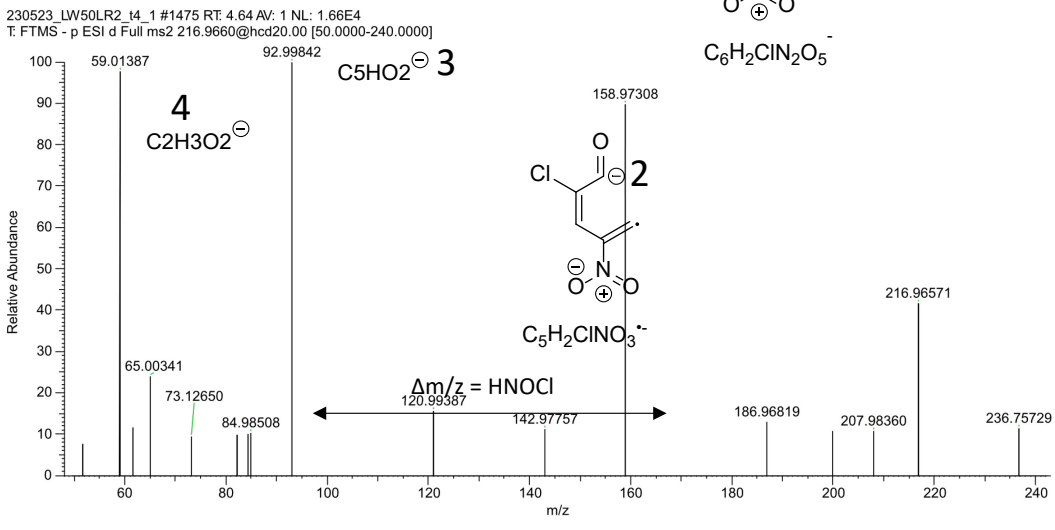

Figure S19. Annotation of 2-chloro-4,6-dinitrophenol

4-Chloro-3-nitrobenzenesulfonic

Nr	Found m/z	Expected m/z	Error (ppm)	Error (mDa)
1	235.94315	235.94259	2.37	0.56
2	171.98116	171.98069	2.73	0.47
3	141.98309	141.98271	2.68	0.38
4	79.9576	79.95736	3.00	0.24

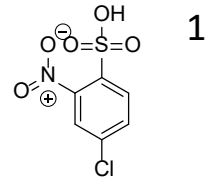

1

$C_6H_4ClNO_5S$

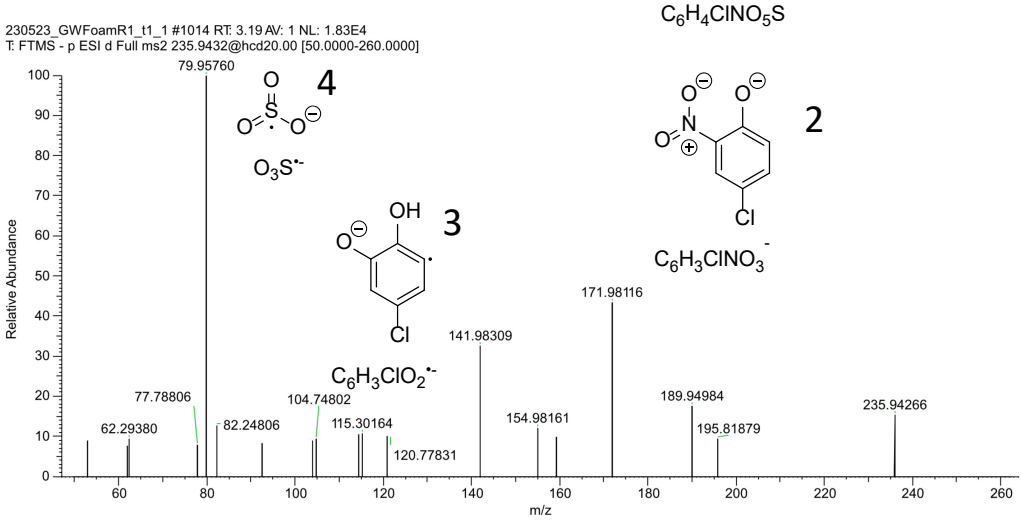

Figure S20. Annotation of 4-chloro-3-nitrobenzenesulfonic acid

3-[(2-Chlorophenyl)amino]-3-

Nr	Found m/z	Expected m/z	Error (ppm)	Error (mDa)
1	212.01257	212.01199	2.74	0.58
2	126.01214	126.0116	4.29	0.54

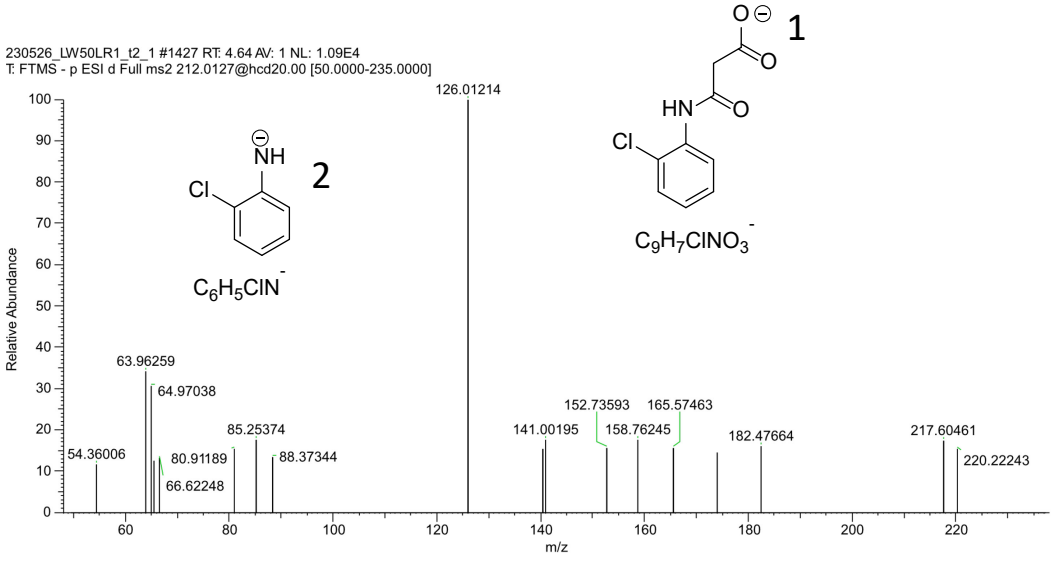

Figure S21. Annotation of 3-[2-chlorophenyl)amino]-3-oxopropanoic acid

2,4-dinitro-6-bromophenol

Nr	Found m/z	Expected m/z	Error (ppm)	Error (mDa)
1	260.9153	260.91526	0.15	0.04
2	230.91734	230.91727	0.30	0.07
3	78.91905	78.91889	2.03	0.16

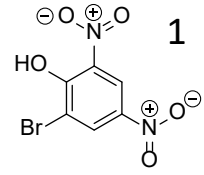

$C_6H_3BrN_2O_5$

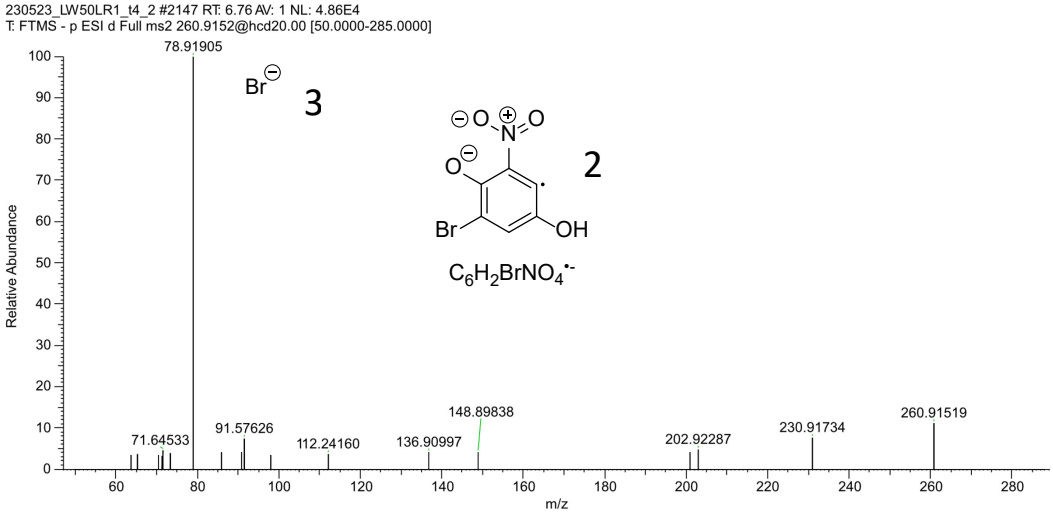

$C_6H_2BrNO_4^{\bullet-}$

Figure S22. Annotation of 2,4-dinitro-6-bromophenol

3,5-Dibromo-4-hydroxybenzoic

Nr	Found m/z	Expected m/z	Error (ppm)	Error (mDa)
1	292.84593	292.84544	1.67	0.49
2	248.85574	248.85561	0.52	0.13
3	168.93015	168.92945	4.14	0.7
4	78.91905	78.91889	2.03	0.16

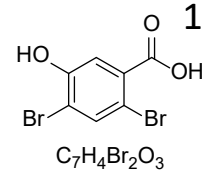

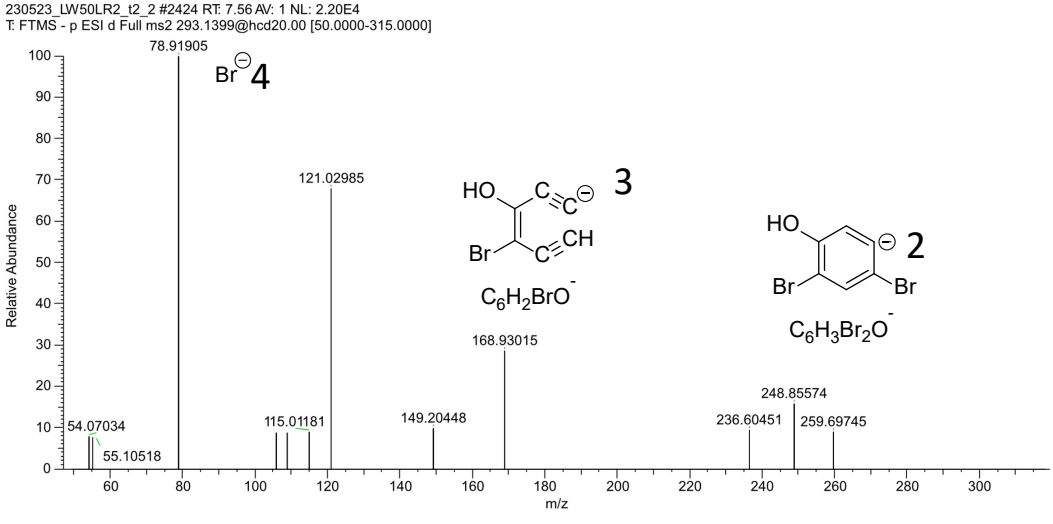

Figure S23. Annotation of 3,5-dibromo-4-hydroxybenzoic acid

Two chlorinated phenoxy carboxylic acids were detected. Chlorprop (ID 2c) was identified with the suspect list and the spectra was compared with one obtained from Massbank, which resulted in CL 2a (Figure S16). Chlorprop has been reported as a herbicide [1]. Mecoprop (ID 5c) was detected through the suspect list and confirmed at CL 2a (Figure S17). Similarly to Chlorprop, Mecoprop is a household herbicide that is widely used and has been reported previously in several different environmental matrices [2]. This was the only compound confirmed using a different spectral database than Massbank, namely The Toxin and Toxin Target Database [3].

Chlorprop

Nr	Found m/z	Expected m/z	Error (ppm)	Error (mDa)
1	199.01716	199.01675	2.06	0.41
2	126.996	126.99562	2.99	0.38
3	71.01395	71.01385	1.41	0.1

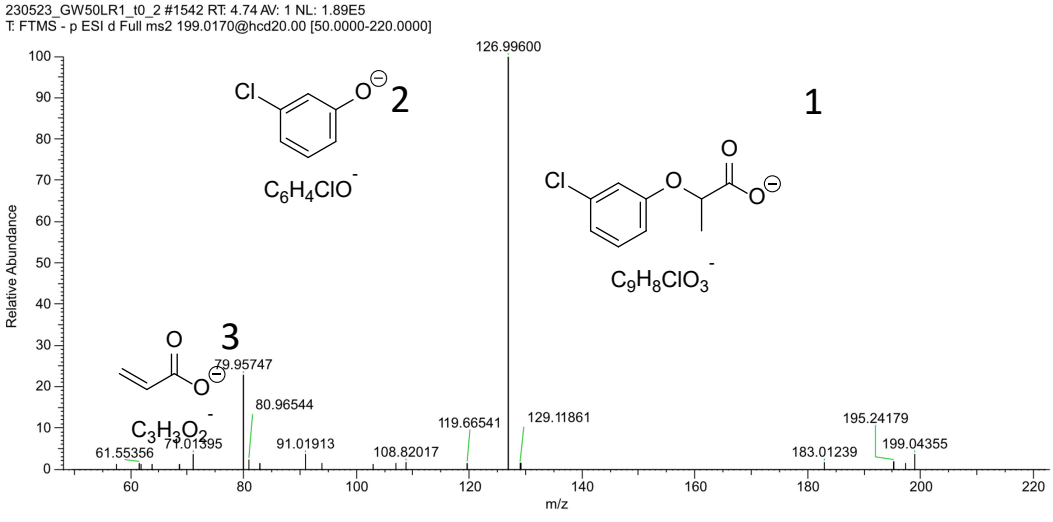

Figure S24. Annotation of the compound Chlorprop.

Mecoprop

Nr	Found m/z	Expected m/z	Error (ppm)	Error (mDa)
1	213.03271	213.0324	1.46	0.31
2	141.01152	141.01127	1.77	0.25
3	71.01389	71.01385	0.56	0.04

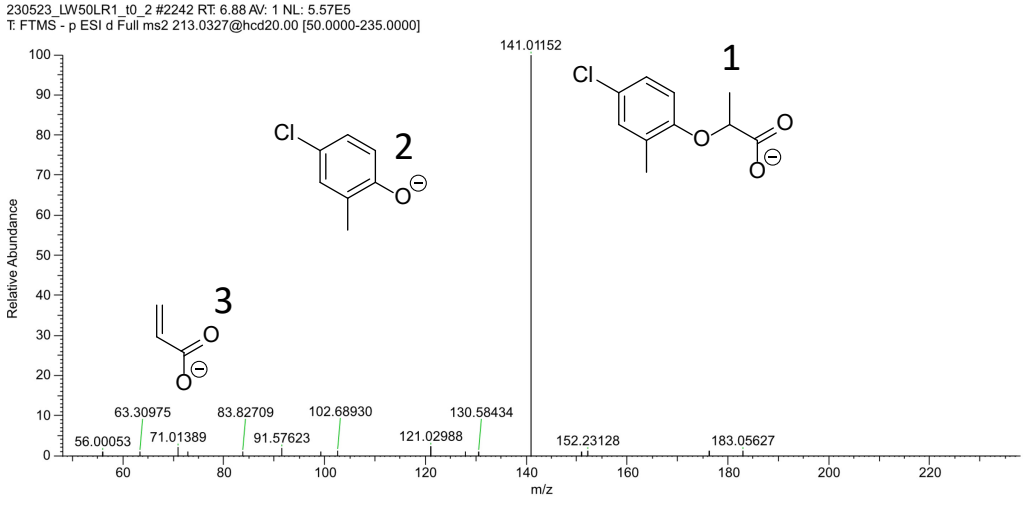

Figure S25. Annotation of the compound Mecoprop.

Three chlorinated sulfonic acids with a benzene backbone were identified. Two isomers of 2-chloro-4-aminotoluene-5-sulfonic (ID 8c) acid were detected. However, the exact position of the isomers was impossible to determine based on mass spectrometry evidence alone, and as such they were given the same name (Figure S18). For the same reason, the CL of the compound was set to 3, as the position of the functional groups could not be determined exactly. 2-Chloro-4-aminotoluene-5-sulfonic acid has historically been used in lake dyes, and has been reported previously in the river Rhine [4,5]. 2,5-Dichlorobenzenesulfonic (ID 9c) acid was detected through the suspect list and had a record in the spectral library at Massbank (Figure S19). However, identification of the compound was more complex due to the presence of two peaks detected in the MS2, which were identified as contamination occurring from a background ion with a m/z

which fit within the isolation window of the instrument. Therefore, the CL was set to 3. 2,5-Dichlorobenzenesulfonic acid is a key reagent used for the production of fuel cells and has been reported previously in groundwater [6,7]. 2,3,4-Trichlorobenzenesulfonic acid (ID 11c) was determined at CL 2b (Figure S20). 2,3,4-Trichlorobenzenesulfonic acid is a precursor in production of various consumer products, one example being golf balls [8]. It has been reported previously in soil samples obtained from a municipal waste incineration plant [9]. 2-(2-amino-4-chlorophenoxy)-5-chlorobenzenesulfonic acid (ID 12c) was detected at CL 3 (Figure S21. It is a precursor used for the synthesis of 1,2,4-benzothidiazine-1,1-dioxide derivatives and has been reported previously in groundwater downstream from a wastewater facility [10,11].

2-Chloro-4-Aminotoluene-5-Sulfonic Acid + isomer

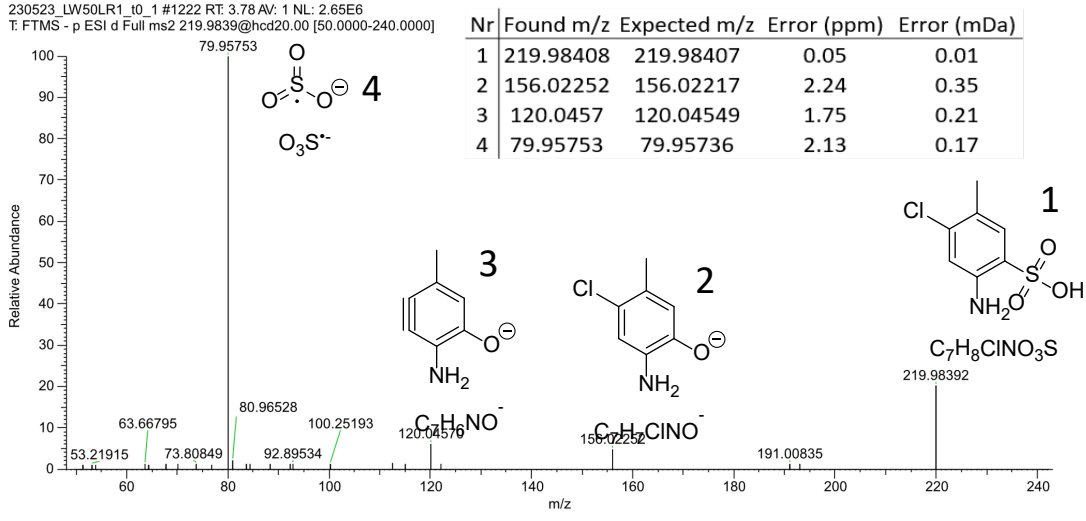

Nr	Found m/z	Expected m/z	Error (ppm)	Error (mDa)
1	219.98408	219.98407	0.05	0.01
2	156.02252	156.02217	2.24	0.35
3	120.0457	120.04549	1.75	0.21
4	79.95753	79.95736	2.13	0.17

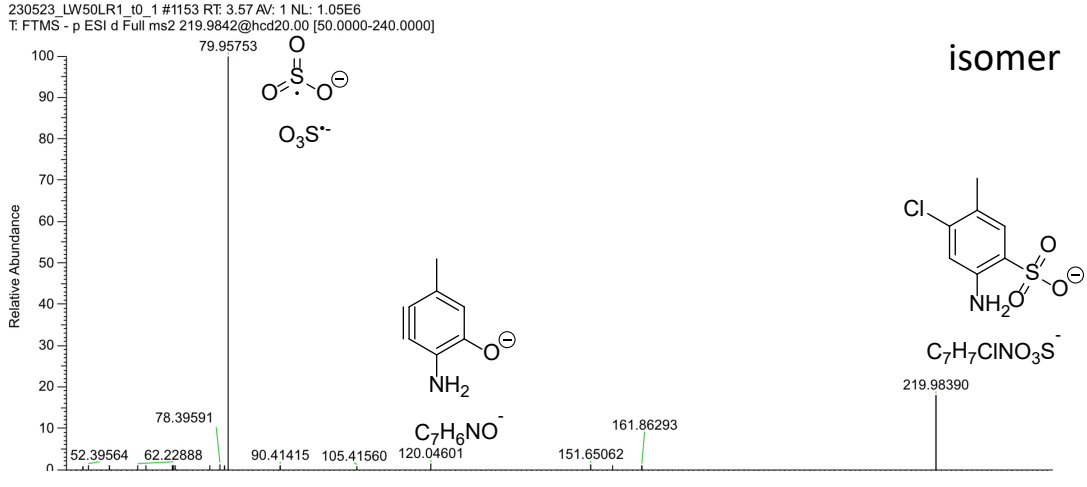

Figure S26. Annotation of the compound 2-chloro-4-aminotoluene-5-sulfonic acid and its isomer.

2,5-Dichlorobenzenesulfonic acid

Nr	Found m/z	Expected m/z	Error (ppm)	Error (mDa)
1	224.91901	224.91854	2.09	0.47
2	160.95734	160.95664	4.35	0.7
3	79.95751	79.95736	1.88	0.15

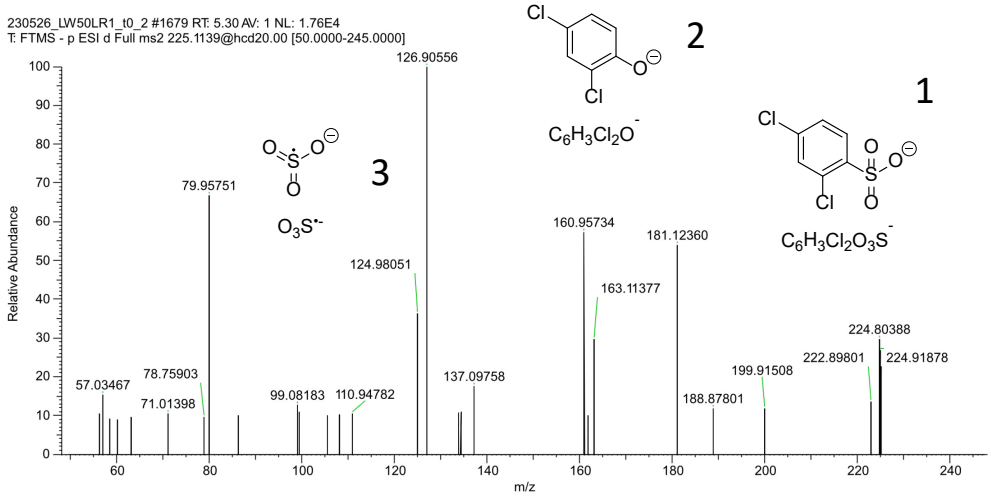

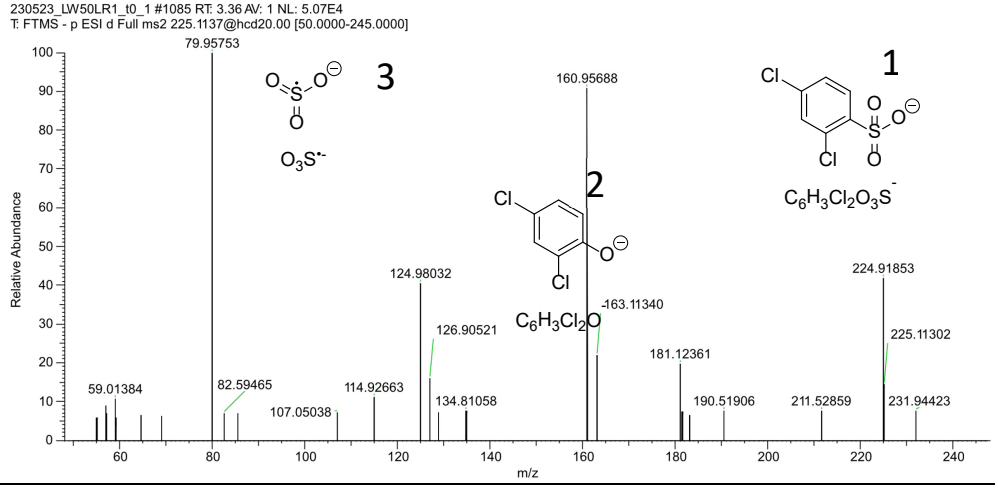

Figure S27. Annotation of the compound 2,5-dichlorobenzenesulfonic acid.

2,3,4-Trichlorobenzenesulfonic acid

Nr	Found m/z	Expected m/z	Error (ppm)	Error (mDa)
1	258.87966	258.87957	0.35	0.09
2	194.91794	194.91767	1.39	0.27
3	158.94124	158.94099	1.57	0.25
4	79.95755	79.95736	2.38	0.19

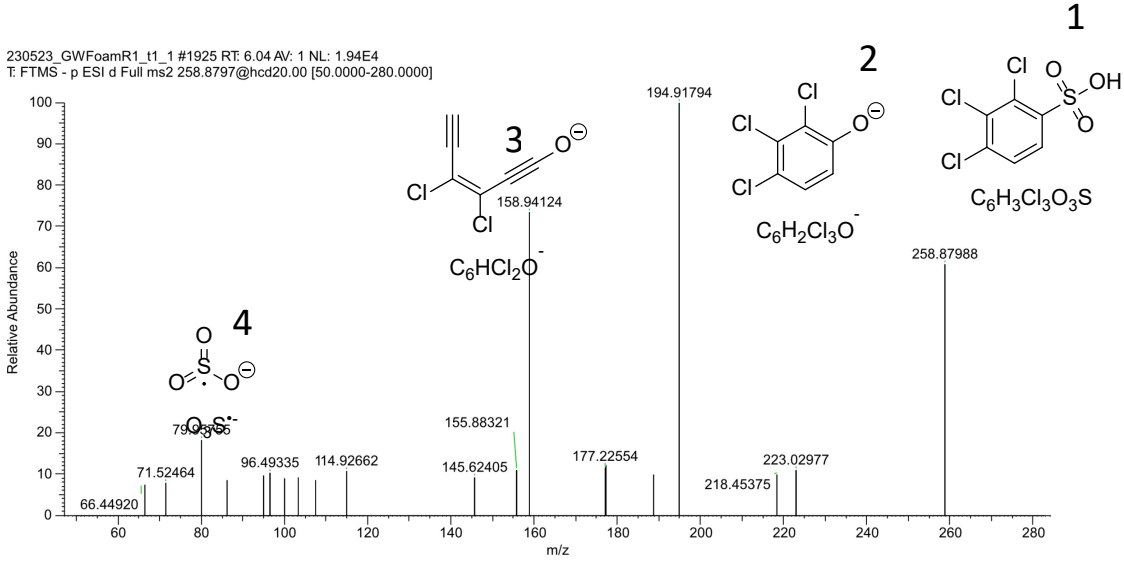

Figure S28. Annotation of the compound 2,3,4-trichlorobenzenesulfonic acid.

2-(2-Amino-4-chlorophenoxy)-5-chlorobenzenesulfonic acid

Nr	Found m/z	Expected m/z	Error (ppm)	Error (mDa)
1	331.95616	331.95566	1.51	0.5
2	251.99869	251.99884	-0.60	-0.15
3	205.94464	205.94461	0.15	0.03
4	141.98297	141.98271	1.83	0.26
5	126.99611	126.99562	3.86	0.49
6	80.96534	80.96519	1.85	0.15
7	79.95755	79.95736	2.38	0.19

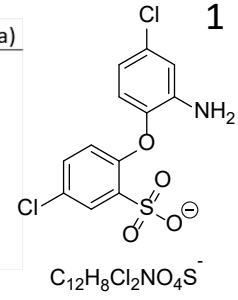

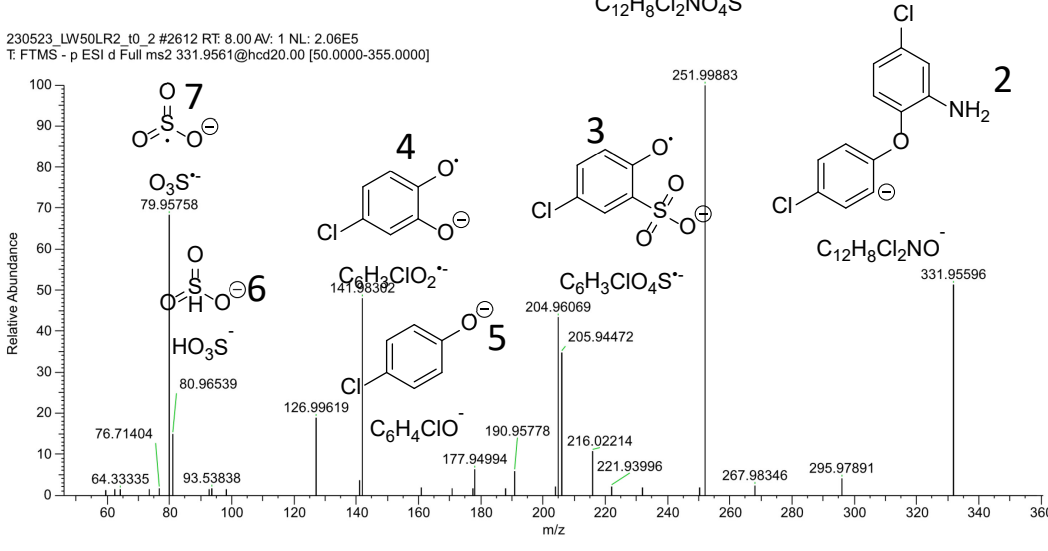

Figure S29. Annotation of the compound 2-(2-amino-4-chlorophenoxy)-5-chlorobenzenesulfonic acid.

2. References

1. National Center for Biotechnology Information. PubChem Annotation Record for , 2-(3-CHLOROPHENOXY)PROPIONIC ACID. https://pubchem.ncbi.nlm.nih.gov/source/hsdb/6594 (2024).

2. Li, L. *et al.* Occurrence, ecological risk, and advanced removal methods of herbicides in waters: a timely review. *Environ. Sci. Pollut. Res.* **31**, 3297–3319 (2023).

3. The Toxin and Toxin Target Database. T3DB: Methylchlorophenoxypropionic acid. http://www.t3db.ca/toxins/T3D0806 (2024).

4. National Center for Biotechnology Information. Azo pigment production - Patent US-2744027-A. https://pubchem.ncbi.nlm.nih.gov/patent/US-2744027-A (2024).

5. Ruff, M., Mueller, M. S., Loos, M. & Singer, H. P. Quantitative target and systematic non-target analysis of polar organic micro-pollutants along the river Rhine using high-resolution mass-spectrometry - Identification of unknown sources and compounds. *Water Res.* **87**, 145–154 (2015).

6. Miyake, J. *et al.* Design of flexible polyphenylene proton-conducting membrane for next-generation fuel cells. *Sci. Adv.* **3**, 1–8 (2017).

7. Hale, S. E. *et al.* Getting in control of persistent, mobile and toxic (PMT) and very persistent and very mobile (vPvM) substances to protect water resources: strategies from diverse perspectives. *Environ. Sci. Eur.* **34**, (2022).

8. National Center for Biotechnology Information. Golf ball - Patent US-2022193494-A1. https://pubchem.ncbi.nlm.nih.gov/patent/US-2022193494-A1#section=Country (2024).

9. Tang, C. *et al.* High-performance nontarget analysis of halogenated organic compounds in tap water, fly ash, soil and sediment using ultrahigh resolution mass spectrometry and scripting approaches based on Cl/Br-specific search algorithms. *Anal. Chim. Acta* **1204**, 339618 (2022).

10. Varano, F., Catarzi, D., Colotta, V., Squarcialupi, L. & Matucci, R. 1,2,4-Benzothiadiazine-1,1-dioxide derivatives as Ionotropic glutamate receptor ligands: Synthesis and structure-activity relationships. *Arch. Pharm. (Weinheim).* **347**, 777–785 (2014).

11. Rao, R. N., Venkateswarlu, N., Khalid, S., Narsimha, R. & Sridhar, S. Use of solid-phase extraction, reverse osmosis and vacuum distillation for recovery of aromatic sulfonic acids from aquatic environment followed by their determination using liquid chromatography-electrospray ionization tandem mass spectrometry. *J. Chromatogr. A* **1113**, 20–31 (2006).

Acta Universitatis Agriculturae Sueciae

Doctoral Thesis No. 2026:34

Per- and polyfluoroalkyl substances (PFAS) are persistent and widespread environmental contaminants. Destructive treatment techniques have been developed to degrade these pollutants. However, such processes may generate transformation products (TPs). This thesis explores the formation of TPs occurring from treatment techniques. Several new TPs were identified as originating from treatment techniques. Their potential toxicity was evaluated with *in silico* techniques. The work in this thesis highlighted the need for complementary untargeted analyses when assessing the performance of advanced destructive treatment techniques.

Svante Bertil Rehnstam received his doctoral education at the Department of Aquatic Sciences and Assessment at the Swedish Univeristy of Agricultural Sciences. He holds a Master's degree in Analytical Chemistry from Uppsala University and a Bachelor's degree in Applied Chemistry from HZ University of Applied Sciences.

Acta Universitatis Agriculturae Sueciae presents doctoral theses from the Swedish University of Agricultural Sciences (SLU).

SLU generates knowledge for the sustainable use of biological natural resources. Research, education, extension, as well as environmental monitoring and assessment are used to achieve this goal.

ISSN 1652-6880
ISBN (print version) 978-91-8124-251-5
ISBN (electronic version) 978-91-8124-281-2